

**ROLE OF ASYMMETRIC SEGREGATION AND THE RIBOSOME ASSOCIATED
COMPLEX IN PRION FORMATION AND PROPAGATION**

A Dissertation
Presented to
The Academic Faculty

by

Rebecca Leigh Howie

In Partial Fulfillment
of the Requirements for the Degree
Doctor of Philosophy in the
School of Biological Sciences

Georgia Institute of Technology

May, 2018

COPYRIGHT © 2018 BY REBECCA HOWIE

**ROLE OF ASYMMETRIC SEGREGATION AND THE RIBOSOME ASSOCIATED
COMPLEX IN PRION FORMATION AND PROPAGATION**

Approved by:

Dr. Yury Chernoff, Advisor
School of Biological Sciences
Georgia Institute of Technology

Dr. William Ratcliff
School of Biological Sciences
Georgia Institute of Technology

Dr. Kirill Lobachev
School of Biological Sciences
Georgia Institute of Technology

Dr. Hong Qin
College of Arts and Sciences
University of Tennessee at Chat.

Dr. Francesca Storici
School of Biological Sciences
Georgia Institute of Technology

Date Approved: April 2, 2018

ACKNOWLEDGEMENTS

I would like to thank all of the many people who have assisted in this work, including my advisor Dr. Yury Chernoff for guidance, my committee members, Gary Newnam for all of his advice and assistance with experiments, Drs. Denis Kiktev and Katy Bruce for encouragement, and my family for love and support of my scientific interests, especially my parents Melanie and Joseph Howie. Most of all, I would like to thank my husband Jamie Grimes for love and support, for waiting up while I worked late nights running experiments in the lab, and for taking care of our Henry while I wrote this.

TABLE OF CONTENTS

ACKNOWLEDGEMENTS	iii
LIST OF TABLES	vi
LIST OF FIGURES	vii
LIST OF SYMBOLS AND ABBREVIATIONS	ix
SUMMARY	x
CHAPTER 1. Background of protein quality control and stress	1
1.1 Prions and amyloids	2
1.2 Prion and amyloid diseases	3
1.3 Yeast prions	4
1.3.1 [<i>PSI</i> ⁺]	6
1.3.2 [<i>URE3</i>]	8
1.3.3 [<i>LSB</i> ⁺]	10
1.4 Chaperone control of prion propagation and curing	12
1.5 The effects of stress on yeast prions	14
1.6 Asymmetric segregation of protein aggregates	17
1.7 The ribosome associated complex	19
1.8 Goal of this work	22
CHAPTER 2. Materials and methods	24
2.1 Basic yeast techniques	24
2.1.1 Media used and phenotypic screening	24
2.1.2 Transformation of yeast strains	24
2.1.3 Mating assay	25
2.1.4 Yeast DNA purification	26
2.2 Construction of yeast strains	27
2.3 Biochemical analysis of proteins	32
2.3.1 Method for protein purification	32
2.3.2 Protein level determination via Western Blot	32
2.3.3 Analysis of protein aggregation: boiled gel	33
2.3.4 Analysis of protein aggregation: SDD-AGE	33
2.3.5 Analysis of intracellular protein distribution: sucrose gradient centrifugation	33
2.4 Prion curing assays	34
2.4.1 Curing of [<i>PSI</i> ⁺] by mild heat-shock	34
2.4.2 Artificial overexpression of HSP104	36
2.4.3 Prion curing by GuHCl	37
CHAPTER 3. Role of the cellular asymmetry apparatus in prion curing by stress	38
3.1 Introduction to Chapter 3	38
3.2 Materials and Methods: Fluorescence microscopy	40
3.3 The effect of <i>SIR2</i> deletion on [<i>PSI</i> ⁺] destabilization during heat shock	41
3.4 The result of <i>LSB2</i> deletion on [<i>PSI</i> ⁺] curing and the necessity of <i>SIR2</i>	45
3.5 The effect of nicotinamide on [<i>PSI</i> ⁺] destabilization during heat shock	46

3.6	The effect of <i>sir2</i> deletion on aggregate recovery and segregation after mild heat shock.	48
3.7	Sup35 co-localization with Hsp104-marked protein aggregates during heat shock.	49
3.8	Discussion of Chapter 3 data	53
3.9	Conclusions of Chapter 3	57
CHAPTER 4. Changes in aggregation due to aging		59
4.1	Introduction to Chapter 4	59
4.2	Materials and methods for aging	60
4.2.1	Purification of aged cells by biotinylation	60
4.2.2	Assay for cellular load of Hsp104-associated aggregates	62
4.2.3	Assay for frequency of spontaneous [<i>PSI</i> ⁺] formation	62
4.3	Age-related changes in cellular load of Hsp104-associated aggregates	63
4.4	Frequency of spontaneous formation of [<i>PSI</i> ⁺] in aged cells	64
4.5	Discussion of Chapter 4 data	67
4.6	Conclusions of Chapter 4	69
CHAPTER 5. The role of the Hsp70-Ssb chaperone and ribosome-associated complex (RAC) in [<i>PSI</i>⁺] destabilization by heat shock		70
5.1	Introduction to Chapter 5	70
5.2	Deletion of <i>ZUO1</i> , <i>SSZ</i> , or <i>SSB</i> and the effect on [<i>PSI</i> ⁺] loss during mild heat shock	71
5.3	Heat shock protein levels in strains deleted in <i>ZUO1</i> or <i>SSB</i>	74
5.4	The intracellular distribution of Ssb during mild heat shock	75
5.5	Discussion of Chapter 5 data	76
5.6	Conclusions of Chapter 5	80
CHAPTER 6. The effect of the ribosome-associated complex on formation of prions beyond [<i>PSI</i>⁺]		81
6.1	Introduction to Chapter 6	81
6.2	Materials and methods for Chapter 6	82
6.2.1	Fluctuation test for formation of prion	82
6.2.2	Heat shock induction of [<i>PRN</i> ⁺] assay	83
6.3	The impact of <i>zuo1Δ</i> on formation of [<i>URE3</i> ⁺]	86
6.4	The effect of <i>ssb1/2Δ</i> on induction of prions by heat shock	89
6.5	Discussion of Chapter 6 data	93
6.6	Conclusions of Chapter 6	95
APPENDIX A. Tables of STRAINS, PLASMIDS, PRIMERS, and Data		98
REFERENCES		106

LIST OF TABLES

Table 1-1 – List of known prions in yeast.	6
Table 3-1 – Percent of cells with Sup35NM aggregates.	51
Table 6-1 – Curability and stability rates of spontaneously formed [<i>URE3</i>].	89
Table 6-2 – Induction of [<i>PSI</i> ⁺] by a prion [<i>PRN</i> ⁺] by mild heat shock in wild-type vs. <i>ssb1/2Δ</i> strains.	92
Table 6-3 – Stability of a prion [<i>PRN</i> ⁺] with [<i>PSI</i> ⁺] inducing effect by mild heat shock in wild-type vs. <i>ssb1/2Δ</i> strains.	92
Table A1 – Strains used in this work.	98
Table A2 – Plasmids used in this work.	100
Table A3 – Primers used in this work.	101
Table A4 – Percent of [<i>psi</i>] (reds and mosaics) for mild heat shock experiments	103
Table A5 – Hsp104-GFP tagged aggregate location data	103
Table A6 – Sup35NM-RFP aggregate location data.	104
Table A7 – Frequencies of [<i>PSI</i> ⁺] in aged, unaged, or average age cells.	104
Table A8 – Frequency of [<i>URE3</i>] spontaneous formation for wild-type vs. <i>zuo1Δ</i> .	105
Table A9 – Rates of [<i>URE3</i>] spontaneous formation for wild-type vs. <i>zuo1Δ</i> .	105

LIST OF FIGURES

Figure 1-1 – System of [<i>PSI</i> ⁺] detection.	7
Figure 1-2 – System for [<i>URE3</i>] detection.	9
Figure 1-3 – Role of the [<i>LSB</i> ⁺] prion as an inducer of [<i>PSI</i> ⁺].	11
Figure 1-4 – Control of formation, propagation, and loss of [<i>PSI</i> ⁺] by cellular factors.	12
Figure 1-5 – Destabilization of [<i>PSI</i> ⁺] by mild heat shock.	16
Figure 1-6 – Asymmetric segregation in yeast.	18
Figure 1-7 – The role of the RAC and Ssb in [<i>PSI</i> ⁺] formation and propagation.	21
Figure 2-1 – Pringle method of gene deletion.	28
Figure 2-2 – Method to copy deletion into our strain background.	29
Figure 2-3 – Procedure to make Hsp104-GFP in our strain background.	31
Figure 2-4 – Procedure for testing destabilization of weak [<i>PSI</i> ⁺] by heat shock.	35
Figure 3-1 – Effects of <i>SIR2</i> deletion on [<i>PSI</i> ⁺] destabilization by heat shock.	42
Figure 3-2 – Heat shock protein levels and changes to [<i>PSI</i> ⁺] aggregates in a heat-shocked <i>sir2Δ</i> strain.	43
Figure 3-3 – Curing by Hsp104 overexpression in a <i>sir2Δ</i> strain.	44
Figure 3-4 – Effect of <i>sir2Δ</i> on curing by mild heat shock in a <i>lsb2Δ</i> background.	46
Figure 3-5 – Effects of nicotinamide addition during heat shock vs <i>sir2Δ</i> .	47
Figure 3-6 – Effects of <i>sir2Δ</i> on recovery from aggregate formation after heat shock.	49
Figure 3-7 – Localization of Sup35NM and Hsp104 after mild heat shock.	50
Figure 3-8 – Proportion of mother-daughter pairs with different aggregate distributions.	52
Figure 3-9 – Changes to morphology in <i>sir2Δ</i> strain.	53
Figure 3-10 – Proposed model for <i>sir2Δ</i> impairment of asymmetric segregation.	57

Figure 4-1 – Enrichment of aged cells in a yeast population by biotin tagging.	61
Figure 4-2 – Average age vs. old wild-type and <i>sir2</i> Δ cells with Hsp104-marked aggregates.	64
Figure 4-3 – Frequency of spontaneous [<i>PSI</i> ⁺] formation during replicative aging in wild-type and <i>sir2</i> Δ strains.	66
Figure 5-1 – Effect of <i>ssb1/2</i> Δ on [<i>PSI</i> ⁺] destabilization during mild heat shock.	72
Figure 5-2 – Effect of addition of <i>SSB2</i> plasmid on [<i>PSI</i> ⁺] destabilization during mild heat shock.	73
Figure 5-3 – Effect of <i>zuo1</i> Δ or <i>ssz1</i> Δ on [<i>PSI</i> ⁺] destabilization during mild heat shock.	74
Figure 5-4 – Hsp levels in <i>ssb1/2</i> Δ or <i>zuo1</i> Δ strains during mild heat shock.	75
Figure 5-5 – Effect of mild heat shock on Ssb localization.	76
Figure 5-6 – The role of Ssb in heat-shock mediated destabilization of [<i>PSI</i> ⁺].	79
Figure 6-1 – Fluctuation test for spontaneous [<i>URE3</i>] formation.	83
Figure 6-2 – Procedure for heat shock induction of a prion [<i>PRN</i> ⁺].	85
Figure 6-3 – Induction of the prion [<i>URE3</i>] in wild-type and <i>zuo1</i> Δ strains.	87
Figure 6-4 – Effect of <i>zuo1</i> Δ on spontaneous formation of the prion [<i>URE3</i>].	88
Figure 6-5. Presence of another prion induces [<i>PSI</i> ⁺] formation.	90
Figure 6-6 – Effect of <i>ssb1/2</i> Δ on induction of a prion [<i>PRN</i> ⁺] with [<i>PSI</i> ⁺] inducing effect by mild heat shock.	91
Figure 6-7 – Curability of [<i>PSI</i> ⁺] colonies induced by a prion [<i>PRN</i> ⁺].	93

LIST OF SYMBOLS AND ABBREVIATIONS

AD	Alzheimer's Disease
PrP	Prion protein
DNA	DeoxyriboNucleic Acid
PCR	Polymerase Chain Reaction
WT	Wild-type
SD	Standard Deviation
CI	Confidence Interval
μ L	microliter
mL	milliter
ADE	adenine
YPD	yeast extract peptone dextrose media
PBS	phosphate buffered saline
P_{GAL}	galactose promoter
RAC	ribosome associated complex

SUMMARY

Self-perpetuating transmissible protein aggregates—prions—are implicated in mammalian diseases and control phenotypic traits in *Saccharomyces cerevisiae*. Yeast heat shock-induced chaperone proteins counteracting stress-induced cytotoxic aggregation also control prion propagation. Heat-damaged proteins that are not disaggregated by chaperones are cleared from daughter cells via asymmetric segregation in cell divisions following heat shock. Heat shock mediated destabilization of $[PSI^+]$, a prion isoform of the yeast translation termination factor Sup35, was previously shown to coincide with the imbalance between the Hsp104 and Hsp70-Ssa chaperones. Here we show that deletion of the *SIR2* gene, required for asymmetric segregation, counteracts $[PSI^+]$ destabilization by heat shock, and Sup35 aggregates are co-localized with aggregates of heat-damaged proteins marked by Hsp104-GFP. These results support the role of asymmetric segregation in prion destabilization. We then investigate the effects of aging on protein aggregation and prion formation and demonstrate that, like other stresses, aging increases aggregation and prion formation. While protein aggregation is increased in cells deficient in asymmetric segregation, prion formation is reduced, implying a role of the cellular asymmetric apparatus in prion formation. We show that depletion of the heat shock non-inducible ribosome-associated chaperone Hsp70-Ssb decreases destabilization of $[PSI^+]$ by heat shock, while disruption of a co-chaperone complex mediating the binding of Ssb to the ribosome increases loss. Ssb is shown to relocate from the ribosome to the cytosol during heat shock and, as Ssb has been shown to antagonize the function of Ssa in prion propagation, these data support the role of the chaperone imbalance in prion destabilization and denote a stress-related role in localization of Ssb. Lastly, we demonstrate that disruption of the Ssb chaperone or the ribosome-associated complex increases formation of prions beyond $[PSI^+]$.

CHAPTER 1. BACKGROUND OF PROTEIN QUALITY CONTROL AND STRESS

Yeast prions both serve as a model for human disease and represent an environmentally alterable phenotype, expanding the potential for heritable diversity and quick environmental adaptation in yeast. Yeast prion formation, propagation, and curing are controlled by a variety of chaperone proteins, most prominently Hsp104, which is required for propagation of all known yeast prions. Hsp104 works together with chaperones Hsp70 and Hsp40 to disaggregate aggregated proteins in yeast, but this system also has the effect of propagating prions by shearing the prion fibers, which are then able to recruit additional monomer. Changes in the balance of these chaperones by overexpression or acute stress such as heat shock may cause the yeast cell to lose the prion, however stresses such as heat or aging are also known to induce prion formation.

Yeast cells practice asymmetric segregation, a Sir2-dependent process by which aggregated and damaged proteins are maintained in the mother cell during budding. Loss of the prion $[PSI^+]$ due to heat stress is known to occur predominantly in the daughter cells, implicating asymmetric segregation in prion loss during this process, but it is currently unknown if prions are segregated asymmetrically with damaged proteins. The ribosome associated complex (RAC) and the associated Hsp70 chaperone Ssb, which work together to ensure proper folding of nascent polypeptides off of the ribosome, have also been shown to prevent formation of the prion $[PSI^+]$. The RAC-Ssb system was recently found to promote $[PSI^+]$ curing during Hsp104 overexpression in the case of RAC deficiency, which causes Ssb to be released to the cytosol. However, it is currently unknown whether the ribosome associated complex and Ssb work to prevent formation of prions generally or if Ssb is able to play a role in $[PSI^+]$ destabilization during heat stress.

1.1 Prions and amyloids

Prions (proteinaceous infectious particles) are self-perpetuating, alternately folded proteins that cause disease in mammals and are communicable in transmission (Prusiner, 1998). Prion proteins contain no change in DNA or amino acid sequence from their normal protein counterparts, rather the difference is a matter of conformation that causes proteins folded typically to alter conformation and, frequently, become incorporated into ordered fibril aggregates. Amyloids, similarly, are proteins that aggregate into insoluble disease-specific aggregates, forming deposits known as plaques, neurofibrillary tangles, or Lewy bodies. Discoverer Stanley Prusiner argued that the differentiating feature between the two is that prions can undergo self-propagation as oligomers and do not need to polymerize into amyloid fibrils; “the self-propagation of an alternative conformational state” is the distinguishing feature for a prion (Prusiner, 2012). However, the major difference is usually considered to be transmissibility (Kushnirov *et al.* 2007)—prions are regarded as a transmissible subclass of amyloids—but this distinction is unclear as some amyloids may be transmissible under extreme conditions such as direct inoculation with brain homogenate (Ridley *et al.* 2006). Prion and amyloid proteins both tend to have characteristic unstructured glutamine/asparagine (Q/N)-rich domains, as well as high β -sheet content in the fibril form, features that are important for achieving the differential conformations responsible for the prion phenotype (Uptain and Lindquist 2002; Chiti and Dobson 2006).

While prions and amyloids are most commonly associated with protein misfolding diseases, functional amyloids have also been found to have biological roles in memory formation (Si *et al.* 2003; Majumdar *et al.* 2012), hormone storage (Maji *et al.* 2009), and biofilm formation (Blanco *et al.* 2012), demonstrating that although amyloids are known for causing disease, their actual functions in the biological world are incredibly diverse

and important. In addition, recent work incorporating them into a variety of biomaterials (Li *et al.* 2018) portends great potential for amyloids in biotechnology.

1.2 Prion and amyloid diseases

Possibly the most infamous of the prion diseases is Creutzfeldt-Jakob Disease (CJD), commonly known as mad cow disease, which is transmitted to humans from cows suffering from bovine spongiform encephalopathy via consumption of infected beef. This disease caused an epidemic first in cows then in humans beginning in 1986 in the United Kingdom (Trevitt and Singh 2003) that terrified consumers and raised public consciousness regarding the deadly potential of prion diseases. Other prion diseases include kuru, which is transmitted between humans via ritualistic cannibalism, scrapie in sheep, and chronic wasting disease (CWD) in mule deer and elk. In all of these diseases, a modified version of the mammalian prion protein, PrP^{Sc}, causes the unmodified cellular prion protein, PrP^C, to be refolded into the fibril, β -sheet-rich prion confirmation, resulting in neurodegenerative disease and, ultimately, death (Prusiner 1998).

While the prion diseases are much more infamous and inspire public fear because of their persistent nature and ease of transmission, the amyloid-based protein misfolding diseases are much more common sources of morbidity and mortality in humans. Alzheimer's Disease (AD), now estimated to be the 3rd leading cause of death in the United States (James *et al.* 2014), is a progressive neurodegenerative disease associated with deposition of amyloid-beta (A β) plaques in the brain. Experiments have demonstrated accumulating evidence for A β as the disease agent of AD: human brain homogenates from Alzheimer's patients, when injected intracerebrally into marmosets, caused development of A β plaques in the brains of those marmosets; this was the first

demonstration that AD could be transmissible (Ridley *et al.* 2006). Furthermore, even synthetic A β peptides have demonstrated capability as disease agents (Stöhr *et al.* 2012). Many other neurodegenerative diseases are associated with misfolded proteins including Parkinson's (α -synuclein) and Amyotrophic Lateral Sclerosis (superoxide dismutase 1), but it is increasingly the case that non-neuropathic diseases are associated with amyloidogenic proteins, for example, type II diabetes is associated with amylin (Chiti and Dobson 2006), medullary thyroid cancer is associated with calcitonin (Chiti and Dobson 2006), and recently even heart disease has been found to be associated with apolipoprotein AI (Audet *et al.* 2012). Given the high incidence of some of these diseases in the population—heart disease is the primary killer of Americans (Heron 2012; Ma *et al.* 2015), diabetes incidence is on the rise correlating with the rise in obesity in the United States and is expected to increase from 14% of the US population in 2010 to between 21 and 33% of the US population by 2050 (Boyle *et al.* 2010), and Alzheimer's is predicted to increase from 4.5 million affected American adults in the year 2000 to 13.2 million in the year 2050 based on the rapid growth of older age groups due to aging and increased survival (Hebert *et al.* 2003)—understanding amyloid disease becomes critical to reducing human morbidity and mortality.

1.3 Yeast prions

The budding yeast *Saccharomyces cerevisiae* is useful in studying Alzheimer's and other protein misfolding diseases, as yeast possess endogenous transmissible amyloids (yeast prions) that produce phenotypically detectable traits and serve as a model for human amyloid disease (Miller-Fleming *et al.* 2008; Tenreiro *et al.* 2010; Liebman and Chernoff 2012). Most yeast prions identified so far possess intrinsically disordered regions that are Q/N rich and are necessary for the self-propagating and aggregation properties of these proteins. Like all known mammalian prion proteins, yeast prions are

also based on highly ordered cross β -sheet polymers (Taneja *et al.* 2007; Liebman and Chernoff 2012). *De novo* formation of prions in yeast occurs when there is a high local concentration of a prion forming protein, which may occur by overexpression or by localization of the prion protein due to cellular factors (Chernova *et al.* 2014). The frequency of this initial induction is increased dramatically when other prions are already present in the cell, and some prions such as $[PSI^+]$ are very rarely or never induced without a secondary prion, such as $[PIN^+]$ to cause initial nucleation, though the secondary prion may not be required for continued propagation (Derkatch *et al.* 2000; Lancaster *et al.* 2010).

In yeast, prions are observed as non-Mendelian heritable genetic elements that may sometimes cause pathogenic effects, but are also proposed to play an important role in yeast biology (Shorter and Lindquist 2005; Inge-Vechtomov *et al.* 2007) allowing for the additional production of alternate phenotypes. Table 1.1 shows a list of known prions in yeast and the altered phenotypes resulting from prion formation. In the lab, these alternate phenotypes allow for the use of yeast prions as models for prion curing, spread, or maintenance in cells, as cells carrying the prion may be easily differentiated from those that do not. In nature, this phenotypic diversity expands the adaptive potential of yeast in various environments by permitting faster phenotypic change in unstable environments (Chernova *et al.* 2014), including selective flocculation (Holmes *et al.* 2013) and resistance to antifungal compounds (Suzuki *et al.* 2012).

While some prions in yeast may represent disease elements (Nakayashiki *et al.* 2005), yeast prions most often impart altered genetic traits by affecting cellular transcriptional or translational regulation and even may provide advantageous characteristics that allow the cell to adapt to environmental stress (Suzuki *et al.* 2012;

Chernova *et al.* 2014). Yeast prions, in this respect, differ from most recognized prions in mammalian cells.

Table 1-1. List of known prions in yeast

Protein	Prion	Protein function	Prion phenotype
Ure2	[<i>URE3</i>]	Regulatory protein in nitrogen metabolism	Use of poor nitrogen source
Sup35	[<i>PSI</i> ⁺]	Translation termination factor	Increases nonsense suppression
Rnq1	[<i>PIN</i> ⁺]/[<i>RNQ</i> ⁺]	Unknown	Increases <i>de novo</i> formation of other prions
Swi1	[<i>SWI</i> ⁺]	Subunit of chromatin remodeling complex	Altered carbon source utilization
Cyc8	[<i>OCT</i> ⁺]	Transcriptional co-repressor	Altered carbon source utilization, flocculation
Mot3	[<i>MOT</i> ⁺]	Transcriptional co-repressor	Change in cell wall composition
Mod5	[<i>MOD</i> ⁺]	tRNA modification enzyme	Increased level of ergosterol and resistance to antifungals
Nup100	[<i>NUP100</i> ⁺]	FG-nucleoporin	Increases the rate of nuclear import
Lsb2	[<i>LSB</i> ⁺]	Binds and inhibits Las17, actin associated	Increases <i>de novo</i> formation of other prions ([<i>PSI</i> ⁺])

1.3.1 [*PSI*⁺]

The yeast prion [*PSI*⁺] is an amyloid form of the translation termination factor Sup35 (Wickner 1994). In normal conformation (the [*psi*⁻] cell), Sup35 encodes release factor 3 (eRF3) which functions with eRF1 to recognize stop codons and release

polypeptide chains at the ribosome (Liebman and Derkatch 1999), shown in Figure 1-1.

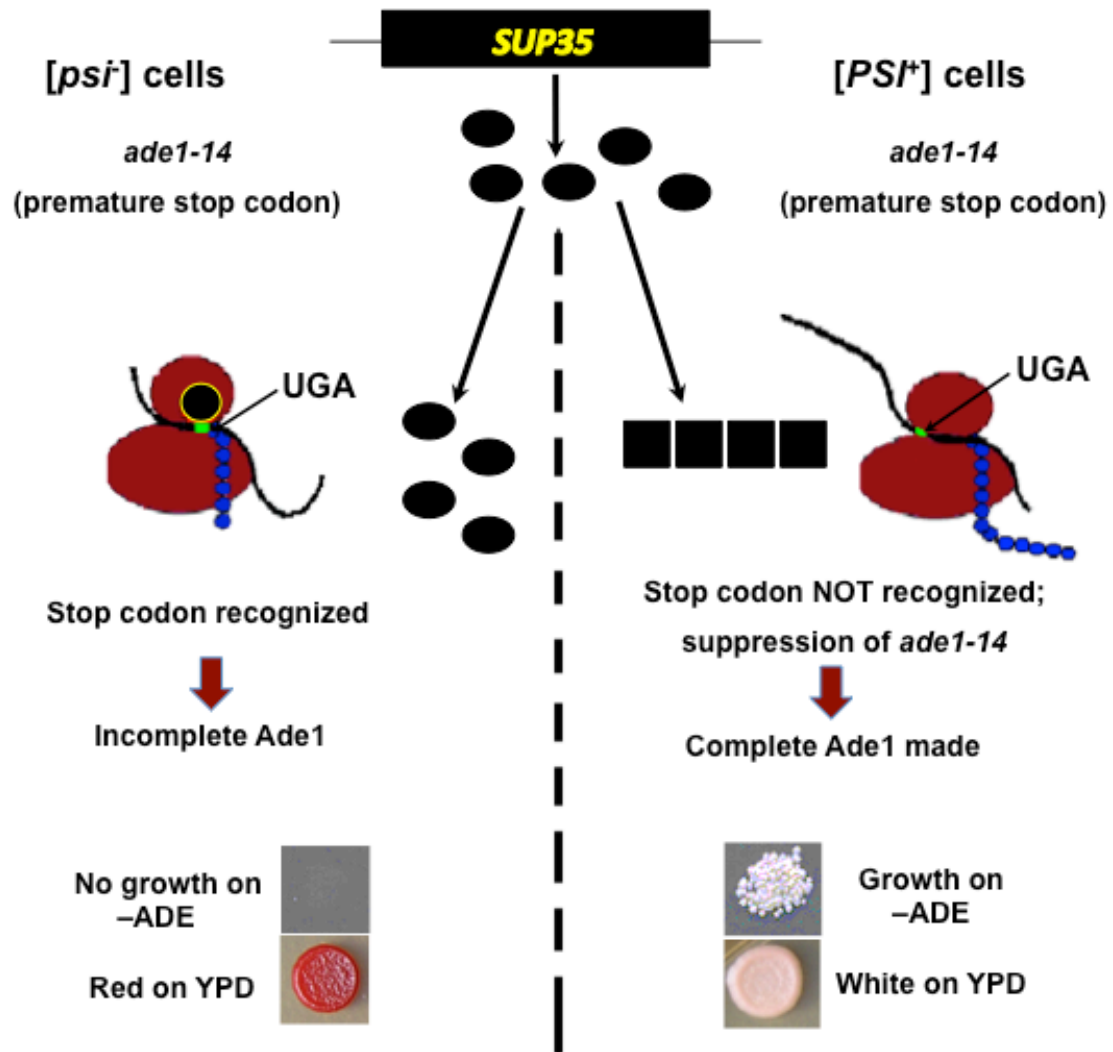


Figure 1-1. System of $[PSI^+]$ detection. $[PSI^+]$ is the aggregated form of the translation termination factor, Sup35. The strain used for detection has premature stop codon in the adenine biosynthesis gene, *ade1-14*. When Sup35 is in the normally monomeric state, it causes reading of the premature stop codon, and adenine is not produced, causing lack of growth on $-ADE$ media and a red color on YPD. When Sup35 is in the aggregated $[PSI^+]$ state, it does not function normally, the stop codon in *ade1-14* is not recognized, and complete Ade1 protein is made allowing growth on $-ADE$ media and causing a pink or white color for growth on YPD.

In $[PSI^+]$ cells, Sup35 is folded into an alternate amyloid form, causing Sup35 to be less efficient in termination and resulting in reduced nonsense suppression in the cell.

The subsequent increase in nonsense codon read-through due to presence of $[PSI^+]$ may then be detected in strains bearing premature stop codons in necessary amino acid biosynthesis genes; specifically strains bearing a premature UGA nonsense mutation in the adenine biosynthesis gene, *ade1-14* are currently used (Kushnirov *et al.* 2007). In these strains, correct translation termination in the $[psi^-]$ cell causes incomplete synthesis of Ade1, causing cells to lack the ability to grow on media lacking adenine (-ADE media), and also causing growth on YPD to be red in color due to build-up of unused products in the adenine biosynthesis pathway. However, if the amyloid form is inherited from the mother cell, or if Sup35 becomes misfolded into the prion form ($[PSI^+]$), the resulting inefficient translational termination causes read-through resulting in production of Ade1. This provides the cell with the ability to grow on -ADE media and causes growth on YPD to be shades of pink or white in color (Tuite and Cox 2007). Changes in the conformation of Sup35 fibrils causes variants of $[PSI^+]$ to arise which are weak (darker pink, less growth on -ADE), strong (whitish or light pink and strong growth on -ADE) or intermediate (somewhere between the two) due to changes in how that particular prion isoform is propagated.

1.3.2 $[URE3]$

The first yeast protein asserted to be a prion was Ure2 (Wickner 1994). Like $[PSI^+]$, $[URE3]$ causes a loss-of-function phenotype as the prion form prevents the protein Ure2 from being active. Ure2 is a transcriptional repressor for genes involved in nitrogen metabolism like *GLN3* and *GAT1* and serves as a regulator of nitrogen catabolism that prevents uptake of allantoate in the presence of other nitrogen sources. As ureidosuccinate (USA), an intermediate in uracil biosynthesis, closely resembles allantoate, the normal form of Ure2 also prevents uptake of USA, causing cells with a *ura2* mutant gene to be unable to grow on -URA media even when USA is added. In

[*URE3*] cells, when Ure2 activity is faulty, *DAL5* which is activated by Gln3, is turned on, allowing cells to take up USA and grow on media lacking uracil (Wickner 1994; Hong *et al.* 2011; Liebman and Chernoff 2012), thus growth on USA media serves as an indicator of [*URE3*]. As this detection method works only in *ura2* strains and requires replica plating to detect [*ura0*], a new reporter assay was developed for the [*URE3*] prion (Hong *et al.* 2011) using the same *ade1-14* background and colorimetric/growth assay that is used in detection of [*PSI⁺*], shown in Figure 1-2.

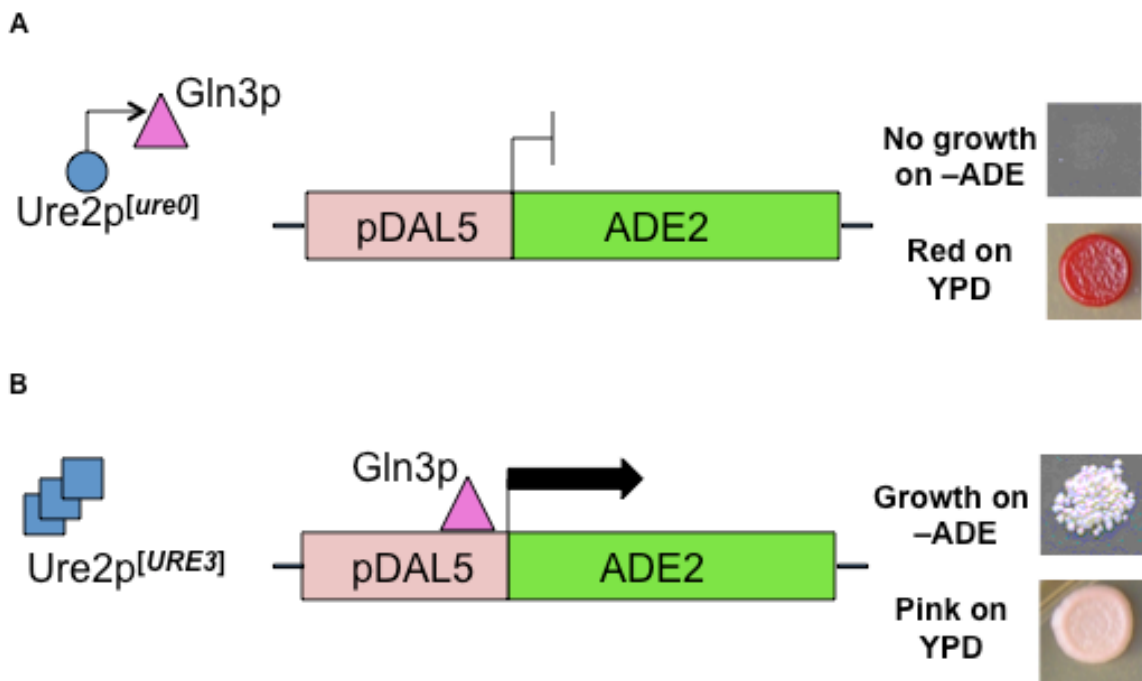


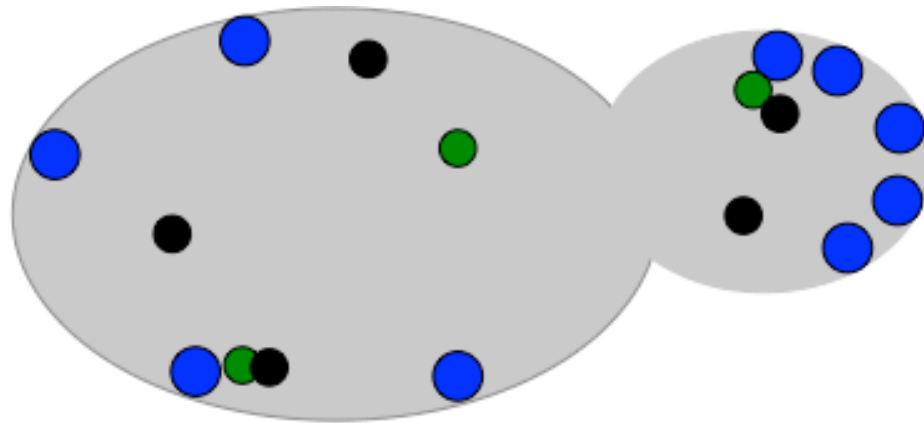
Figure 1-2. System for [*URE3*] detection. [*URE3*] works at the transcription level. A) Ure2 in normal [*ure0*] state. Ure2 antagonizes Gln3, and prevents transcription of *ADE2*. Colonies are red on YPD due to the lack of Ade2p, and cannot grow on $-ADE$. B) In [*URE3*] cells, aggregated Ure2 does not antagonize Gln3, Gln3 activates the *DAL5* promoter and turns on transcription of *ADE2*, causing adenine to be produced. Colonies are white or pink on YPD and grow on $-ADE$.

In this new strain, used in our work, the *ADE2* gene is placed under the *DAL5* promoter. In [*ure0*] cells, the normal Ure2 antagonizes Gln3, and prevents transcription of *ADE2*. In

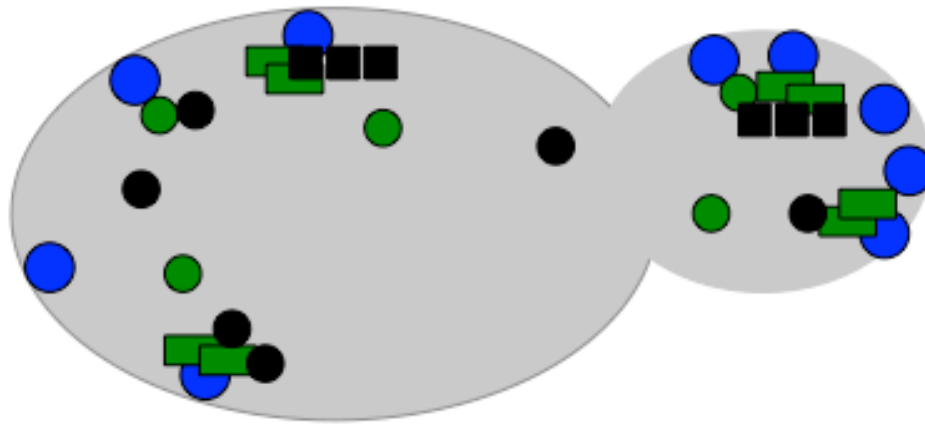
[*URE3*] cells, aggregated Ure2 does not antagonize Gln3, Gln3 activates the *DAL5* promoter and turns on transcription of *ADE2*, causing adenine to be produced. The result is a phenotype identical to that of the [*PSI*⁺] reporter assay, wherein absence of the prion causes growth on YPD to be red and prevents the cell from growing on media lacking adenine. Presence of the prion is indicated by white or pink color on YPD and the ability to grow on –ADE media.

1.3.3 [*LSB*⁺]

One of the most recent yeast prions to be described (Chernova *et al.* 2017), [*LSB*⁺] is a prion form of the short-lived actin-associated protein Las17-binding protein 2, also sometimes termed Pin3 due to its suspected role in prion induction (Madania *et al.* 1999). When Lsb2 is overproduced, it promotes overproduced Sup35 to the [*PSI*⁺] form (Chernova *et al.* 2011). Lsb2 levels are increased in the cell during thermal stress, localize to actin patches, and act as a promoter of [*PSI*⁺], possibly by creating high local concentrations of both Lsb2 and Sup35 (Chernova *et al.* 2011). Although Lsb2 itself is ubiquitinated and quickly degraded, this role in promoting the prion form in thermal stress has caused it to be deemed a “stress-dependent prion modifier” (Chernova *et al.* 2014) or a “memory of cellular stress” (Chernova *et al.* 2017). Aside from biochemical assays to detect aggregated Lsb2, the major method of detection of [*LSB*⁺] is through its induction of [*PSI*⁺]. In a background without other secondary prions such as [*PIN*⁺], induction of [*PSI*⁺] is essentially non-existent, even with overproduction of Sup35. However, during heat shock (thermal stress), Lsb2 is induced and forms a prion, which then causes increased induction of [*PSI*⁺] when Sup35 is overproduced, shown in Figure 1-3. This effect is dependent on Lsb2, as *lsb2Δ* strains do not induce [*PSI*⁺] when Sup35 is overproduced post-heat shock (Chernova *et al.* 2017).



Normal environmental conditions
Lsb2 expressed at low levels



Environmental stress
Lsb2 expression increases



Figure 1-3. Role of the $[LSB^+]$ prion as an inducer of $[PSI^+]$. Under normal conditions, Lsb2 is expressed at low levels. Under environmental stress, Lsb2 expression increases and Lsb2 localizes to cortical actin patches along with Sup35. $[LSB^+]$ is formed, and promotes conversion of Sup35 to prion ($[PSI^+]$).

1.4 Chaperone control of prion propagation and curing

Prion formation may be caused by stress, defects in protein folding, or overexpression or high protein concentration, but maintenance of yeast prions in the cell requires a balance of several different heat-shock proteins (Hsps), chaperone proteins that assist in re-folding and sequestering misfolded proteins. This balance is shown in Figure 1-4.

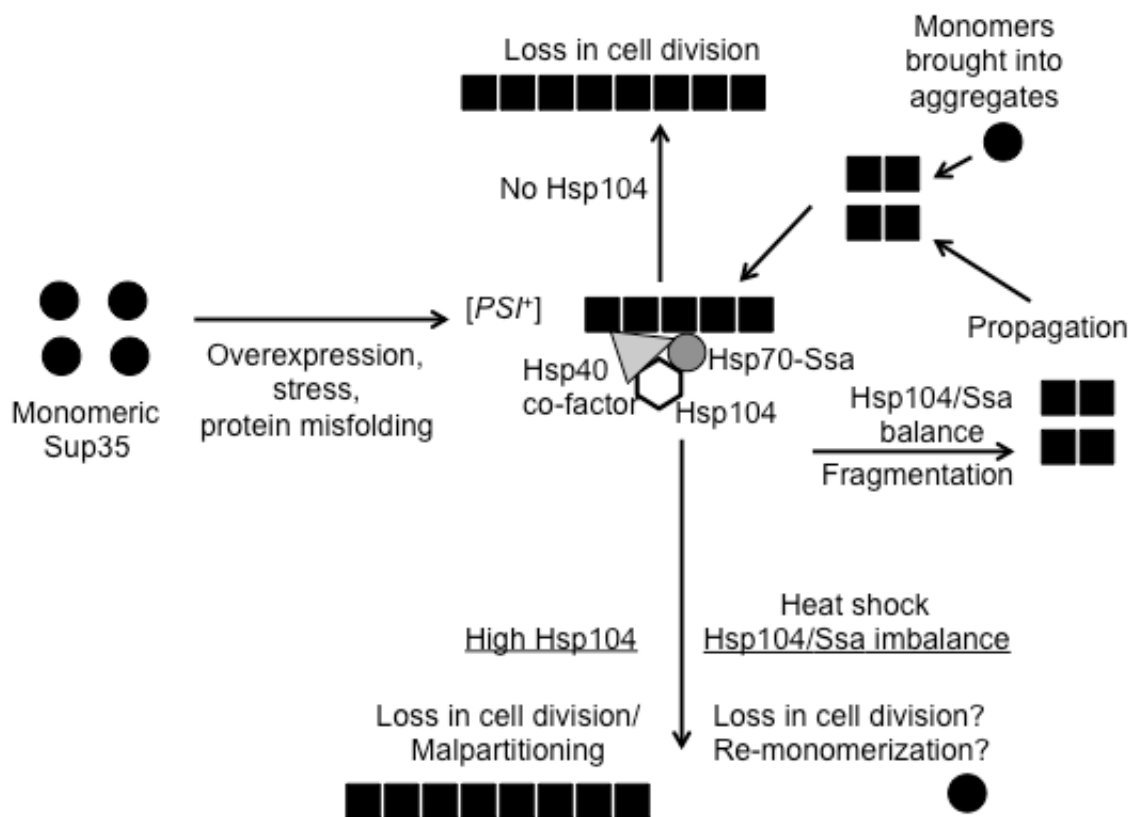


Figure 1-4. Control of formation, propagation, and loss of $[PSI^+]$ by cellular factors. $[PSI^+]$ propagation depends on a balance of Hsp104, Hsp70-Ssa, and Hsp40 co-factors to shear large prion fibers into seeds that can incorporate monomer and propagate the prion. Overexpression of Sup35 or defects in protein folding may cause formation but high levels of Hsp104 relative to Ssa or no Hsp104 causes loss. Heat shock, in which an imbalance in the levels of Hsp104 and Ssa occurs, is hypothesized to cause loss in cell divisions.

In particular, the chaperone protein Hsp104 is required for yeast prion propagation, and inhibition of Hsp104 via passage on guanidine hydrochloride (GuHCl) cures all known yeast prions (Tuite and Cox 2007; Kushnirov *et al.* 2007; Liebman and Chernoff 2012). This is because Hsp104, along with other chaperones, breaks the prion fibers into pieces that allow for replication of the prion; those pieces can then incorporate additional monomer and lengthen and be fragmented again, increasing levels of prion in the cell in order to keep up with prion lost to the daughter cell during cell division (Reidy and Masison 2011; Chernova *et al.* 2014). Aggregated proteins as well as thermally denatured proteins are disaggregated using a primary Hsp70/40 chaperone system that works in conjunction with Hsp104, disaggregating and threading these proteins through the axial channel of the hexameric Hsp104 complex (Glover and Lum 2009) to allow refolding to the native state. In yeasts, this system includes the cytosolic proteins Hsp70 Ssa (encoded by *SSA1-4*) (Verghese *et al.* 2012) and the Hsp40s Ydj1 and Sis1 (Liebman and Chernoff 2012). The current model of disaggregation holds that Hsp70-Ssa is assisted by an Hsp40 to recruit Hsp104 to the aggregated protein. These Hsps then work in concert to extract a monomer from the fiber or aggregate (Reidy and Masison 2011). In the case of a prion, extracting a monomer from the middle of the fiber has the effect of splitting the fiber into two, allowing each fragment to then recruit more monomer and increasing prion numbers in the cell, shown as the fragmentation and propagation portion of Figure 1-4. The Hsp104/Hsp70-Ssa/Hsp40 machinery seems to be generally required for propagation of yeast prions, though different prions may be recognized by different Hsp70/Hsp40, as different Ssa members and different Hsp40s have different effects on the various prions (Moriyama *et al.* 2000; Sharma and Masison 2008; Reidy and Masison 2011; Matveenko *et al.* 2018). Another co-chaperone, Sgt2, was recently included in this system, as it seems to aid accessibility of the Hsp104/70/40 complex to the prion (Kiktev *et al.* 2012).

While Hsp104 is required for propagation of all known prions, Hsp104 overexpression cures at least some of the known prions (Chernoff *et al.* 1995; Suzuki *et al.* 2012; Matveenko *et al.* 2018); this curing is best characterized for [PSI⁺]. The reason for this duality of Hsp104 seems to be that Hsp104 propagation of prions is associated with the M-domain of Hsp104 (Dulle *et al.* 2014) and involves Hsp70/40, while curing of prion by overexpression requires the N-terminal domain (Hung and Masison 2006) and seems to work by another mechanism, possibly via trimming the ends of prion fibers (Park *et al.* 2012) and re-monomerizing (Park *et al.* 2014), or by malpartitioning/asymmetric segregation (Ness *et al.* 2017), and requires a relative deficit of Ssa, with evidence indicating that Hsp104 binds the prion fiber without Ssa and so is unable to fragment the fiber (Chernova *et al.* 2014). This inability to create new prion “seeds” results in loss of the prion during cell division (Ness *et al.* 2017), also shown in Figure 1-3. Re-monomerization of prion fibers by Hsp104 overexpression has been argued (Klaips *et al.* 2014; Park *et al.* 2014), but recent evidence points to malpartitioning of prion between mother and daughter cell (Ness *et al.* 2017), though this mechanism is still under debate.

1.5 The effects of stress on yeast prions

Like all other studied eukaryotes, yeast have a cellular response to stress known as the heat shock response, which is a major protective component against proteotoxic stress in a wide variety of organisms, and with which problems are linked to aging and disease (Feder and Hofmann 1999; Anckar and Sistonen 2011). Interestingly, this response is activated in humans during exercise (Smith *et al.* 2014; Lancaster *et al.* 2004; Sadowska-Krępa *et al.* 2006) and declines during aging (Kayani *et al.* 2008), thus understanding of the heat shock response in model organisms may provide insight into human disease process, prevention, and treatment. The heat shock response is

provoked to some extent in yeast by metabolic stress, such as growth on minimal media, and also by thermal stress, and serves as a means of control between yeast and their environment. The yeast prion $[PSI^+]$ is resistant to prolonged growth at high temperature when Hsp levels are proportionally increased, however it is destabilized by short-term heat shock followed by a return to normal growth temperature (Tuite *et al.* 1981, Newnam *et al.* 2011, Klaips *et al.* 2014) as shown in Figure 1-5.

Hsp104 and Ssa are both induced by heat shock, however Hsp104 levels rise faster in the yeast cell, and prion destabilization coincides with the period of maximal imbalance between Hsp104 and Hsp70-Ssa (Newnam *et al.* 2011). Prion loss is promoted in the absence of some cytoskeleton-associated proteins (Chernova *et al.* 2011; Ali *et al.* 2014), occurs primarily in cell divisions following heat shock, and is asymmetric, which may be explained either by asymmetric segregation of prion aggregates (Newnam *et al.* 2011, Ali *et al.* 2014) or by asymmetric accumulation of Hsp104 and re-monomerization of $[PSI^+]$ (Klaips *et al.* 2014). Recently, the non-heat shock-inducible Hsp70 Ssb, which is normally associated with the ribosome, was found to dissociate from the ribosome during metabolic stress and antagonize Ssa, playing a role in curing of $[PSI^+]$ (Kiktev *et al.* 2015), but whether this plays a role in $[PSI^+]$ curing during mild heat shock has not been investigated.

Stress may also induce formation of some prions. Lsb2, for example, is a protein that is transiently expressed at higher levels during heat stress, forming $[LSB^+]$, which was found to promote $[PSI^+]$ (Chernova *et al.* 2017). *De novo* appearance of $[PSI^+]$ itself is dependent on the yeast heat-shock transcription factor (Park *et al.* 2006), and changes to the stress-induced Hsp104, Hsp70-Ssa, or other chaperones alters formation of $[PSI^+]$ or $[URE3]$ (Liebman and Chernoff 2012).

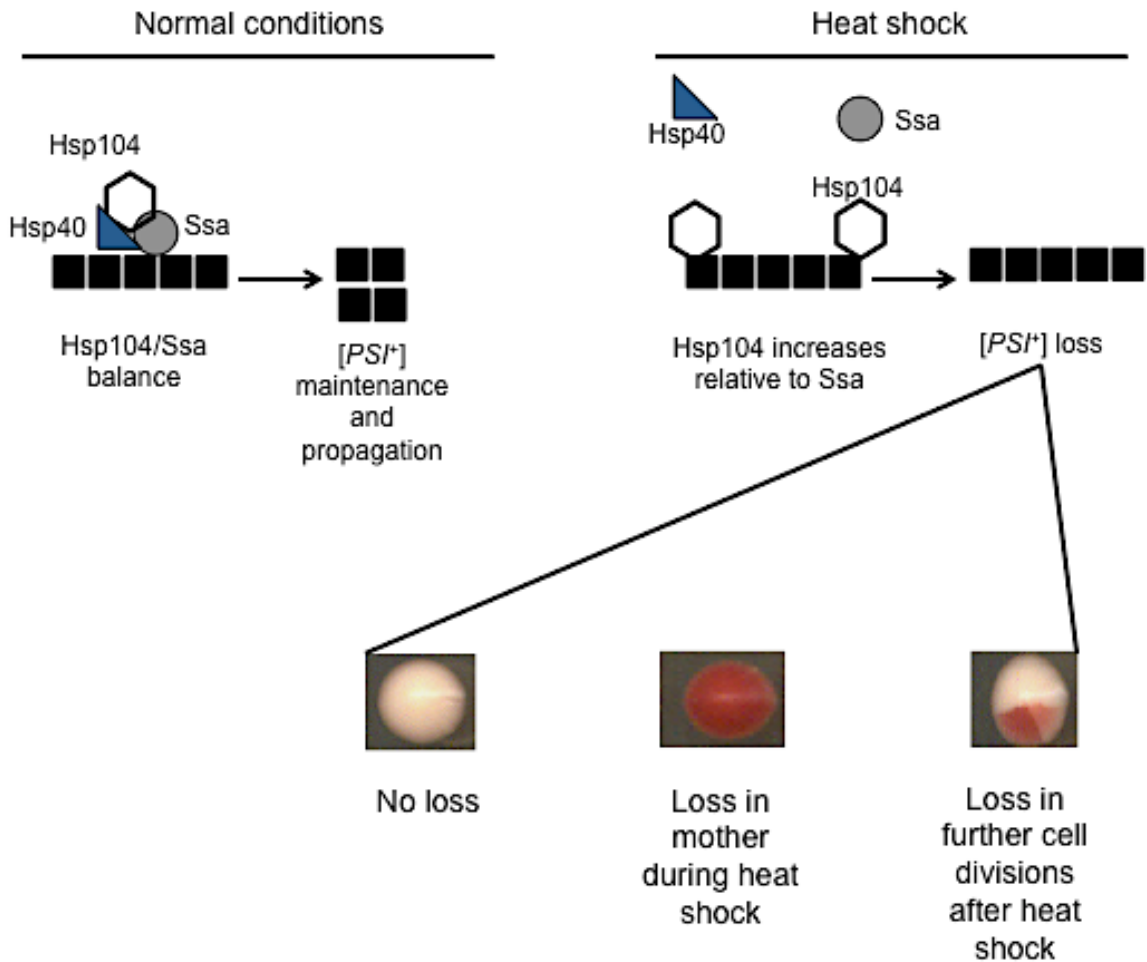


Figure 1-5. Destabilization of $[PSI^+]$ by mild heat shock. During normal growth, Hsp104 and Ssa, along with Hsp40, fragment $[PSI^+]$ which causes it to be propagated and maintained. During mild heat shock, Hsp104 levels rise faster than Ssa levels. The imbalance of Hsp104 and Ssa prevents fragmentation and causes a period of $[PSI^+]$ loss, until Ssa levels increase so that the normal ratios are obtained once more. The resulting colonies are pink (no loss), red (loss of $[PSI^+]$ during heat shock in the mother cell), and mosaics, which indicate that $[PSI^+]$ is lost in later divisions after heat shock. $[PSI^+]$ loss after heat shock is predominantly in daughter cells.

In addition to thermal stress, aging is another factor that may be regarded as a form of stress, and protein misfolding is increased in aged cells (Cohen *et al.* 2012).

Changes to Hsp104 levels and the heat shock response occur with age (Calderwood *et al.* 2009), but studies examining the effect of aging on aggregation and prion formation have been limited.

1.6 Asymmetric segregation of protein aggregates

S. cerevisiae practice asymmetric cell division, a process during which oxidized and other damaged proteins are preferentially retained in the mother cell while the daughter cell receives undamaged proteins (Aguilaniu *et al.* 2003). This process is required for the daughter cell to have full replicative ability and is linked to cellular aging of the mother in yeast, but recently has also been found to play a role in aging in mammalian neuronal stem cells (Moore *et al.* 2015). Possible mechanisms in the process of asymmetric segregation are shown in Figure 1-6 and include (1) retention by passive factors, (2) retention by active factors, and (3) retrograde transport of aggregates by active means. In passive retention, sequestration in the mother cell is mostly due to the formation of the daughter cell off of the bud neck. The small size of the bud neck prevents most damaged proteins from entering the daughter cell in the first place, and any transport back to the mother cell is the result of random movement rather than active transport (Zhou *et al.* 2011), as in Figure 1-6A. Retention may also be active (Zhou *et al.* 2014), requiring tethering protein aggregates to maternal organelles by actin cables (Figure 1-6B). Retrograde transport is a more debated mechanism of asymmetric segregation, wherein a feature called the polarisome forms on the far side of the budding daughter cell and is connected to the mother cell by actin filaments (Figure 1-6C). Aggregated and damaged proteins are moved back from the daughter cell to the mother cell along these filaments (Liu *et al.* 2010).

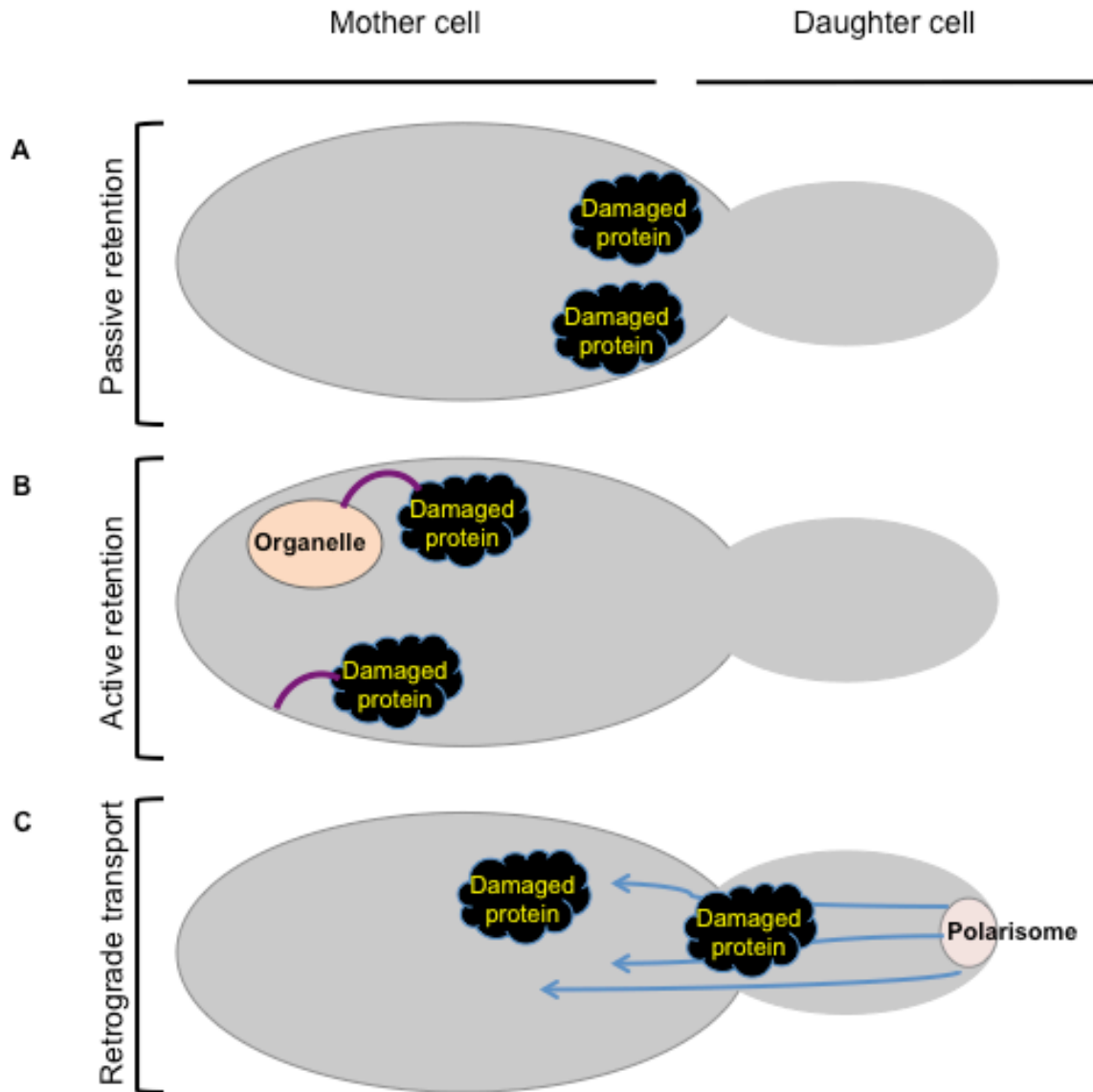


Figure 1-6. Asymmetric segregation in yeast. During cell division, and especially after stress, oxidatively damaged and aggregated proteins are kept in the mother cell. There are three proposed mechanisms for maternal retention of protein aggregates as shown. A) Passive retention: The bud neck acts as a diffusion barrier for aggregates causing segregation in the mother, B) Active retention: Aggregates are tethered to the mother cell or to maternal organelles, preventing aggregates going into the daughter, C) Retrograde transport: Aggregates are moved from the daughter cell back into the mother along actin filaments.

Although the exact method of asymmetric segregation is debated, it is largely agreed that the diffusion effect preventing aggregated proteins entering the daughter cell in the first place plays a role in asymmetric segregation, and all sides seem to agree that actin appears to interact with Hsp104 and that this interaction is vital to maintain asymmetric segregation (Erjavec *et al.* 2007; Zhou *et al.* 2011; Liu *et al.* 2011).

The yeast protein Sirtuin2 (Sir2) is an NAD⁺ dependent deacetylase that targets histones, CCT chaperonin and others, is implicated in aging, and is crucial for asymmetric segregation of oxidatively damaged proteins after cell division (Erjavec *et al.* 2007), with deletion of *SIR2* causing defects in actin folding (Liu *et al.* 2010) and impairment of maternal retention of protein aggregates (Song *et al.* 2014). The effect of Sir2 on actin is presumed to be due to the targeting of the chaperonin CCT, which refolds non-native actin into native actin. Sir2, the cellular actin machinery, and the heat shock protein Hsp104 have all been established as necessary components of asymmetric distribution of carbonylated proteins (Aguilaniu *et al.* 2003; Erjavec *et al.* 2007; Liu *et al.* 2010).

It is currently unknown how prions are segregated or shared between mother and daughter cells and whether or not prions are treated in the same manner as damaged and aggregated proteins after stress, but curing of the yeast prion [*PSI*⁺] was previously found to occur asymmetrically after mild heat shock (Newnam *et al.* 2011), with greatest loss of [*PSI*⁺] in the daughter cells.

1.7 The ribosome associated complex

Many factors in protein production, including ribosomal crowding, protein sequence, and protein structure, can lead to initial misfolding of nascent polypeptides coming off of the ribosome. To counteract this, eukaryotic cells have a ribosome associated complex (RAC), formed from Ssz1 and Zuo1 in yeast, as well as the RAC-associated Hsp70 chaperone Ssb (encoded by *SSB1* and *SSB2*), which aid in folding the nascent polypeptide. These components have been found to be especially important in proper folding of prion proteins in yeast, with deletion of RAC components leading to increased spontaneous and induced formation of $[PSI^+]$ (Amor *et al.* 2015) and deletion of *SSB1/2* causing increased $[PSI^+]$ formation (Chernoff *et al.* 1999) and widespread protein aggregation (Willmund *et al.* 2013). Overexpression of Ssb in conjunction with Hsp104 was previously found to enhance $[PSI^+]$ curing (Chernoff *et al.* 1999), and deletion of both *SSB1* and *SSB2* together was demonstrated to antagonize $[PSI^+]$ destabilization by *HSP104* overexpression (Chernoff *et al.* 1999). Recently, in RAC-disrupted strains, the heat shock non-inducible (Lopez *et al.* 1999) ribosome-associated Ssb was shown to move to the cytosol and increase destabilization of $[PSI^+]$ by *HSP104* overexpression via interference with the cytosolic chaperone Ssa (Kiktev *et al.* 2015), as shown in Figure 1-7. Growth in poor synthetic media was also shown to cause Ssb to move to the cytosol in wild-type cells. Ssb has now been proposed as a possible component of $[PSI^+]$ curing during stress by antagonizing the Hsp104-Ssa-Sup35 interaction (Kiktev *et al.* 2015), but this model is yet to be tested.

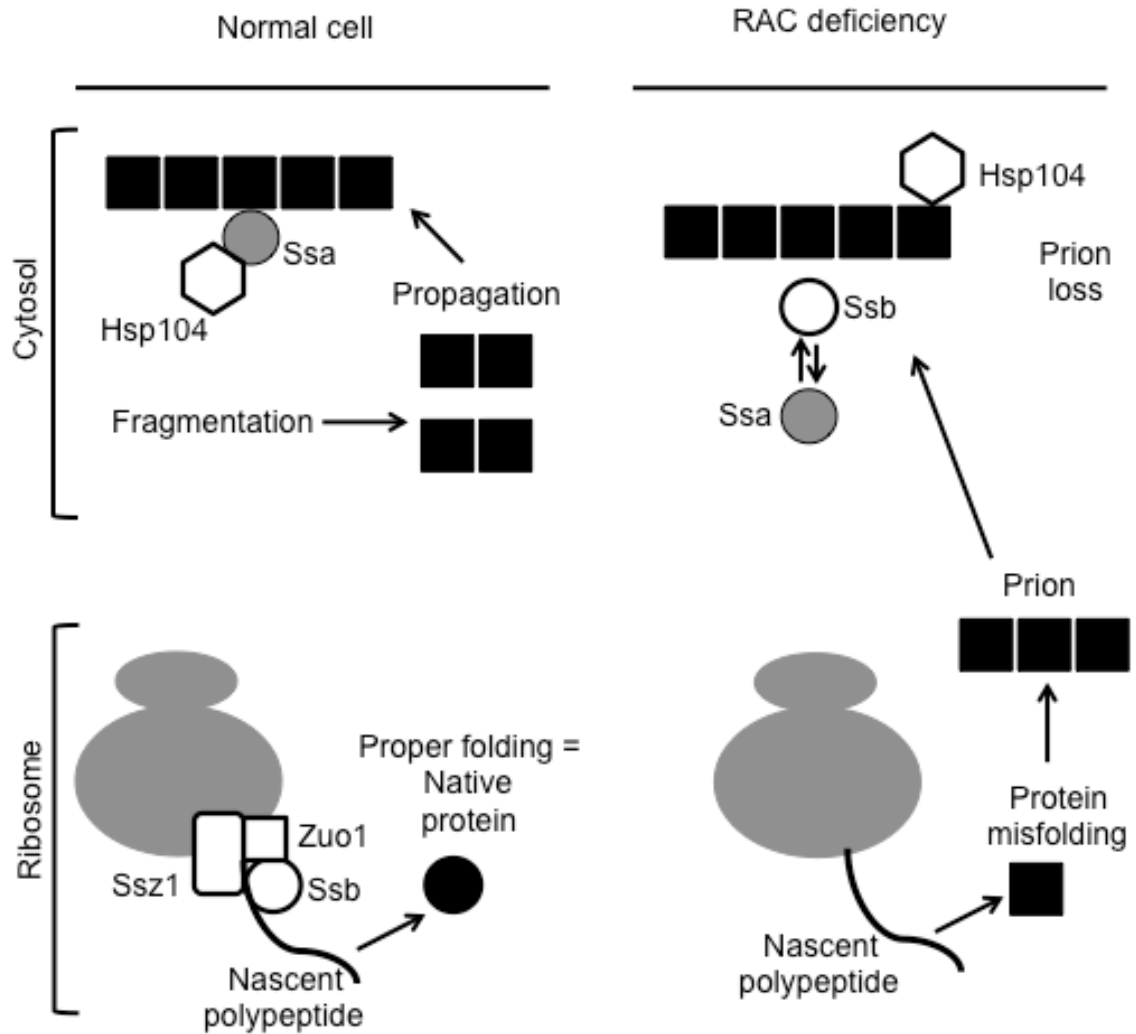


Figure 1-7. The role of the RAC and Ssb in $[PSI^+]$ formation and propagation. Modeled from Kiktev *et al.* 2015. During normal growth, Hsp104 and Ssa fragment $[PSI^+]$ in the cytosol, while Ssb and the RAC (along with others) cause nascent polypeptides to fold correctly into their native structure off the ribosome. When RAC is not present on the ribosome, protein misfolding causes increased formation of $[PSI^+]$. Ssb is released to the cytosol, where it antagonizes Ssa. This prevents fragmentation of the prion and causes subsequent loss in the daughter during cell division.

1.8 Goal of this work

The understanding of prion formation and curing in yeast is potentially helpful to comprehending the pathways of prion and amyloid formation and curing in mammalian cells for purposes of drug development targets; additionally this knowledge is helpful in understanding how yeast may respond to environmental stress by using prions to create quick phenotypic change. The picture of curing during heat shock is currently incomplete, and while the roles of Hsp104 and Ssa are somewhat determined, it is still unknown what role if any Ssb plays in curing by thermal stress and whether curing is due to asymmetric aggregate retention in the mother cell. Because of the demonstrated role in preventing aggregated proteins from being distributed to the daughter cell, we theorized that Sir2 could affect the distribution of prions, possibly playing a role in curing of $[PSI^+]$ in yeast. While some information regarding the role of the RAC in prion formation is known, it remains to be determined whether this information is generalizable to all prions or only a feature of $[PSI^+]$. The goal of this work is a better understanding of the effects of asymmetric segregation by Sir2 and the RAC-released Ssb on heat shock promoted destabilization of $[PSI^+]$, as well as a clearer picture of protein misfolding causing prion formation, including the necessity of the RAC to prevent prion formation and the potential of aging to serve as a prion-inducing stress. Specifically, this work aims to define the role of asymmetric segregation in $[PSI^+]$ destabilization by heat shock, determine whether Ssb plays a role in $[PSI^+]$ destabilization by heat shock, investigate the role of the ribosome associated complex in prion formation, and explore the effects of aging on prion formation. The results implicate the Sir2-dependent apparatus of cell asymmetry in heat shock-dependent prion destabilization, reveal a role for the heat shock non-inducible chaperone Ssb in prion destabilization by stress, support the anti-

prion effect of the ribosome-associated complex in prion formation, and demonstrate an increase in protein aggregation and prion formation with aging.

CHAPTER 2. MATERIALS AND METHODS

2.1 Basic yeast techniques

2.1.1 *Media used and phenotypic screening*

Yeast media and protocols were as described previously (Sherman 2002). Rich organic medium (YPD) contained 1% yeast extract, 2% peptone and 2% dextrose (glucose). Synthetic dropout (SD) media are designated by the supplements that are missing (e.g. -ADE for the synthetic medium lacking adenine) and contained 0.17% yeast nitrogen base without amino acids or ammonium sulfate, 0.5% ammonium sulfate, 2% glucose and 13 nutrition supplements (adenine, arginine, histidine, isoleucine, leucine, lysine, methionine, phenylalanine, threonine, tryptophan, tyrosine, uracil and valine) unless noted for dropout. Yeast were grown at 30°C unless otherwise stated.

In order to examine phenotype for each yeast strain, single colonies from purified cultures were patched to YPD and grown at 30°C overnight. This primary plate was then used to velveteen the same colonies to various types of media in order to examine the metabolic phenotype for each colony. Velveteening was performed by placing a piece of sterile velveteen fabric onto a replicating block, then placing the primary plate over the velveteen face-down in order that the cells from the plate were transferred onto the velveteen. The plate was then removed and the plates for metabolic testing were placed on the velveteen, one at a time and always in the same order, in order to transfer some of the cells to each plate. Each phenotype screening profile began with YPD and ended with YPG in order to verify that viable cells were still available for growth, as all usable colonies should grow on both of these media types.

2.1.2 *Transformation of yeast strains*

Transformation of yeast cells was performed similarly to the previously described method (Gietz *et al.* 1992). Briefly, a pre-culture of the yeast strain was grown overnight in 10mLs of YPD. This pre-culture was used to inoculate a 50mL flask of YPD the following day; this culture was incubated at 30C for 2-4 hours. The culture was transferred to two sterile Oakridge tubes and spun down at 3,000 rpm for 10 min., the supernatant was poured off, the cells were washed with 10mL of Tris-EDTA buffer (TE), then spun down again. The TE was removed, and the cells were re-suspended in 10mLs of 0.1M Lithium acetate Tris-EDTA buffer (LiAc-TE) then incubated at 30C for 30-60 min with shaking. Cells were then centrifuged again, the supernatant was removed, and the cells were re-suspended in 0.5-1.0mL of 0.1M LiAc-TE (depending on number of transformations, 100µL per transformation). For each transformation, 100µL of cells was placed into a microfuge tube along with 10µg of transforming DNA and 20µg of carrier DNA. For each transforming attempt, one transformation had no transforming DNA (negative control). Transformations were incubated for 30 min at 30C, then 700µL of Lithium acetate-Polyethelene glycate-Tris-EDTA buffer (LiAc-PEG-TE) was added to each tube, and tubes were incubated for an additional 60 min at 30°C. Cultures were heat shocked at 42°C for 5 min, then placed at 4°C overnight. The following day, cultures were spun down at 3000 rpm for 2 minutes, the supernatant was removed, and cells were re-suspended in 250µL dH₂O. For each tube, 100 µL was plated onto the appropriate selective media, and plates were incubated 3-4 days to obtain transformative colonies.

2.1.3 *Mating assay*

Pre-cultures of strains to be checked as well as proven *MAT_a* and *MAT_α* strains (mating type check strains) were grown on YPD at 30°C overnight. Growth from the

overnight culture of the strain being checked was used to streak two horizontal lines across a fresh YPD plate. Growth from each of the mating type check strains were then streaked perpendicular to (crossing) the first streak. Plates were incubated at 30°C overnight, then velveted to SD plates selective for diploids based on genotype, which were incubated at 30°C for 2 days and checked for growth every 24 hours. For nicotinamide-added variants of this experiment, NAM was added to the pre-culture growth plates as well as the YPD and SD mating plates.

2.1.4 Yeast DNA purification

For purification of yeast DNA for PCR, overnight pre-cultures of the strains were grown by inoculating 10mLs YPD and incubating overnight at 30°C with 220 rpm shaking. These pre-cultures were centrifuged at 2,000 rpm for 5 min and the cells were re-suspended in 0.5 mL of 1M sorbitol, 0.1M Na EDTA (pH 7.5) and transferred to 1.5 mL microfuge tubes. To each tube, 20µL of 4mg/mL lyticase was added, and cultures were incubated at 37°C for 60-90 min. Cultures were centrifuged at 14,000 rpm for 1 min, the supernatant was discarded, and cells were re-suspended in 0.5mL of 50mM Tris-CL (pH 7.4), 20mM NaEDTA. To each tube, 55µL of 10% SDS was added, cultures were mixed by inversion, then incubated at 65°C for 30 min. To each tube, 0.2 mL of 5M potassium acetate was added, tubes were mixed by inversion, and tubes were placed on ice for 60 min. Tubes were then centrifuged at 14,000 rpm for 5 min, the supernatant was transferred to a fresh tube, and 0.75mL of isopropanol was added to each tube. Tubes were mixed by inversion, centrifuged again for 5 min, supernatant removed and pellet was washed with 70% EtOH then dried briefly. The pellet was re-suspended in 0.4mL of TE, then 22µL of 1mg/mL RNase A was added and cultures were incubated at 37°C for 30min. An equal volume (~420µL) of chloroform:isoamylalcohol (24:1 ratio) was

added to each tube; tubes were mixed well, spun at 14,000 rpm for 1 min, and the aqueous (top) layer was transferred to a fresh microfuge tube. A 1/10 volume (usually about 84 μ L) of 3M sodium acetate was added to each tube, mixed, then DNA was precipitated with 2 volumes (~0.84mL) of 100% EtOH by inversion. Tubes were centrifuged at 14,000 rpm for 15 min to pellet DNA, then DNA was washed three times with 70% EtOH. The supernatant was poured off of each tube, pellets were dried, and pellets were re-suspended in 50 μ L of TE.

2.2 Construction of yeast strains

Deletion strains were derivatives of strain OT55, a weak [*PSI*⁺] strain. Deletions with exception of *zuo1* Δ and *ssb2* Δ were obtained via the Pringle method (Longtine *et al.* 1998) as shown in Figure 2-1. Primers were designed with the gene specific sequence at the 5' end and tags for deletion added at the 3' end. PCR was performed using these primers and the desired Pringle marker plasmid as template. PCR product was transformed via lithium acetate transformation (Gietz *et al.*, 1992), plated to selective media, plates were incubated 3-4 days at 30°C, and transformants were restreaked on selective media to purify colonies. Single colonies were chosen and patched to YPD, then velveted to selective media to determine phenotype. Potentials with desired phenotype (identical to OT55 except growth on selected marker media) were checked via PCR to determine whether the desired gene had been successfully deleted.

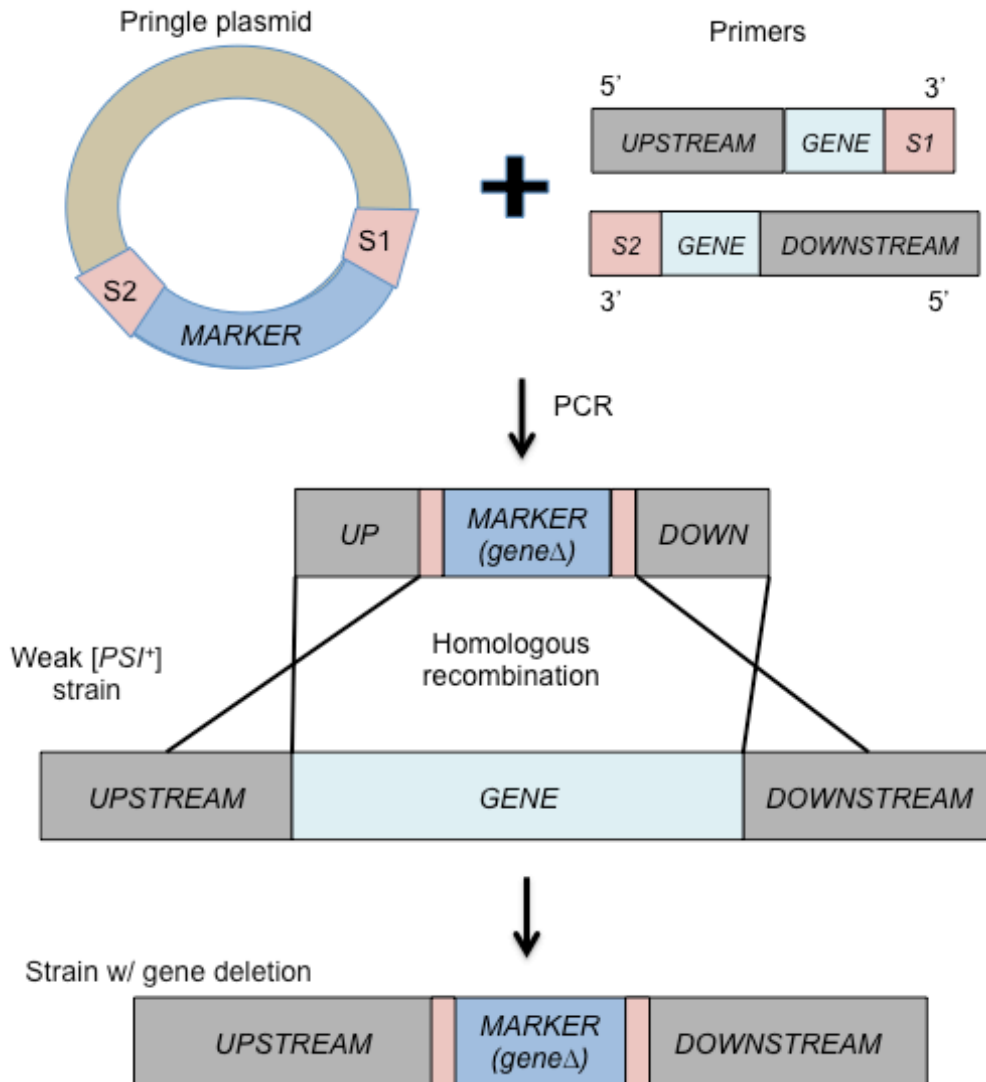


Figure 2-1. Pringle method of gene deletion. Primers are designed to include either just upstream of the gene being deleted through the start codon and a sequence homologous to sequence on the Pringle plasmid. When PCR is run, this creates a fragment with 20bp homology to just upstream/slightly internal to the gene being deleted, the marker from the plasmid, and about 20bp homology to just downstream/end of the gene being deleted. When transformed into the desired strain, homologous recombination causes the gene to be replaced with the marker.

For strains with *zuo1 Δ* or *ssb2 Δ* deletions (including *ssb1/2 Δ*), a different method as shown in Figure 2-2 was used to copy the deletion from a different background and place it in the OT55 background. Briefly, PCR was used to copy a segment of DNA from

slightly upstream of the gene in question to downstream, with approximately 100bp of homology on each side of the gene in question. Fragments were then transformed as described into the desired strain, homologous recombination caused the deleted segment to be incorporated in place of the gene, and resulting strains were checked for phenotype as described and for incorporation of gene deletion by PCR.

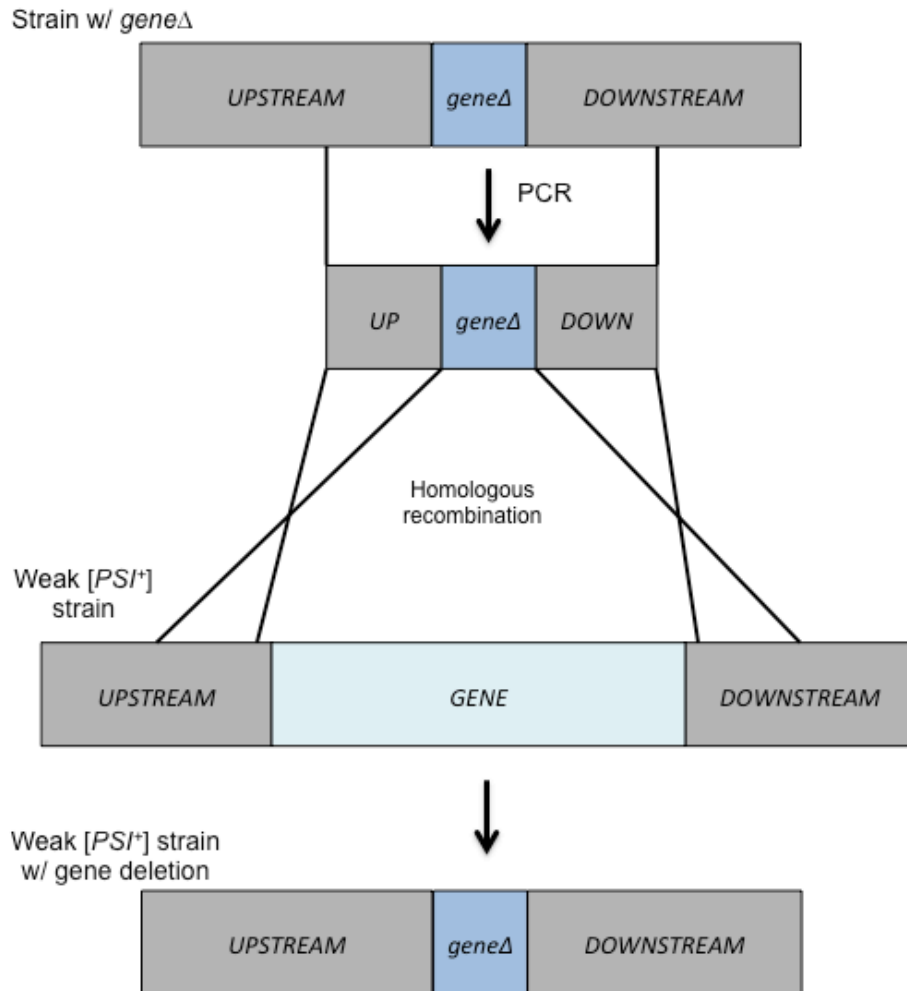


Figure 2-2. Method to copy deletion into our strain background. PCR was used to copy a fragment with the desired deletion from a strain that already contained that deletion. PCR fragment included at least 100 bp of homology to the regions upstream and downstream of the deleted gene. Fragment was transformed into our weak [PSI⁺] strain and recombined via homologous recombination. Transformants were checked for correct phenotype and then checked for integration by PCR.

Strains with GFP on chromosomal *HSP104* were constructed in a similar manner, but with slight differences in the fragment for recombination. As shown in Figure 2-3, the strain with Hsp104-GFP was obtained from the Nystrom lab (Erjavec *et al.* 2007). Primers were designed to amplify a stretch from the end of the *HSP104* gene to several hundred bp into the following gene (*YLLCΔ1*). PCR was performed to amplify a fragment containing the end of HSP104, including the GFP tag, to *YLLCΔ1*. This fragment was then transformed as previously described into our weak [*PSI⁺*] strain and resulting recombinants were checked by PCR for integration as well as by phenotype analysis and fluorescence microscopy to ensure working GFP.

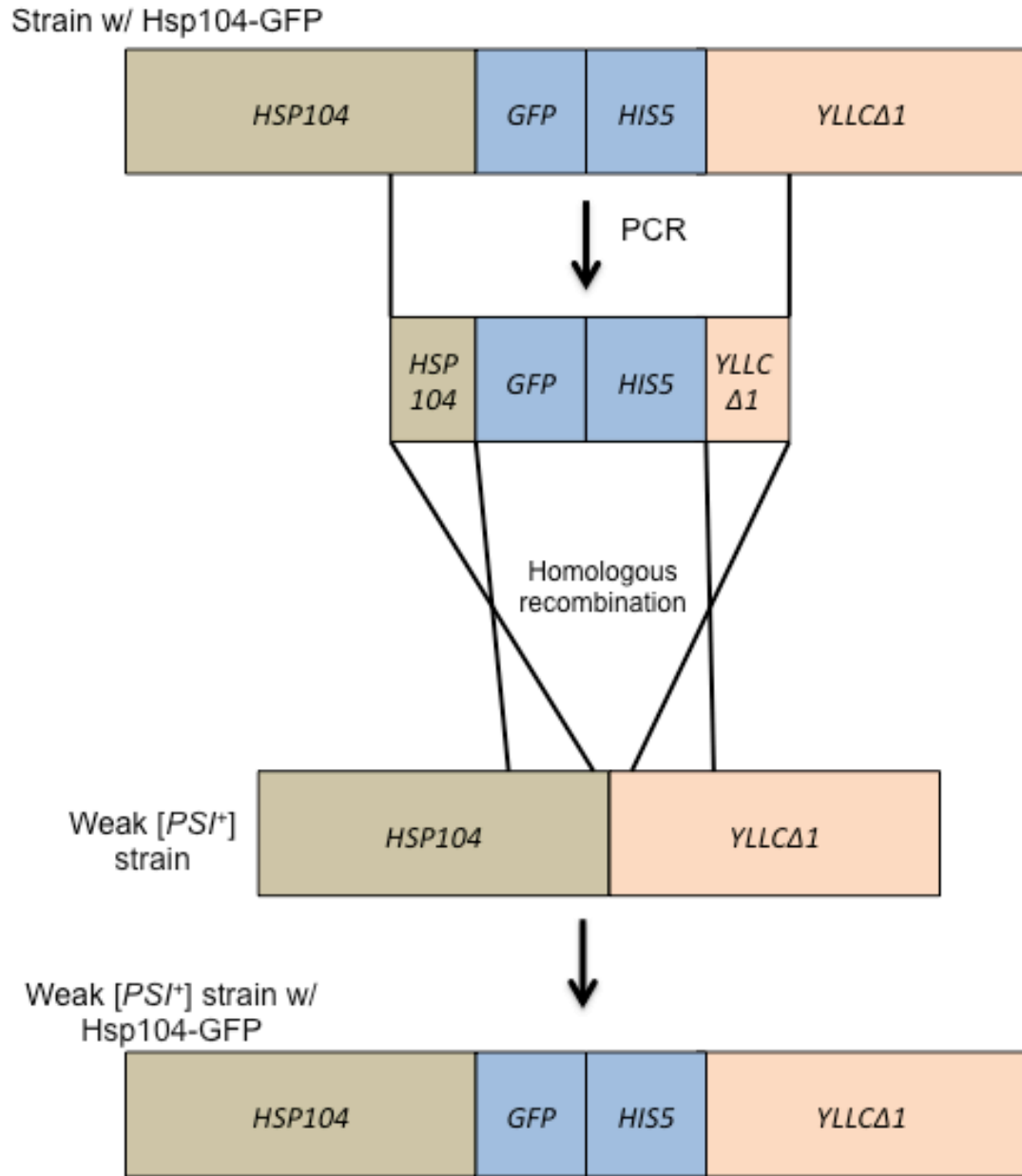


Figure 2-3. Procedure to make Hsp104-GFP in our strain background. Strain with Hsp104-GFP was obtained from another lab. PCR was used to copy the end of the Hsp104 gene through several hundred bp of the following gene so that fragment had over 100bp homology at each end to the wild-type strain. Fragment was transformed into our weak [*PSI*⁺] strain and recombined via homologous recombination. Transformants were checked for correct phenotype and then checked for integration by PCR.

2.3 Biochemical analysis of proteins

2.3.1 Method for protein purification

For protein isolation with heat shock, yeast cultures were grown as follows: overnight pre-culture diluted to OD₆₀₀~0.1, grown two hours, then moved to 39°C for the specified time. Cultures were precipitated by centrifugation and were transferred to 1.5 ml centrifuge tubes, washed with and resuspended in 200 µl of lysis buffer (50 mM Tris-HCl pH 7.5, 1x complete mini protease inhibitor cocktail from Roche, 3 mM phenylmethanesulfonylfluoride). Cells were disrupted by agitation with an equal volume of glass beads for 8 min in a cold room at 4°C. Cell debris was spun down at 4000 g for 2 min, and the supernatants were adjusted with lysis buffer and used for electrophoresis and Western analysis as described below.

2.3.2 Protein level determination via Western Blot

For denaturing polyacrylamide gel electrophoresis (SDS-PAGE) and Western analysis, protein samples were incubated with 0.25x volume of 4x loading buffer (240 mM Tris-HCl pH 6.8, 8% SDS, 40% glycerol, 12% 2-mercaptoethanol and 0.002% bromophenol blue) at room temperature for 10 min, boiled in a water bath for 10 min, and run in a 10% SDS-polyacrylamide gel with 4% stacking gel in Tris-Glycine-SDS running buffer (25 mM tris, 192 mM glycine, 0.1% SDS, pH 8.3), followed by electrotransfer to a Hybond-ECL nitrocellulose membrane (GE Healthcare Life Sciences), pre-blocking with 5% non-fat milk, and probing with the appropriate antibody. Visualization was chemiluminescent and utilized the appropriate secondary HRP (horseradish peroxidase) conjugate antibody and ECL.

2.3.3 *Analysis of protein aggregation: boiled gel*

Boiled gel analysis was performed in the same manner as the SDS-PAGE, except that protein samples were not boiled prior to loading in the gel. Instead, the samples were loaded into the SDS-PAGE gel and run for about 1.5 hrs, so that soluble protein could enter the gel and run for sufficient distance. Electrophoresis was then paused and wells were filled with a new portion of acrylamide to trap aggregated protein that remained in the wells. After polyacrylamide had solidified, the whole gel was placed into a boiling water bath for 10–15 min, cooled down and replaced into the electrophoresis setup, and electrophoresis was resumed. As boiling destroyed polymers, protein from the aggregated fraction was now capable of moving in the gel. After about 2 hrs of electrophoresis, Western blotting was performed followed by reaction to antibodies as described.

2.3.4 *Analysis of protein aggregation: SDD-AGE*

For separation of prion aggregates by SDD-AGE as described previously (Bagriantsev *et al.* 2006), yeast extracts were incubated with 0.25 volume of 4x loading buffer (240 mM Tris-HCl pH 6.8, 8% SDS, 40% glycerol, 12% 2-mercaptoethanol and 0.002% bromophenol blue) at room temperature for 10 min, and run in 1.8% Tris-Acetate EDTA (TAE)-based agarose gel with 0.1% SDS followed by protein transferred to a nitrocellulose Protran membrane (Whatman) by capillary blotting. Membranes were reacted to appropriate antibodies after pre-blocking in 5% non-fat milk.

2.3.5 *Analysis of intracellular protein distribution: sucrose gradient centrifugation*

For sucrose density gradient centrifugation, cells were collected and disrupted as described above, except for using a gradient buffer (20 mM HEPES pH 7.5, 1 mM

EGTA, 5 mM MgCl₂, 10 mM KCl, 10% glycerol, 1x complete mini protease inhibitor cocktail from Roche, 3 mM phenylmethanesulfonylfluoride and 100 µg/ml of cycloheximide). One hundred microliters of a protein extract containing 30–50 µg of total protein as measured by Bradford assay was loaded on a sucrose cushion composed of 100 µl of 20%, 200 µl of 30% and 200 µl of 40% sucrose in the gradient buffer. Samples were centrifuged in 1.4 ml (11 × 34 mm) thick wall polycarbonate tubes, using a TLS-55 rotor on an Optima TLX-120 ultracentrifuge (Beckman) at 259,000 g for 80 min. Fractions of 200 µl each were collected beginning from the top of the gradient; the solid pellet was re-suspended in 200 µl of gradient buffer. Equal amount of samples were prepared, resolved on SDS-polyacrylamide gel and analyzed by Western blotting as described above.

2.4 Prion curing assays

2.4.1 Curing of [PSI⁺] by mild heat-shock

Mild heat-shock was performed as previously described (Newnam, 2011), and as shown in Figure 2-4. Cultures were plated on YPD and grown at 25°C for 7-10 days and [PSI⁺] colonies from this plating were used to inoculate 10 mL YPD liquid, which were grown overnight at 25°C with 180 rpm shaking. Overnight pre-cultures were then diluted in 50 mL YPD liquid to OD₆₀₀ ~ 0.1 and grown at 25°C with 180 rpm shaking for 2 hours. After 2 hours, cultures were sampled (T = 0), then moved to a 39°C water bath (shaking at 180 rpms). Samples were taken after 30 minutes, 45 minutes, 1 hour, 2 hours, and 4 hours of heat shock.

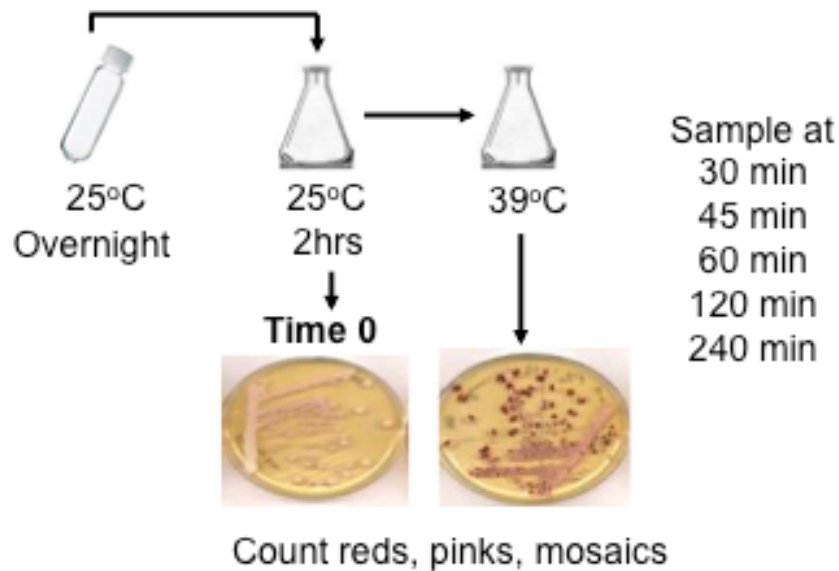


Figure 2-4. Procedure for testing destabilization of weak $[PSI^+]$ by heat shock. Pre-cultures of 10mL YPD are grown overnight at 25°C, then diluted into 50mL YPD to $OD_{600}=0.1$. Cultures are grown for 2 hours at 25°C, sampled, then moved to 39°C and sampled at the stated time. Aliquots of 10 μ L are plated to YPD and streaked for single colonies. Plates are grown at 25°C for 7-14 days, then the numbers of red, mosaic, and pink colonies are counted. Reds and mosaics are considered “cured”.

Each sample was streaked using 10 μ L of the undiluted sample onto YPD plates for prion curability assays. Plates were grown at 25°C for 7-10 days to allow growth and full color development. $[PSI^+]$ (light pink), $[\psi si^-]$ (red), and partially cured $[PSI^+]/[\psi si^-]$ (mosaic) colonies were counted by visual inspection, and red + mosaic colonies constituted the “cured” fraction. For viability of mild heat shock, 200 μ L culture were sampled, serial dilutions were prepared, and cultures were spotted onto YPD plates (4 μ L per spot), then grown at 25°C for ~5 days. Thermotolerance viability assays were performed at 45 and 50°C for 1-8 minutes after diluting as described but allowing cells to grow about 12 hours to $OD_{600} \sim 0.7$ then aliquotting 500 μ L of culture into 1.7 mL microfuge tubes. In this case, cells were placed on ice directly after heat shock then diluted/spotted and grown as described.

For heat-shock experiments with nicotinamide (NAM), 2.5 M filter-sterilized solution of nicotinamide (Sigma) powder in water was added to YPD plates for initial plating, to liquid YPD for pre-culture and for heat shock culture, and to YPD plates used for plating post-heat shock. Procedure was identical to that described previously except that cultures were diluted into 10mL YPD +/- NAM in 50mL Oakridge tubes, which were used for heat shock.

2.4.2 Artificial overexpression of *HSP104*

Strains were transformed via lithium-acetate transformation as previously described (Gietz *et al.* 1992) with plasmids bearing *HSP104* under the galactose-inducible promoter ($P_{GAL}HSP104$). Resulting colonies were purified on selective media and patched to YPD then replica plated to selective media to check phenotype; transformants with similar [*PSI*⁺] phenotype (similar growth on –ADE, similar color on YPD) were selected for experimentation. For qualitative analysis, patched transformants were velveteened to Gal media selective for the plasmid, then velveteened to YPD and –ADE selective for plasmid. Plates were grown for 7 days then visually examined to check for curing (red on YPD, no growth on –ADE).

For quantitation experiments, selected transformants were used to inoculate 10 mL liquid synthetic media selective for plasmid. Cultures were grown overnight with 220 rpm shaking at 30°C, then diluted to a total of 2×10^5 cells in 50 mLs synthetic media possessing 2% galactose and 2% raffinose instead of glucose in order to induce *HSP104*. Cultures were sampled at T= 0 (prior to dilution into gal media), 12 hours, and 24 hours, washed in water, and plated onto synthetic media selective for plasmid. Plates were grown at 30°C for 3 days, then velveteened to YPD and –ADE selective for plasmid

in order to determine curing rates for each strain. Plates were grown for 7 days, then visually examined, and cured vs. non-cured or partially cured colonies were enumerated.

2.4.3 Prion curing by GuHCl

To determine whether strains could be cured of respective prions by passage on guanidine hydrochloride (GuHCl), each strain was first streaked onto YPD for single colonies. Single colonies were then patched onto YPD containing 5mM (2mM for *zuo1Δ* strains) GuHCl, grown for 3 days at 30°C, then serially patched to YPD + GuHCl an additional 2 times. The final patch of growth for each culture was then streaked onto YPD for individual colonies, grown 1 day, velveteened to YPD and –ADE, and visually examined and counted to determine percentage of curing via color on YPD (red if cured) and growth on –ADE (growth indicating non-cured).

CHAPTER 3. ROLE OF THE CELLULAR ASYMMETRY APPARATUS IN PRION CURING BY STRESS

S. cerevisiae practices asymmetric cell division, so that mother and daughter (bud) cells are morphologically distinguishable from each other. After stress, asymmetric distribution leads to stress-damaged proteins being preferentially retained in the mother cell and cleared from the daughter cell, a process necessary for the daughter to maintain full replicative ability. In yeast, asymmetric segregation of damaged proteins in cell divisions is known to depend on several cellular components, including Hsp104, the actin cytoskeleton, and the NAD⁺ dependent deacetylase Sir2. The yeast prion [PSI⁺] is known to be destabilized by short-term mild heat shock followed by a return to normal growth temperature. We show that this destabilization is promoted in the absence of some cytoskeleton-associated proteins. We also show that [PSI⁺] destabilization by heat shock is dependent on Sir2 in a manner similar to the effect of heat shock on distribution of other protein aggregates, and that Sup35 aggregates co-localize with Hsp104-marked aggregates of heat-damaged proteins after heat shock, demonstrating the role of the asymmetric segregation apparatus in prion destabilization by heat shock. Our data indicate that behavior of prion aggregates during and after heat shock resembles the behavior of stress-damaged aggregates after heat shock, and prions are asymmetrically segregated to the mother cell, causing prion loss in the daughters.

3.1 Introduction to Chapter 3

S. cerevisiae practices asymmetric cell division, with the mother cell retaining damaged proteins, such that mother and daughter (bud) cells are morphologically distinguishable from each other. After stress, asymmetric distribution of cytoplasm serves as a “last line” of defense, as stress-damaged proteins, which are not

disaggregated by chaperones, are preferentially retained in the mother cell and cleared from the daughter cell, restoring its proliferation ability (Aguilaniu *et al.* 2003). Preferential recovery of daughter cells is an adaptive feature, as daughter cells are at the start of replicative life span and will undergo more cell divisions than aging mothers. In yeast, asymmetric segregation of damaged proteins in cell divisions depends on several cellular components, including Hsp104, the actin cytoskeleton, and the NAD⁺ dependent deacetylase Sir2 (Aguilaniu *et al.* 2003; Erjavec *et al.* 2007; Tessarz *et al.* 2009; Liu *et al.* 2010). It has been proposed that Sir2 promotes asymmetric segregation via deacetylating the chaperonin CCT, which in turn modulates folding of actin (Liu *et al.* 2010).

The yeast prion [*PSI*⁺] is resistant to prolonged growth at high temperature when Hsp levels are proportionally increased, however it is destabilized by short-term heat shock followed by a return to normal growth temperature (Tuite *et al.* 1981, Newnam *et al.* 2011, Klaips *et al.* 2014). Prion destabilization by short-term mild heat shock coincides with the period of maximal imbalance between Hsp104 and Hsp70-Ssa, as Hsp104 is accumulated faster during heat shock (Newnam *et al.* 2011). Prion loss is promoted in the absence of some cytoskeleton-associated proteins (Chernova *et al.* 2011, Ali *et al.* 2014), occurs primarily in cell divisions following heat shock, and is asymmetric, which may be explained either by asymmetric segregation of prion aggregates (Newnam *et al.* 2011, Ali *et al.* 2014) or by asymmetric accumulation of Hsp104 (Klaips *et al.* 2014). Thus, the behavior of prion aggregates during heat shock shows a resemblance to the behavior of stress-damaged aggregated proteins.

3.2 Materials and Methods: Fluorescence microscopy

Strains with Hsp104-GFP were built as described, and proven Hsp104-GFP strains were then subjected to the Pringle method as described to obtain *sir2Δ* strains. Isolates containing Hsp104 tagged with GFP on the C-terminal end were grown on YPD plates for 5-6 days at 25°C. Single colonies from this plate were then used to inoculate 10 mL liquid YPD preculture, which was grown overnight at 25°C/200 rpm shaking. Pre-cultures were diluted into 50 mLs YPD broth to $OD_{600} = 0.1$, and allowed to grow at 25°C for 2 hours. Cultures were sampled for T= 0, moved to a shaking water bath at 42°C or 39°C for 30 min, then moved back to 25°C for recovery. Cultures were sampled after the stated amount of time of recovery. For each time point, 500 μL of culture was sampled to a microcentrifuge tube and spun down at 3,000 rpm for 2 minutes, after which the supernatant was poured off and the cells were re-suspended into 30-50 μL dH₂O. Ten microliters of each sample was then placed on a microscope slide and sealed with clear nail polish to prevent drying. Slides were visualized at 100x oil immersion using GFP excitation with an Olympus Bx2 fluorescence microscope. Cells were classified into listed categories based on general fluorescence or aggregates in mother vs. daughter cells, and in some cases the numbers of aggregates in cells were counted and classified (one large, 2-3, many small, etc.).

For co-localization experiments, strains were transformed with a plasmid containing Sup35NM-RFP, and initial pre-culture was performed in liquid media selective for the plasmid. Dilution of pre-culture and heat shock were then identical to Hsp104-GFP associated aggregate localization study, except that heat shock for Sup35NM-RFP co-localization was conducted at 39°C for 1 hour, then flasks were moved back to 25°C for recovery. Excitation for RFP was performed prior to that for GFP to minimize cross-reactivity.

3.3 The effect of *SIR2* deletion on $[PSI^+]$ destabilization during heat shock

Along with Hsp104, the NAD⁺ dependent protein deacetylase Sir2 (sirtuin) has been shown to control asymmetric segregation of aggregated oxidatively damaged proteins in cell divisions following heat shock (Aguilaniu *et al.* 2003, Liu *et al.* 2010). To determine whether Sir2 also plays a role in heat shock-induced destabilization of $[PSI^+]$, we constructed a weak $[PSI^+]$ strain bearing the *sir2*Δ deletion and compared effects of mild heat shock at 39°C on this strain and the isogenic wild type strain containing the same variant of prion. Indeed, we observed that deletion of *SIR2* dramatically reduced loss of $[PSI^+]$ during and after mild heat shock (Figure 3-1A,B). Notably, deletion of *HST2*, another sirtuin not shown to be involved in asymmetric segregation of heat-damaged proteins, exhibited a significantly milder effect (Figure 3-1A). Deletion of *SIR2* did not affect thermotolerance and viability, even at 50°C heat shock (Figure 3-1C). To determine if *sir2*Δ influences levels of heat shock proteins (Hsp104 and Hsp70-Ssa) involved in $[PSI^+]$ propagation, and/or alters patterns of Sup35 aggregation, we compared aggregation of Sup35 and levels of Hsps in the isogenic and “isoprionic” *sir2*Δ and wild-type strains before and during heat shock. Western analysis indicated that Hsp104 and Hsp70-Ssa are produced at comparable levels in the levels in the *sir2*Δ and wild-type cultures before heat shock, and show identical dynamics of heat shock-induced accumulation in both cultures (Figure 3-2A), with Hsp104 accumulating faster than Ssa, in agreement with our previous observations for the wild-type strain (Newnam *et al.* 2011).

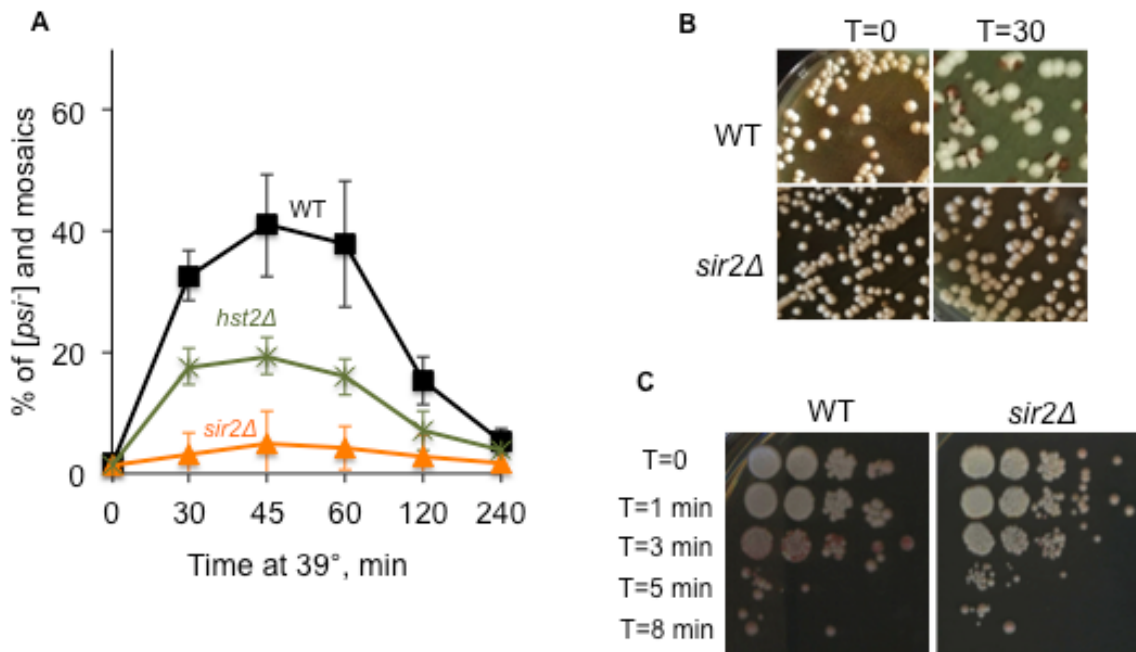


Figure 3-1. Effects of *SIR2* deletion on $[PSI^+]$ destabilization by heat shock. (A) Quantitative assay of curing by mild heat shock for *sir2Δ* compared to *hst2Δ*. Deletion of *SIR2* antagonizes $[PSI^+]$ destabilization by mild heat shock. Deletion of *HST2* does not have an equivalent effect. Cells were heat shocked at 39°C; cured number includes red and mosaic colonies. WT (wild-type) is a compilation of all runs. Error bars indicate standard deviation. (B) Wild type and *sir2Δ* cultures before and after 30 min heat shock at 39°C, note the lack of increase in red and mosaic colonies at T=30 in the *sir2Δ* strains. (C) Deletion of *SIR2* does not affect viability during high (50°C) heat shock. Cells were placed at 50°C and sampled after listed time, then dilution plated. See Table A4 for percent curing and SD.

“Boiled gel” procedure (see Materials and Methods) showed that *sir2Δ* somewhat increased the proportion of monomeric versus polymeric Sup35 protein in the yeast cells prior to heat shock, however *sir2Δ* caused a lack of further increase in accumulation of monomeric protein during heat shock (Figure 3-2B). Analysis of aggregate distribution by sizes, using semi-denaturing gel electrophoresis (SDD-AGE)

indicated that while Sup35 aggregates in the heat shocked wild-type cells are shifted up compared to non-shocked culture (suggestive of an overall increase in aggregate size,

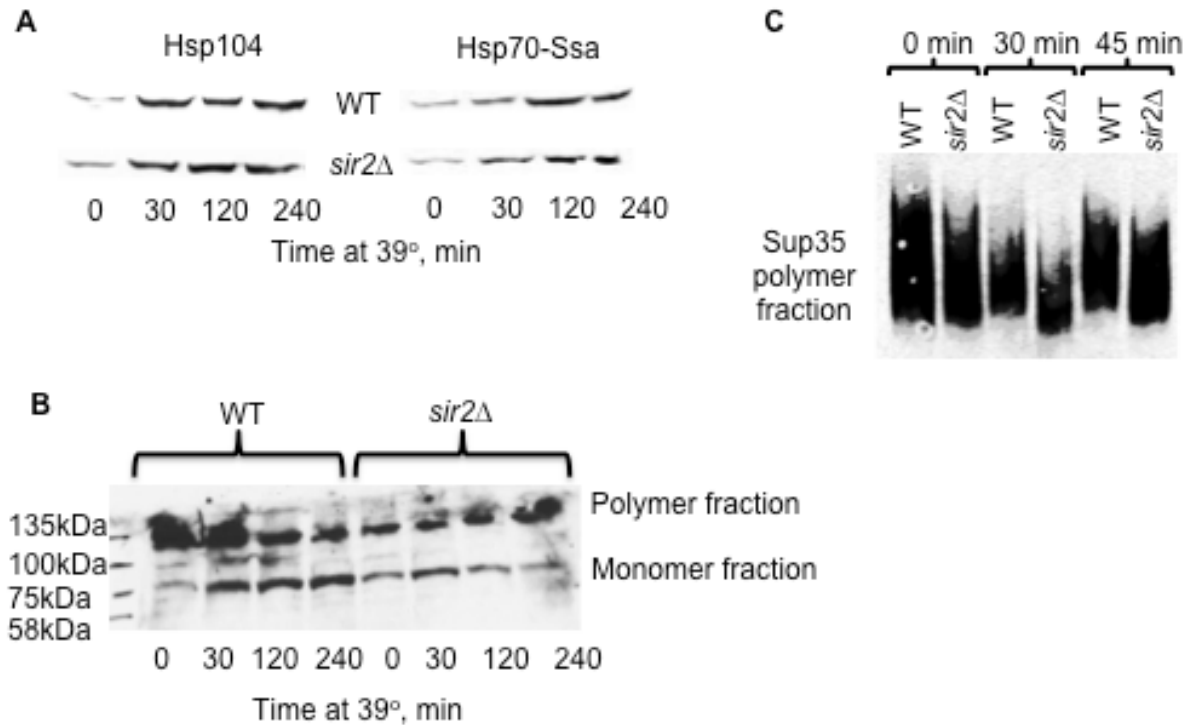


Figure 3-2. Heat shock protein levels and changes to $[PSI^+]$ aggregates in a heat-shocked *sir2Δ* strain. (A) Hsp levels are not altered by *sir2Δ*. Purified proteins were analyzed by Western blot for Hsp104 and Hsp70-Ssa levels. (B) Deletion of *SIR2* increases monomer in the cell prior to heat shock and decreases it later in heat shock. Purified proteins were analyzed by boiled gel SDS-PAGE tagged with Sup35-antibody. (C) Deletion of *SIR2* decreases Sup35 polymer size during heat shock. Purified proteins from heat shock were run on SDD-AGE and tagged with Sup35 antibody.

previously described by Newnam *et al.* 2011), that during heat shock, Sup35 aggregates in heat shocked *sir2Δ* cells are shifted down compared to non-shocked cells, suggestive of an overall decrease in aggregate size (Figure 3-2C). As smaller aggregates are more efficiently transmitted to daughter cells and produce more seeds for prion propagation, these data are in agreement with more efficient transmission of $[PSI^+]$ prion in the *sir2Δ* cells compared to wild-type cells in cell divisions following heat shock.

We then asked if *sir2* Δ acts on [*PSI*⁺] curing by artificial Hsp104 overexpression in the same direction as in the case of heat shock. For this purpose, we transformed wild-type and *sir2* Δ strains containing weak [*PSI*⁺] variant with a plasmid containing the *HSP104* gene under the control of galactose-inducible (P_{GAL}) promoter and performed quantitation as described (Materials and Methods). The cultures were incubated in galactose medium turning on the overexpression of Hsp104, aliquots were plated onto glucose medium where overexpression is turned off, and proportions of plasmid containing cells keeping or losing [*PSI*⁺] were determined. We found that [*PSI*⁺] curing by Hsp104 overexpression was delayed in *sir2* Δ cells as indicated by the increased proportion of colonies that grew on -ADE medium and retained lighter color on YPD (Figure 3-3). However in contrast to its effect during heat shock, *sir2* Δ did not entirely abolish [*PSI*⁺] curing by artificial overexpression of Hsp104. Notably, *sir2* Δ did not show any significant effect on [*PSI*⁺] curing by 5mM guanidine hydrochloride (GuHCl), an agent inactivating Hsp104 (data not shown).

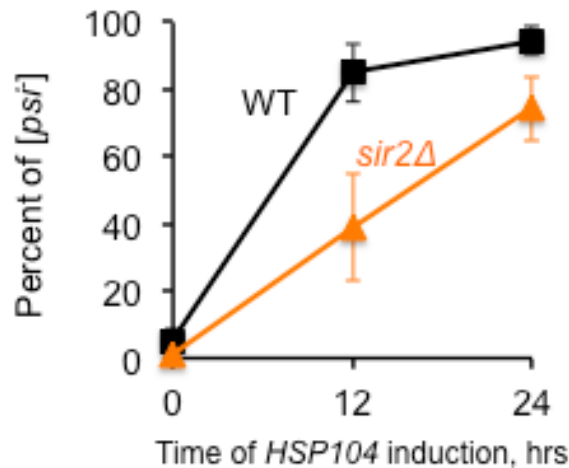


Figure 3-3. Curing by Hsp104 overexpression in a *sir2* Δ strain. Deletion of *SIR2* delays [*PSI*⁺] curing by Hsp104 overexpression as indicated by growth on -ADE. Strains transformed with Gal-*HSP104* were induced and sampled at 0, 12, and 24 hours. Error bars indicate standard deviation.

3.4 The result of *LSB2* deletion on *[PSI⁺]* curing and the necessity of *SIR2*

It has previously been demonstrated that Sir2 deficiency leads to actin cytoskeletal deficiencies (Erjavec *et al.* 2007; Liu *et al.* 2010), suggesting that association of aggregates with the actin cytoskeleton and actin cables prevents transmission of these aggregates into the daughter cell during asymmetric segregation (Tessarz *et al.* 2009; Liu *et al.* 2010). We found that deletion of the protein coding for the yeast actin assembly protein Lsb2 increased *[PSI⁺]* destabilization by heat shock (published in Chernova *et al.* 2011). We then checked to see if *[PSI⁺]* destabilization in the *lsb2Δ* strain is Sir2-dependent, and found that *sir2Δ/lsb2Δ* cells were indistinguishable from *sir2Δ* cells in regard to lack of *[PSI⁺]* loss after mild heat shock (Figure 3-4). This shows that the effect of *sir2Δ* on *[PSI⁺]* is epistatic to *lsb2Δ*, in agreement with the notion that the effect of Sir2 might be mediated by the alterations of the actin cytoskeleton.

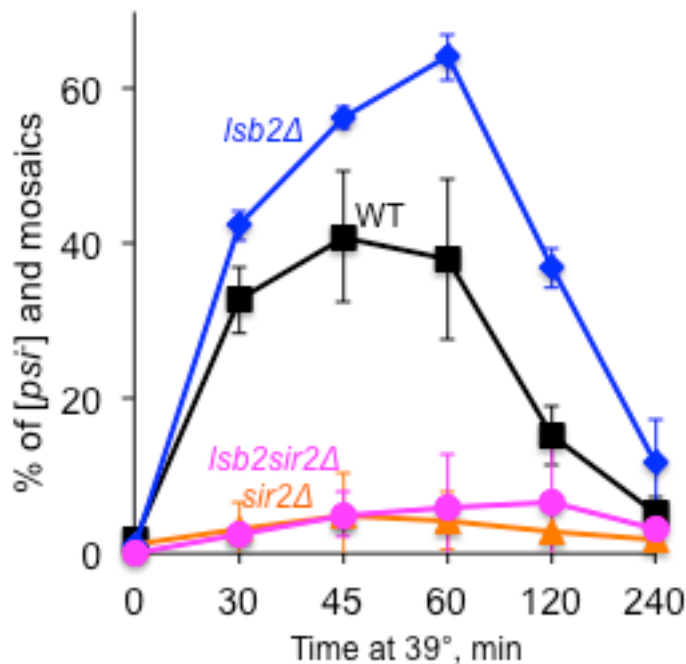
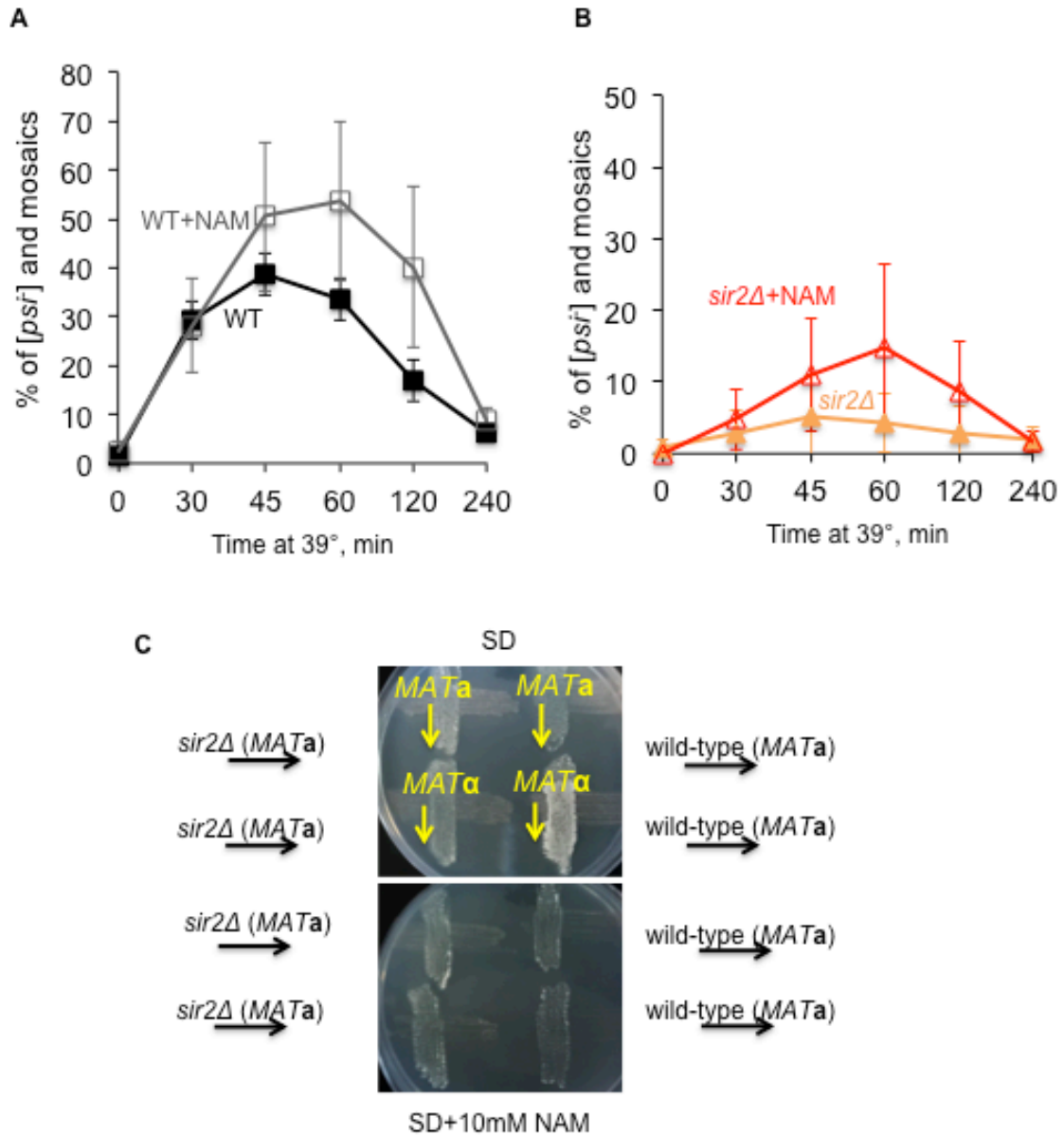


Figure 3-4. Effect of *sir2Δ* on curing by mild heat shock in a *Isb2Δ* background. Quantitative assay of curing by mild heat shock for *sir2Δ* compared to *Isb2Δ*. Deletion of *SIR2* antagonizes $[PSI^+]$ destabilization by mild heat shock, while *Isb2Δ* dramatically increases curing by heat shock, but *Isb2sir2Δ* returns the strain to *sir2Δ* curing levels. Cells were heat shocked at 39°C; cured number includes red and mosaic colonies. WT is a compilation of all wild-type runs. Error bars indicate standard deviation. See Table A4 for percent curing and SD.

3.5 The effect of nicotinamide on $[PSI^+]$ destabilization during heat shock

Nicotinamide (NAM) is known to negatively regulate Sir2 and has been shown to inhibit Sir2-dependent gene silencing in yeast (Bitterman *et al.* 2002) and to antagonize asymmetric distribution of aggregated heat damaged proteins in cell divisions (Liu *et al.* 2010). We checked whether or not addition of NAM is able to alter $[PSI^+]$ destabilization by heat shock to a level similar to that of *sir2Δ*. Surprisingly, addition of 10 mM NAM to yeast cultures during heat shock did not impair, and in most repeats of the experiment, increased $[PSI^+]$ curing in the wild-type strain (Figure 3-5A).



NAM addition during heat shock also slightly promoted [*PSI*⁺] curing by heat shock in *sir2*Δ cells (Figure 3-5B). Notably, this concentration of NAM was sufficient to inhibit yeast mating (Figure 3-5C), an effect that depends on inhibition of Sir2 and the resulting activation of normally silent mating type cassettes (Bitterman *et al.* 2002). This confirms that Sir2 was indeed inhibited by NAM. A potential explanation for the lack of impairment of [*PSI*⁺] curing by NAM is provided by the observation that NAM slightly promotes [*PSI*⁺] curing by heat shock in *sir2*Δ cells, which indicates that in addition to inhibiting Sir2, NAM facilitates heat shock mediated [*PSI*⁺] curing via a Sir2 independent mechanism.

3.6 The effect of *sir2* deletion on aggregate recovery and segregation after mild heat shock.

Previous data indicates that [*PSI*⁺] loss in the first cell division after heat shock preferentially occurs in daughter cells (Newnam *et al.* 2011, Ali *et al.* 2014). Likewise, aggregates of oxidatively damaged proteins, associated with the Hsp104 chaperone are preferentially accumulated in mother cells (Erjavec *et al.* 2007). By using the integrated gene coding for GFP-tagged Hsp104, we confirmed that Hsp104-GFP marked protein aggregates indeed appear as small dots during mild heat shock (39° or 42°) followed by coalescence of these small aggregates into one larger aggregate located in the mother cells during recovery from heat shock (Figure 3-6A,B). This mother-specific aggregate accumulation was specifically less pronounced in the *sir2*Δ strain, which retained a higher proportion of mother/daughter pairs with aggregates in both cells even after 120 min of recovery (Figure 3-6A).

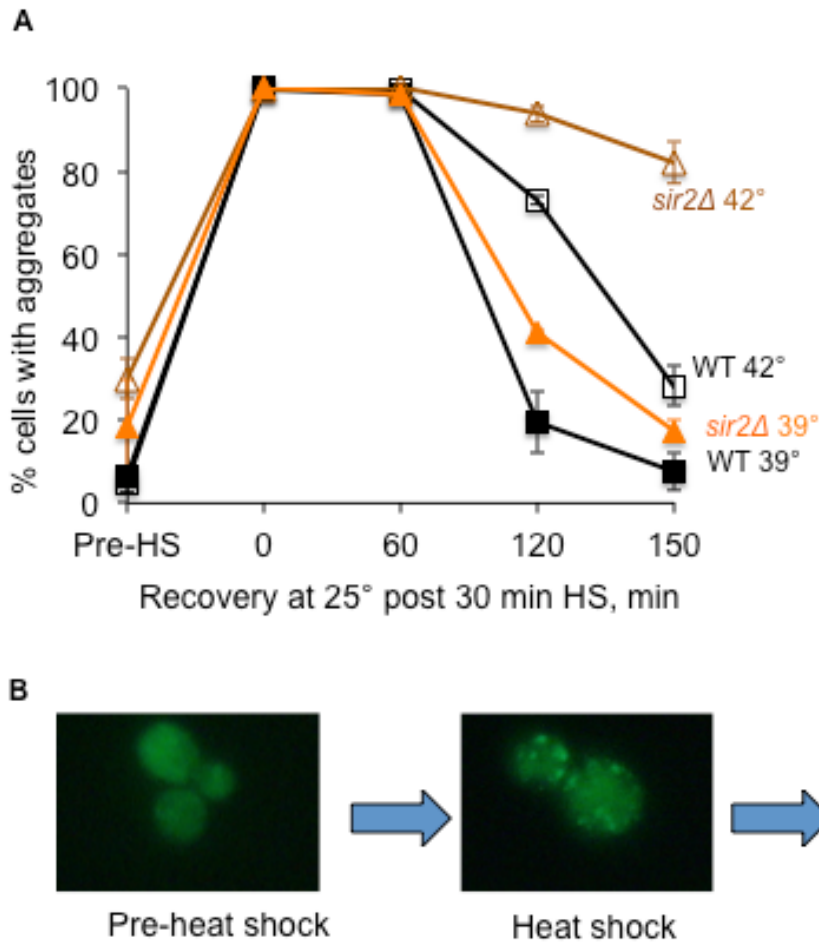


Figure 3-6. Effects of *sir2Δ* on recovery from aggregate formation after heat shock. Fluorescence microscopy of cultures with chromosomal *HSP104* tagged with GFP and subjected to 30 minutes at 39°C or 42°C then recovered at 25°C for the amount of time stated. Zero minutes post-heat shock indicates no recovery time. (A) Deletion of *SIR2* delays post-heat shock recovery of Hsp104-GFP marked aggregates. Error bars indicate standard deviation. (B) Recovery process. Pre-heat shock, cells are generally fluorescent. Just after heat shock, Hsp104-marked aggregates can be seen in all cells. Over time, these aggregates disappear and the cell returns to generalized fluorescence.

3.7 Sup35 co-localization with Hsp104-marked protein aggregates during heat shock.

To check the behavior of Sup35 prion aggregates after heat shock in comparison to Hsp104-GFP, we transformed a centromeric plasmid pYCL-Sp-SUP35NMSC-DsRed

coding for Sup35NM-RFP under the Sup35 promoter, into the same Hsp104-GFP strains and subjected them to mild heat shock followed by recovery. As typical for the tagged Sup35 with moderate expression levels, cells containing cytologically detectable Sup35NM-RFP aggregates were not common in the non-heat-shocked culture. These cells became more numerous in the heat-shocked cultures, although they were still not as frequent as the cells with Hsp104-GFP aggregates, which appear in all cells after heat shock. We detected co-localization of Sup35NM-RFP with Hsp104-GFP aggregates in the majority of heat shocked mother-daughter pairs of both wild-type and *sir2Δ* strains (Figure 3-7A,B).

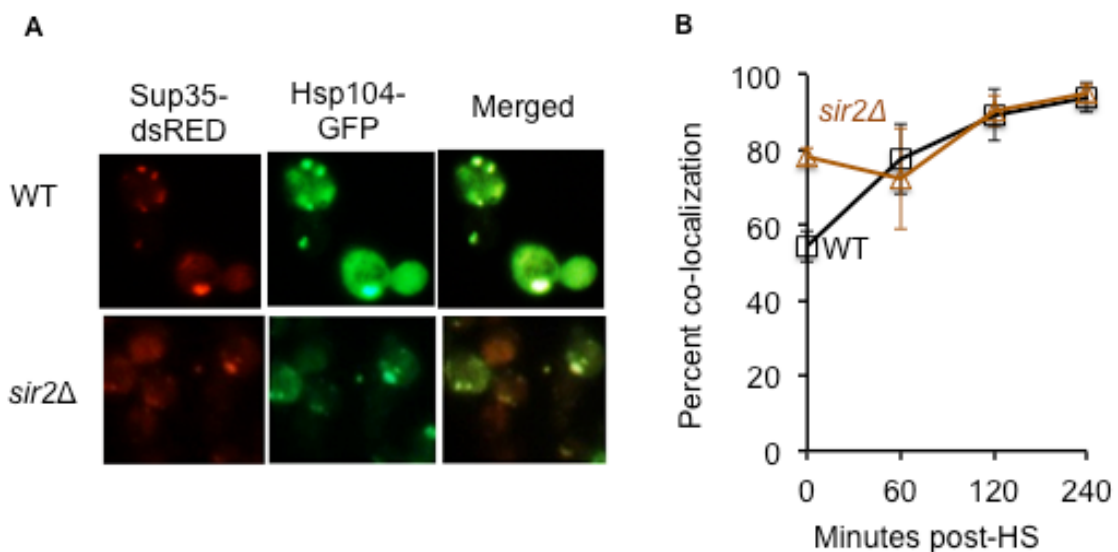


Figure 3-7. Localization of Sup35NM and Hsp104 after mild heat shock. Sup35NM co-localizes with Hsp104 marked aggregates, and this does not change in *sir2Δ* cells (A) Sup35NM-RFP co-localizes with Hsp104-GFP after heat shock at 42°C. (B) Percent of Sup35NM-RFP and Hsp104-GFP aggregates that co-localize at 1hr intervals. *SIR2* deletion does not prevent co-localization. Cultures were grown at 25°C, sampled, then subjected to 1 hr at 42°C, after which they were returned to 25°C for recovery and sampled at one-hour intervals. Zero minutes post-heat shock indicates no recovery time.

A minority of cells possessed Sup35NM-RFP aggregates pre-heat shock, but a majority did so after heat shock (Table 3-1).

Table 3-1. Percent of cells with Sup35NM aggregates.

	Pre-heat shock	T=0 (heat shock)	60min recovery	120 min recovery	240 min recovery
WT	15% (10/67)	63% (29/46)	57% (26/46)	73% (66/91)	78% (18/23)
<i>sir2Δ</i>	22% (12/55)	85% (56/66)	90% (57/63)	91% (81/89)	76% (41/54)

Dynamics of the distribution of the Sup35NM-RFP aggregates between the mother and daughter cells during recovery after heat shock generally followed that of the Hsp104-GFP aggregates (Figure 3-8A,B) demonstrating increased accumulation of aggregates in mother cells. Hsp104-GFP was found in the daughter only with some frequency in *sir2Δ*, whereas this was not the case for wild-type (Figure 3-8A). In the case of Sup35NM-RFP, asymmetry was somewhat less clear (Figure 3-8B). Once again, this asymmetry was impaired by *sir2Δ*. Notably, we also saw that the *sir2Δ* strain frequently formed chained cells indicative of incomplete separation of cells after cell division (Figure 3-9). Delay in cell separation might provide an additional explanation for the impaired asymmetry of aggregated distribution in *sir2Δ* cells.

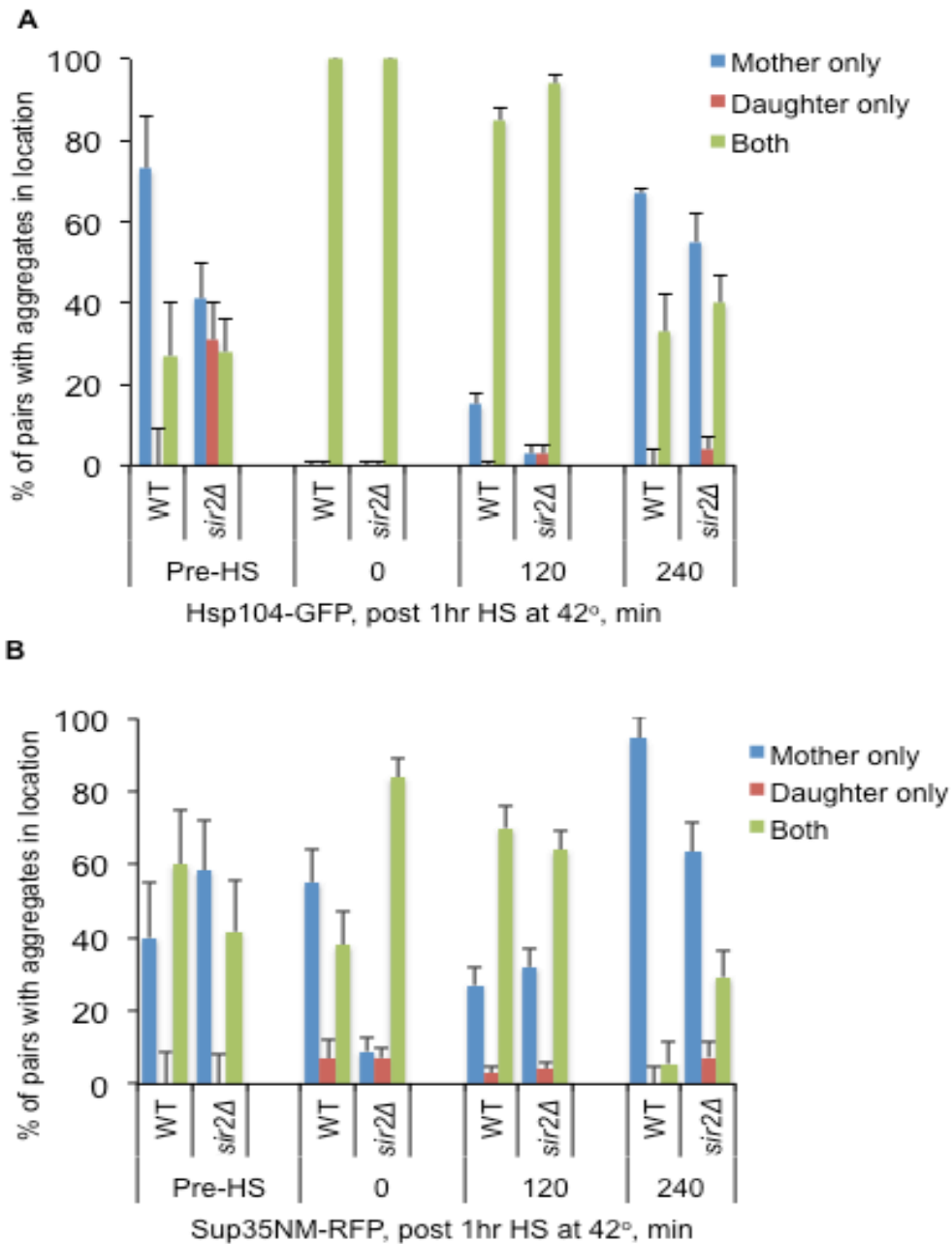


Figure 3-8. Proportion of mother-daughter pairs with different aggregate distributions. Aggregates are in daughter only or both mother and daughter more frequently in *sir2Δ* cells. Strains with chromosomal *HSP104* tagged with GFP were transformed with Sup35NM-dsRED plasmid and heat shocked for 1 hour at 42°C followed by recovery at 25°C (A) Hsp104-GFP aggregates are more frequently in daughters pre-heat shock and in both post-heat shock in the *sir2Δ* strain. (B) Sup35NM-RFP aggregates are found in both or daughter only for a longer period after heat shock in the *sir2Δ* strain. Error bars indicate standard error for compiled experiments. See Tables A5 and A6 for details.

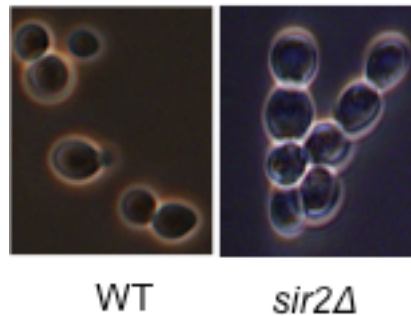


Figure 3-9. Changes to morphology in *sir2Δ* strain. *SIR2* deletion causes delayed cytokinesis, with a chained cell phenotype.

3.8 Discussion of Chapter 3 data

The data here strongly support the role of asymmetric protein segregation in heat shock mediated destabilization of $[PSI^+]$ by showing that the deletion of *SIR2*, coding for an NAD^+ -dependent protein deacetylase (sirtuin) previously implicated in the control of cell asymmetry, prevents destabilization of the $[PSI^+]$ prion by heat shock. Asymmetric segregation of oxidatively damaged proteins has previously been shown to be dependent on both Sir2 and Hsp104 (Aguilaniu *et al.* 2003; Erjavec *et al.* 2007; Tessarz *et al.* 2009; Liu *et al.* 2010). It has been proposed that the effect of *sir2Δ* is due to increased acetylation of the chaperonin CCT that impacts actin folding and thus influences actin-dependent retention and/or retrograde transport of heat-damaged proteins (Liu 2010). Involvement of the actin cytoskeleton in $[PSI^+]$ destabilization by heat shock agrees with our results showing that deletion of the actin assembly protein Lsb2 further increases $[PSI^+]$ loss at high temperature (Chernova *et al.* 2011, Ali *et al.* 2014). Moreover, we show that *sir2Δ* is epistatic to Lsb2 in regard to heat-shock mediated $[PSI^+]$ destabilization, indicating that both Sir2 and Lsb2 proteins are likely to

act on $[PSI^+]$ via the same pathway (Figure 3-4). Our data also point to a delay of cytokinesis in the *sir2* Δ strains (Figure 3-9), which may also impair asymmetry of cytoplasm distribution due to a longer period of time available for the movement of cytoplasmic components from the mother to daughter cell, in accordance with the diffusion model of asymmetric segregation (Zhou *et al.* 2011). It should be noted that the “active” (via actin cytoskeleton) and “passive” (via diffusion) models of cell asymmetry are not necessarily mutually exclusive, as both processes may contribute to asymmetric distribution of protein aggregates. However, our observation that *sir2* Δ prevents an increase in the size of Sup35 prion polymers detected during heat shock (Figure 3-2C) suggests that the role of Sir2 is not achieved entirely through a passive mechanism. If increases in aggregate size occur due to assembly of larger protein complexes promoted by Hsp104 and the actin cytoskeleton, leading to subsequent asymmetric segregation, this assembly appears to be impaired in the *sir2* Δ cells. Decreased assembly of large complexes may increase accessibility of prion polymers for the newly immobilized protein and polymer fragmentation machinery, further decreasing polymer size (Figure 3-2C) and proportion of monomeric protein (Figure 3-2B) in the heat shocked *sir2* Δ cells.

In either case, the effects of *sir2* Δ on prion aggregates appear to parallel its effects on the aggregates of heat damaged proteins. Two differences between these experimental models could, however, be detected. First, deletion of the gene *HST2*, coding for another sirtuin and not specifically implicated in chaperonin deacetylation, did not appear to have any impact on asymmetric segregation of prion aggregates (Liu *et al.* 2010). However, *hst2* Δ did somewhat decrease $[PSI^+]$ destabilization by heat shock in our hands (Figure 3-1A). Still, the effect of *sir2* Δ was much stronger than that of *hst2* Δ . Second, treatment with NAM, an inhibitor of the deacetylase activity of Sir2, impaired

asymmetric retention of heat-damaged proteins (Liu *et al.* 2010) but did not decrease [PSI⁺] destabilization in our assay (Figure 3-5A,B). This is due to the fact that NAM itself increases heat-shock promoted [PSI⁺] destabilization via a yet unknown Sir2-independent mechanism.

The co-localization of Sup35NM with Hsp104 aggregates observed in this work indicates that Sup35 is segregated along with Hsp104-tagged aggregates into mother cells post heat stress, a process which promotes curing of [PSI⁺] and which is impaired in *sir2*Δ cells. Two scenarios may explain the asymmetry of prion loss after heat shock: 1) asymmetric segregation of prion aggregates *per se*, leading to their accumulation in mother cells and resulting in clearance from daughter cells, which therefore accumulate newly synthesized Sup35 protein in the non-prion form, as proposed previously (Newnam *et al.* 2011) and by Ness *et al.* (2017) for curing by Hsp104 overexpression, and 2) asymmetric mother-specific accumulation of Hsp104 that in turn leads to a defect in prion maintenance, as proposed by Klaipe *et al.* 2014. Experimental evidence could be provided in favor of both models. Indeed, fluorescently tagged Hsp104 is associated with aggregates of stress-damaged proteins and accumulated together with them in mother cells, apparently playing an important role in this process (Liu *et al.* 2010). Our data confirm mother-specific accumulation Hsp104-marked protein aggregates in cell divisions following heat shock, and alterations of this asymmetry in *sir2*Δ cells (Figure 3-8A). On the other hand, our data also show that aggregated clumps of Sup35 prion polymers, increased in size after stress, co-localize with the Hsp104-marked aggregates of heat-damaged proteins (Figure 3-7), and show a tendency of Sir2-dependent mother-specific accumulation in cell divisions following stress (Figure 3-8B).

The two models described above are not mutually exclusive, especially taking into account recent data indicating that excess Hsp104 cures [PSI⁺] via a malpartitioning

mechanism, rather than through monomerization (Ness *et al.* 2017). Apparently, Hsp104 may protect cells from toxic effects of protein aggregation in two ways: a) via direct disaggregation and refolding of aggregated proteins when working in complex with Hsp70-Ssa/Hsp40, and b) by promoting aggregate retention in the mother cell when acting in combination with the cytoskeletal machinery. The latter process represents a second line of defense, becoming crucial when levels of aggregate accumulation are too high and Hsp104/Hsp70-Ssa/Hsp40 promoted disaggregation is insufficient for survival, or inactivated when Hsp104 is present in excess of Hsp40-Ssa, which occurs after a short-term stress due to the fact that Ssa levels are not increased during stress as rapidly as are levels of Hsp104. As previously proposed (Liebman and Chernoff 2012), Hsp104 acts on prion aggregates in a manner similar to its effect on heat-damaged protein aggregates. Thus, in cell divisions following stress, both prion aggregates and aggregates of heat damaged proteins, which are assembled into large structures via interactions with each other and Hsp104, are preferentially retained in mother cells. This results in preferential prion clearance from the daughter in the first post-stress divisions as reported (Newnam *et al.* 2011). However, the mother cells retain prion aggregates as part of larger protein complexes, having a lesser ability of transmission into the daughters (Derdowski *et al.* 2010) and contain increased levels of Hsp104, promoting aggregate malpartitioning. This results in the unstable inheritance of prion aggregates in subsequent divisions of mother cells, as reported by Klaips *et al.* 2014. Deletion of *SIR2* partly restores asymmetric distribution of both protein aggregates and Hsp104, thus antagonizing stress-induced prion loss, as shown in Figure 3-10. Our observation that *sir2* Δ also decreases $[PSI^+]$ curing by excess Hsp104 points to similarity between the effects of stress-induced curing and artificial Hsp104 overproduction. However, artificial Hsp104 overproduction is not accompanied by massive aggregation of other proteins, thus making the dependence of prion stabilization on Sir2 less evident.

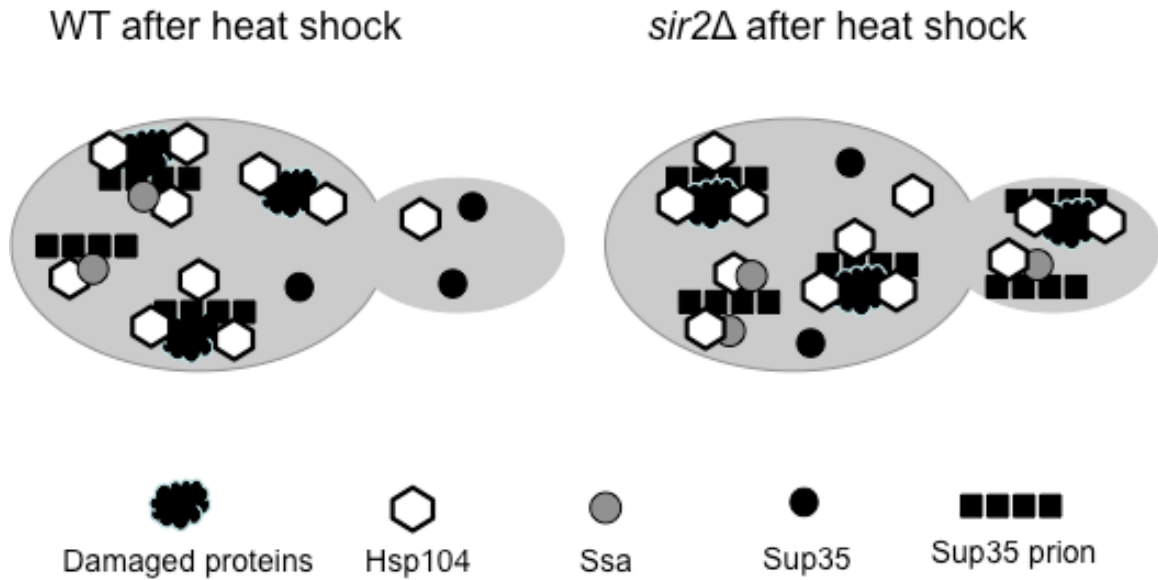


Figure 3-10. Proposed model for *sir2Δ* impairment of asymmetric segregation. Prions segregate with heat-damaged proteins after heat shock; *sir2Δ* impairs segregation of aggregates, slowing transfer of large aggregates to mother cells. Impaired segregation, possibly due to actin defects or incomplete cytokinesis, allows for increased fragmentation of prion into prion seeds, causing daughter cell to inherit the prion.

3.9 Conclusions of Chapter 3

- Deletion of *SIR2*, coding a NAD⁺ deacetylase involved in the control of cell division asymmetry, antagonizes [*PSI*⁺] destabilization by mild heat shock
- Deletion of *SIR2* decreases [*PSI*⁺] curing by artificially overproduced Hsp104
- Inhibition of heat shock mediated [*PSI*⁺] destabilization in the *sir2Δ* cells is not associated with detectable changes in the levels of Hsp104 or Ssa induction during heat shock.
- Loss of Lsb2, a yeast actin assembly protein, increases [*PSI*⁺] destabilization by heat shock

- Increased $[PSI^+]$ destabilization in an *lsb2Δ* strain is Sir2-dependent.
- Nicotinamide (NAM), an inhibitor of Sir2 deacetylase, does not replicate *sir2Δ* on $[PSI^+]$ during heat shock due to ability of NAM to promote $[PSI^+]$ destabilization in a Sir2-independent fashion.
- Cytologically detectable punctated structures formed by Sup35 prion aggregates (marked by Sup35NM-dsRED) during and after heat shock co-localize with Hsp104-marked aggregates of heat-damaged proteins.

CHAPTER 4. CHANGES IN AGGREGATION DUE TO AGING

Stress and aging are intimately connected—stress may influence aging and vice versa, but mild stress may also prolong life and delay the aging process—and it is arguable that the process of aging itself may be thought of as a form of slow stress, as damaged and aggregated proteins are accumulated in both processes. As stress was shown to increase protein aggregation, and recovery from this aggregation was shown to be Sir2-dependent, we hypothesized that formation of both protein aggregates and prion increases with age and that deletion of *SIR2* would exacerbate this. Here we show that aging increases formation of Hsp104-associated protein aggregates but the prion [*PSI*⁺] is only definitively increased in *sir2Δ* cells with aging. Furthermore, impairment of the asymmetric segregation system by deletion of *SIR2* had opposing effects on formation of Hsp104-associated protein aggregates and the prion [*PSI*⁺], causing increased aggregate formation but decreasing *de novo* [*PSI*⁺] formation. These results confirm the association of aggregation with aging and suggest a dual role in the asymmetric segregation system for both counteracting aggregation due to stress and assisting the *de novo* formation of the prion [*PSI*⁺].

4.1 Introduction to Chapter 4

Increased aggregation and oxidative damage to proteins are associated with both stress and aging in yeast (Erjavec *et al.* 2007; Hill *et al.* 2017), and yeast are known to use some of the same mechanisms to counteract these two processes, including the segregation of oxidatively damaged proteins into the mother cell, which happens both after acute stress (Liu *et al.* 2010) and during the aging process (Aguilaniu *et al.* 2003; Erjavec *et al.* 2007). The actin cytoskeleton, Sir2, and Hsp104 have all been linked to inheritance of damaged proteins during aging (Aguilaniu *et al.* 2003; Tessarz *et al.* 2009)

and post-heat shock (Liu *et al.* 2010). Stress is then known to both increase aggregation of proteins in yeast, and conversely, instigate the sequestration of these aggregates into the mother cell during budding. Both curing of the prion [*PSI*⁺] (Newnam *et al.* 2011) and induction of *de novo* [*PSI*⁺] (Chernova *et al.* 2017) during mild heat stress have been linked to the asymmetric segregation system and Sir2, but the effects of aging on the asymmetric segregation system and prion formation are not well defined, though it is known that Sir2 levels decrease in aged cells (Dang *et al.* 2009). We therefore examined whether changes to the asymmetric segregation apparatus by deletion of *SIR2* affect whether Hsp104-associated aggregates are increased in aged cells and how aging affects the formation of [*PSI*⁺] in wild-type and *sir2Δ* cells.

4.2 Materials and methods for aging

4.2.1 Purification of aged cells by biotinylation

Purification of old yeast cells was performed as previously described (Sinclair and Guarente 1997) and as shown in Figure 4-1. In brief, an overnight cell culture grown in YPD was diluted in 50 mL YPAD (Yeast extract Peptone Dextrose media with 3x adenine) and grown for at least 6 hours to an OD₆₀₀ = 0.7. Cells were harvested, washed twice in phosphate-buffered saline (PBS), and resuspended in 1mL of PBS. A portion of the cells was diluted and counted using a hemocytometer, and 8-10 mg of EZ-Link-NHS-LC-LC-Biotin (Pierce) was added to approximately 1x10⁷ yeast cells in PBS. Cells were rotated gently for 15 min at room temperature then washed 3 times in PBS and resuspended in 1mL YPAD. YPAD medium (200 mLs) was inoculated with the biotinylated cells, which were grown for ~13 hours (approximately 5-7 generations) at 30°C (OD₆₀₀ <1.0). The cells were harvested by centrifugation, resuspended in PBS, and incubated on a rotator with 250 μL washed streptavidin magnetic beads (New England

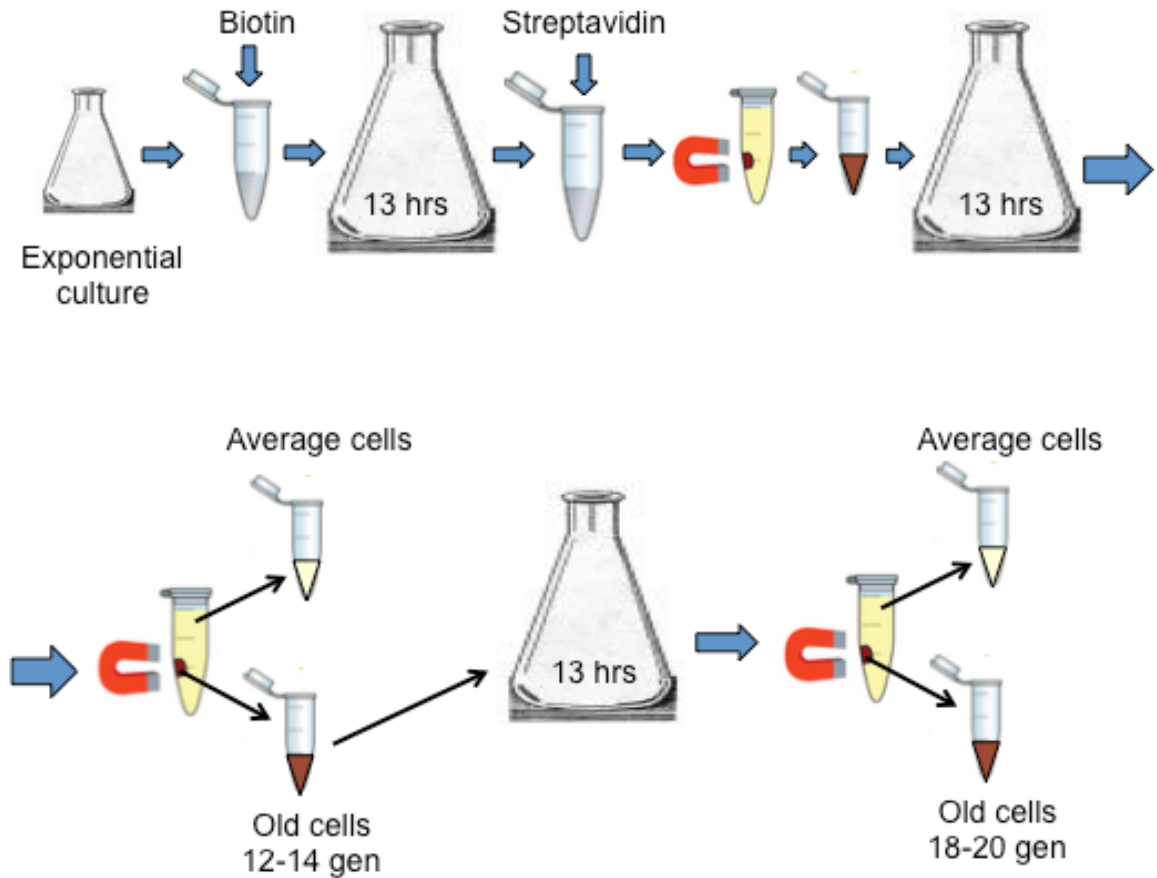


Figure 4-1 Enrichment of aged cells in a yeast population by biotin tagging. Yeast cultures are grown exponentially ($OD_{600} < 1.0$) for 6 hours, then 1×10^7 cells are tagged by adding biotin for 2 hours. Cells are washed, then used to inoculate 200 mL YPAD and grown overnight ($OD_{600} < 1.0$), centrifuged, and washed in cold 1xPBS. Biotin is added and cells are rotated at 4°C for 2 hours. Magnets are then taped to tubes and kept at 4°C for 20 minutes to allow cells to settle. Fractions of loose cells are removed without disturbing the magnetically tagged cells on the tube. This is repeated 13-14 times, until daughter cells have been removed, then purified cells are used to inoculate another 200 mL YPAD for growth overnight. Magnetic purification is repeated to obtain the aged population of cells, with approximate generations based on OD_{600} increases during growth.

Biolabs) in 5 mL PBS at 4°C for about 2h. Following the incubation, the tubes were taped to strong magnets and allowed to settle for 20 minutes, then free cells were gently removed from the tubes. Cold YPAD was added, the remaining cells were gently resuspended and allowed to settle; this wash process was repeated at least 11 times

until there was no apparent improvement in purity of the old cells and hemocytometer counts indicated no more than 1×10^7 cells/mL. The purified culture was used to inoculate another 200 mL of YPAD and the process was repeated to age cells for ~14 generations or repeated twice to aged for ~18 generations. Strains deleted of *SIR2* were aged approximately 14 generations, as replicative lifespan is decreased in these strains.

4.2.2 Assay for cellular load of Hsp104-associated aggregates

In order to check age-related changes in cellular load of Hsp104-associated aggregates, wild-type and *sir2Δ* strains with chromosomal Hsp104-GFP were biotin-aged for 12-15 (*sir2Δ*) or 14-18 (wild-type) generations and examined by fluorescence microscopy for aggregates. “Average” age cells that were removed from the purified aged mother population were compared to the “aged” mother population. Numbers of aggregates per cell were enumerated and compared for the four populations: wild-type average age, wild-type old, *sir2Δ* average age, and *sir2Δ* old. For statistical purposes, experiments were compiled together and cells were classified as having or not having aggregates, with populations compared by Fisher’s Exact test, significance $p \leq 0.05$.

4.2.3 Assay for frequency of spontaneous $[PSI^+]$ formation

To determine frequency of spontaneous $[PSI^+]$ formation, wild-type and *sir2Δ* cells were aged an average of 14 generations, and wild-type were also aged additionally to an average of 18 generations so that cultures could be compared based on similar generational aging but each culture could also be analyzed at close to the end of expected lifespan. Fractions of purified “old”, “average” cells removed during purification from old, and biotinylated but “unaged” (T=0), cells were plated to –ADE plates and allowed to grow at 30°C for 21 days. For unaged and old populations, aliquots of 10, 100, and 880 μ L were plated to –ADE, with the remaining 10 μ L diluted and plated to

YPD to determine viable cells/mL. Aged cell counts by hemocytometer were used to determine the number of cells plated per aliquot. The “average” cell populations were then counted by hemocytometer and diluted so that an identical number of cells were plated from the “average” population for each “old” plating. The plating that yielded reasonably countable numbers of colonies was used to determine frequency for each culture.

4.3 Age-related changes in cellular load of Hsp104-associated aggregates

The effects of stress on cellular protein aggregation as identified by Hsp104-GFP-marked aggregates have been previously studied (Liu *et al.* 2010; Zhou *et al.* 2011; Saarikangas and Barral 2015), but studies of the effects of aging on aggregation and the role of Sir2 have been limited, and in the case of both *sir2Δ* and wild-type, “aged” cells have generally only meant an increase of only 10-12 generations compared to a younger population (Erjavec *et al.* 2007), and most of this work has reported on asymmetry of aggregates rather than changes in aggregate load. In order to see if yeast display age-related changes in cellular loads of Hsp104-associated aggregates, and to see if Sir2 plays a role in total aggregate load, we biotin-labeled and aged both wild-type and *sir2Δ* strains possessing chromosomal Hsp104 tagged with GFP and compared the number of aggregates per cell for “old” and “average” aged cells. Results are shown in Figure 4-2.

Very few wild-type average age cells had aggregates. Aged cell populations of both wild-type and *sir2Δ* cells had statistically higher proportions of cells with aggregates than average age cells from the same populations (Figure 4-2A). Wild-type aged cells and *sir2Δ* average age populations had similar proportions of cells with aggregates, but aged *sir2Δ* cell populations had statistically more cells with aggregates than the wild-

type aged and *sir2Δ* average age populations. Most cells with aggregates had only one dot, as seen in Figure 4-2B.

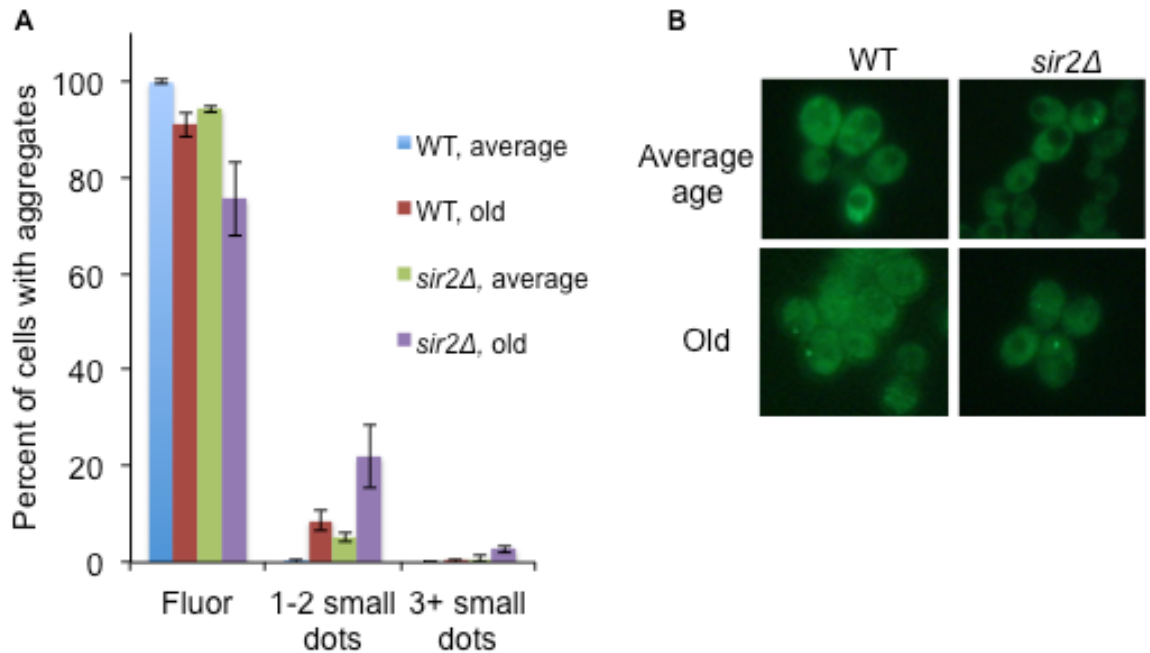


Figure 4-2. Average age vs. old wild-type and *sir2Δ* cells with Hsp104-marked aggregates. (A) Aged cells have similar levels of Hsp104-marked aggregates as *sir2Δ* strains. Wild type and *sir2Δ* strains with chromosomal *HSP104-GFP* were enriched for aged cells by biotin purification for an average of 14-18 generations, then checked for aggregates by fluorescence microscopy. Average and old cells are significantly different in terms of aggregates for each strain (classed as have aggregates or no aggregates for comparison). There is no difference in wild type old and *sir2Δ* average. (B) Wild type and *sir2Δ* cells both gain aggregates with age, but average age *sir2Δ* cells have more aggregates than wild-type. Error bars indicate standard error from compilation of experiments.

4.4 Frequency of spontaneous formation of $[PSI^+]$ in aged cells

Changes in formation of the prions $[PSI^+]$ and $[URE3]$ in aging yeast have been previously explored (Shewmaker and Wickner 2006) with no significant change detected, however, cultures in those experiments were aged for only about 10

generations, while normal yeast replicative lifespan is 20-30 generation (Steffen *et al.* 2009), thus it is possible that cells tested were not old enough to demonstrate detectable changes in $[PSI^+]$ formation.

In order to assess whether aged cells have a higher rate of $[PSI^+]$ spontaneous formation and to determine whether Sir2 and the asymmetric segregation apparatus play a role in possible changes to $[PSI^+]$ formation, $[psi^-][PIN^+]$ wild-type and *sir2Δ* cultures were enriched for aged cells by biotinylation and plated to determine frequency of spontaneous $[PSI^+]$ formation. Starting frequencies (“unaged”, T=0) varied quite a bit for this experiment, and while the wild-type did not show a significant increase in $[PSI^+]$ formation between T=0 and aged 14 generations cells, there was an increase of about 10-fold for *sir2Δ* (Figure 4-3).

The increase in $[PSI^+]$ formation between unaged (T=0) cells and aged 18 generations cells was not statistically significant for wild-type due to high deviation in formation frequency of aged wild-type cells. “Average” fractions, which were removed from the aged cells and used as a comparison here and in previous work (Shewmaker and Wickner 2006), varied quite a bit in $[PSI^+]$ formation and were not significantly different from either unaged (T=0) cells or old cells (Appendix Table A6).

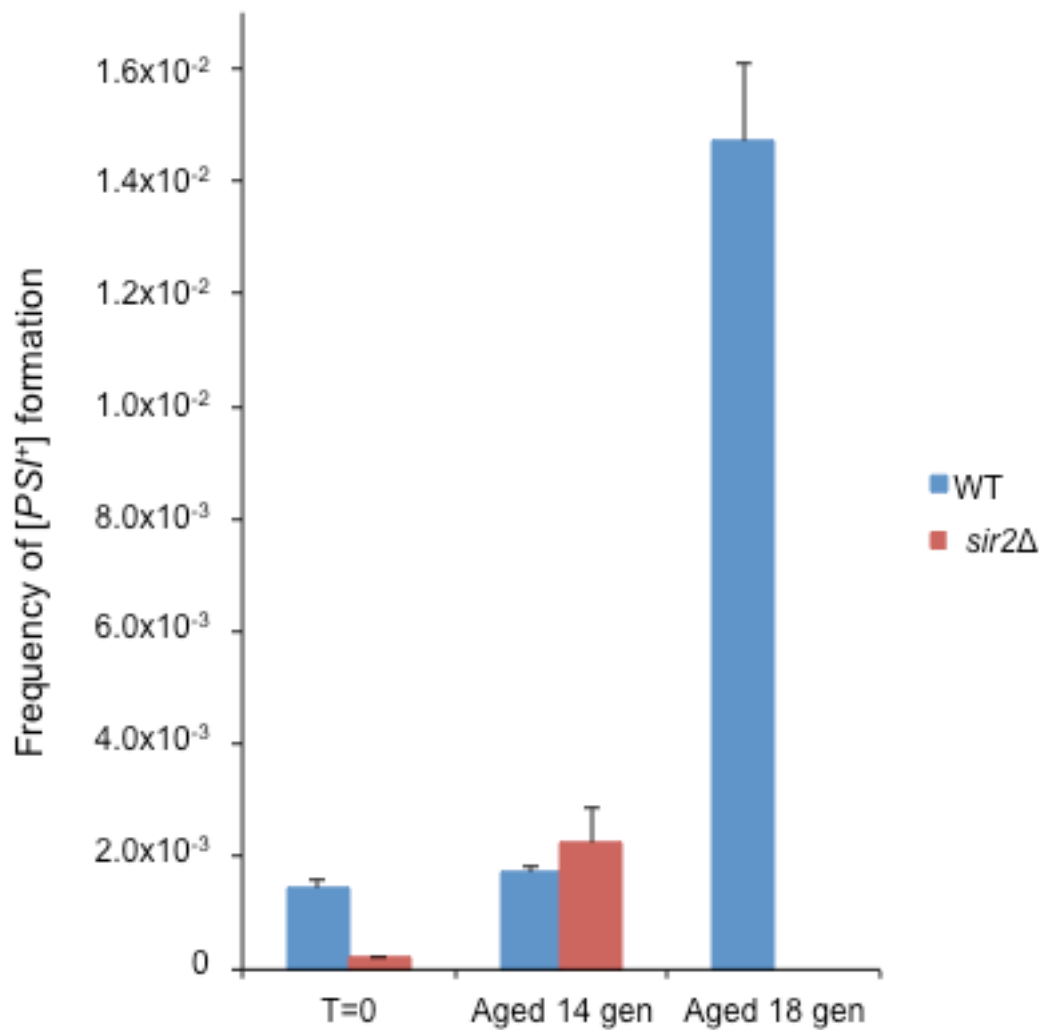


Figure 4-3. Frequency of spontaneous $[PSI^+]$ formation during replicative aging in wild-type and $sir2\Delta$ strains. Wild type and $sir2\Delta$ $[psi^-]$ strains were biotin-aged and plated to $-ADE$ to determine frequency of spontaneous $[PSI^+]$ formation. Aging increased appearance of $[PSI^+]$ in both strains. Three colonies from each strain were passaged on GuHCl to check curability; all were curable. Graph shows one experiment, error bars indicate standard error calculated from proportion of $[PSI^+]$ cells out of total cells plated. See Table A7 for all frequencies.

4.5 Discussion of Chapter 4 data

The finding here that aging causes increases in protein aggregation correlates well with previous studies (Erjavec *et al.* 2007; Hill *et al.* 2017) looking at aggregate formation and asymmetry of aggregates between aged cells and their daughters. While average age *sir2Δ* cells were similar in terms of aggregate load to aged wild-type, the fact that *sir2Δ* cells demonstrated further aggregation with age indicates that deterioration of the asymmetric segregation apparatus is not the only factor in age-dependent aggregate formation. The substantial increase in aggregation frequency for the *sir2Δ* cells compared to wild-type does however indicate that Sir2 plays an anti-aggregate role, most likely because asymmetric segregation is Sir2-dependent (Erjavec *et al.* 2007), and protein aggregates are usually segregated asymmetrically to mother cells during cell division. Without this asymmetry, daughter cells inherit aggregates more frequently and so more cells would be expected to possess aggregates from an earlier—newborn—point in the cell lifespan as opposed to aggregates forming after several cell divisions as has been described (Erjavec *et al.* 2007). Aging would be expected to amplify this, as cells form aggregates with age, seen here in both wild-type and *sir2Δ* cells (Figure 4-2).

Background frequencies of $[PSI^+]$ formation were substantially lower in *sir2Δ* cells compared to wild-type, but increased appreciably with aging 14 generations, whereas wild-type at the same generational aging did not show increased formation of $[PSI^+]$, as shown in Figure 4-3. One possible explanation for this is the loss of asymmetry in the *sir2Δ* cells. Aggregation is apparently increased with age in both strains (Figure 4-2), but in the *sir2Δ* strain these aggregates are diluted and so concentrations of aggregated Sup35 may not be as high as for the wild-type strain, making formation of $[PSI^+]$ less frequent. It is also possible that during aging, wild-type cultures accumulate more cells with aggregates, but asymmetric division prevents spread of aggregates to daughter

cells from old mother in wild-type, causing colonies from old mothers to be prion-free. In contrast, if $[PSI^+]$ forms in the *sir2Δ* cells, it is readily transmitted to daughters, causing colonies from those cells to be $[PSI^+]$ with higher frequency. It is also possible that wild-type cells aged 14 generations are not analogous to *sir2Δ* cells at the same age because *sir2Δ* shortens lifespan and the *sir2Δ* cells are at the end of expected lifespan while the wild-type are not. Indeed, the wild-type that were aged 18 generations were much more similar to *sir2Δ* aged 14 generations in terms of the increased $[PSI^+]$ formation compared to T=0, with a 2-10-fold increase in $[PSI^+]$ for wild-type at that age and about a 10-fold increase in $[PSI^+]$ for the *sir2Δ* cells, however variation in the wild-type at that age meant that even that difference was not significant. Much of the variation in this experiment came from the variation in starting frequencies, and changes were similar across different aging groups, but could not be grouped together because of variation in numbers. High variation in starting $[PSI^+]$ frequencies may be due to variations in proportions of aged cells in the culture. Plates used for starting cultures varied from 7 days to 10 days old, and it was recently found that cells with aged chronological lifespan (CLS) have higher rates of $[PSI^+]$ formation (Speldewinde *et al.* 2017).

It may seem contradictory that *SIR2* deleted cells demonstrated a lower frequency of *de novo* $[PSI^+]$ formation than wild-type, yet had higher cellular load of Hsp104-associated aggregates, especially as *sir2Δ* prevents destabilization of $[PSI^+]$ during heat stress as found previously in this work. These results may be explained by a role of the actin cytoskeleton in asymmetric segregation. Chernova *et al.* (2017) found that $[PSI^+]$ formation during heat stress was induced by Lsb2 localizing to actin patches in the cortical actin skeleton. The localized Lsb2 forms $[LSB2^+]$, which in turn induces formation of $[PSI^+]$. In addition to this finding for heat stress, actin was recently found to be

required for formation of $[PSI^+]$ during oxidative stress-induction (Speldewinde *et al.* 2017). The same actin, however, is necessary in asymmetric segregation, thus keeping aggregated proteins and $[PSI^+]$ in the mother cell during budding after heat stress and causing curing in the daughter. It is reasonable then, that disruption of actin by *SIR2* deletion (Liu *et al.* 2010) would inhibit formation of $[PSI^+]$ by disrupting concentration of Lsb2 and Sup35 at actin patches, but also would inhibit loss by disrupting asymmetric segregation of aggregates into the mother cell.

4.6 Conclusions of Chapter 4

- The process of aging in yeast is associated with increased formation of both Hsp104-associated protein aggregates and the prion $[PSI^+]$.
- Deletion of *SIR2* is concomitant with an increase in the frequency of cells possessing Hsp104-associated aggregates relative to the wild-type strain in both aged and unaged populations.
- Deletion of *SIR2* is associated with reduced *de novo* formation of $[PSI^+]$ relative to the wild-type strain in both aged and unaged populations.

CHAPTER 5. THE ROLE OF THE HSP70-SSB CHAPERONE AND RIBOSOME-ASSOCIATED COMPLEX (RAC) IN $[PSI^+]$ DESTABILIZATION BY HEAT SHOCK

The yeast Hsp70 chaperone Ssb is associated with translating ribosomes via the ribosome associated complex (RAC), which consists of the Hsp40 Zuo1 and Hsp70-Ssz1 and is found at the ribosomal exit tunnel to help correctly fold proteins. Overexpression of Ssb or release of Ssb from the ribosome to the cytosol by RAC deletion is known to promote $[PSI^+]$ curing by overproduction of Hsp104. Ssb release from the ribosome was previously implicated to impair the function of the Hsp104/Hsp70-Ssa chaperone complex in prion propagation by antagonizing Ssa. As the effect of heat shock on $[PSI^+]$ is known to coincide with an alteration of the Hsp104/Ssa balance, we hypothesized that Ssb plays a role in $[PSI^+]$ destabilization by heat shock. Here we show that depletion of the heat shock non-inducible chaperone Ssb decreases heat shock mediated destabilization of $[PSI^+]$, while disruption of the RAC components increases $[PSI^+]$ loss. These effects are not associated with changes in levels or kinetics of induction of the Hsp104 and Ssa proteins in cells defective by Ssb or RAC. Our data demonstrate that Ssb relocates from the ribosome to the cytosol during heat stress. As Ssb has been shown to antagonize the function of Ssa in prion propagation, these data support the role of the chaperone imbalance in prion destabilization and uncover the role of stress-induced re-localization of a stress non-inducible protein in the heat shock response.

5.1 Introduction to Chapter 5

The protein complex composed of the chaperone Hsp104, the major cytosolic member of the Hsp70 chaperone family (Ssa), and the co-chaperone Hsp40 plays the major role in disaggregation and solubilization of stress-damaged proteins in yeast

(Glover and Lindquist 1998; Glover and Lum 2009). Notably, the same chaperone complex is crucial for the propagation of most known yeast prions, including $[PSI^+]$ (Liebman and Chernoff 2012). The balanced action of the Hsp104 and Hsp70-Ssa/Hsp40 proteins breaks prion fibrils into oligomers, initiating new rounds of prion propagation (Kushnirov and Ter-Avanesyan 1998; Reidy and Masison 2011; Chernova *et al.* 2014). When Hsp104 is artificially overproduced in excess of Hsp70-Ssa/Hsp40, it antagonizes propagation of $[PSI^+]$ and some (but not all) other prions (Chernoff *et al.* 1995; Matveenko *et al.* 2018). This occurs due to the fact that Hsp104 binds prion fibrils independently of Hsp70-Ssa/Hsp40 (Winkler *et al.* 2012), resulting in prion loss due to malpartitioning in cell divisions (Ness *et al.* 2017). Another member of the Hsp70 family, Ssb, which is normally associated with the ribosome and acts in folding newly synthesized polypeptides, promotes $[PSI^+]$ elimination by excess Hsp104 when accumulated in the cytosol instead of the ribosomal fraction (Chernoff *et al.* 1999, Kiktev *et al.* 2015, Chernoff and Kiktev 2016). This effect of cytosolic Ssb has been shown to be due to its ability to antagonize binding of Ssa to prion aggregates (Kiktev *et al.* 2015, Chernoff and Kiktev 2016). While the effect of Ssb then has been demonstrated to play a role in $[PSI^+]$ curing by Hsp104 overexpression, it is unknown whether this mechanism also functions in destabilization of $[PSI^+]$ by mild heat shock.

5.2 Deletion of *ZUO1*, *SSZ*, or *SSB* and the effect on $[PSI^+]$ loss during mild heat shock

The ribosome-associated chaperone Hsp70-Ssb promotes $[PSI^+]$ curing by artificially overproduced Hsp104 (Chernoff *et al.* 1999), and release of Ssb from the ribosome to the cytosol in strains lacking one or both components of the ribosome-associated chaperone complex (RAC), Hsp40-Zuo1 and/or Hsp70-Ssz1, also leads to increased $[PSI^+]$ curing by excess Hsp104 and destabilization of some weak variants of

[*PSI*⁺] (Kiktev *et al.* 2015). It was previously shown that Ssb release is accompanied by a decrease in the proportion of Ssa bound to the Sup35 aggregates, suggesting that cytosolic Ssb impairs the function of the Hsp104/Hsp70-Ssa/Hsp40 chaperone complex in prion propagation by antagonizing Ssa (Kiktev *et al.* 2015, Chernoff and Kiktev 2016). As the effect of heat shock on [*PSI*⁺] coincides with an alteration of the Hsp104/Ssa balance, we checked whether Ssb plays a role in [*PSI*⁺] destabilization by heat shock. For this purpose, we deleted either one or both *SSB* genes (*SSB1* and/or *SSB2*) in the weak [*PSI*⁺] strain and subjected it to mild heat-shock at 39°C. Indeed, deletion of either one (*ssb1*Δ or *ssb2*Δ) or both (*ssb1/2*Δ) of the *SSB* genes dramatically impaired [*PSI*⁺] destabilization by mild heat shock, as shown in Figure 5-1.

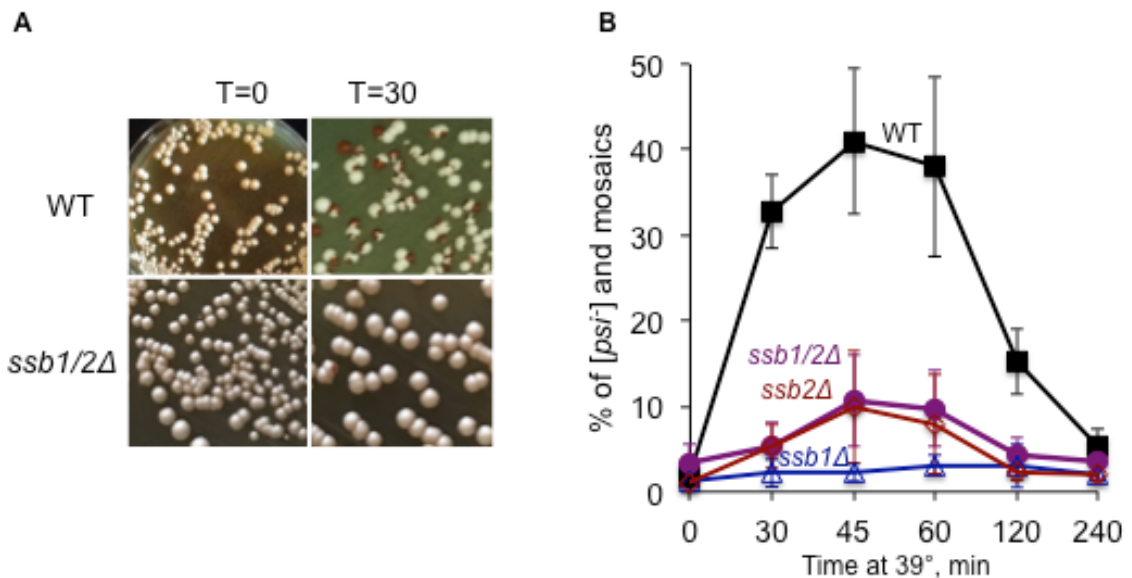


Figure 5-1. Effect of *ssb1/2*Δ on [*PSI*⁺] destabilization during mild heat shock. (A) Deletion of *SSB1/2* prevents curing. (B) Quantitative mild heat shock assay showing that *ssb1/2*Δ antagonizes [*PSI*⁺] destabilization by mild heat shock. Deletion of either *SSB1* or *SSB2* has an effect indistinguishable from the double deletion. WT (wild-type) is a compilation of all runs. Error bars indicate standard deviation. See Table A4 for percent curing and SD.

Reintroduction of Ssb2 on a centromeric plasmid (p366-6) into the *ssb1Δ* strain returned the wild-type result for destabilization of $[PSI^+]$ by mild heat shock (Figure 5-2) in a very limited preliminary trial (only one sample per strain and plasmid). Addition of the same *SSB2* plasmid to the *ssb1/2Δ* strain had no apparent effect as curing was still low, however addition of *SSB2* plasmid to the wild-type strain caused increased destabilization of $[PSI^+]$ as seen in Figure 5-2.

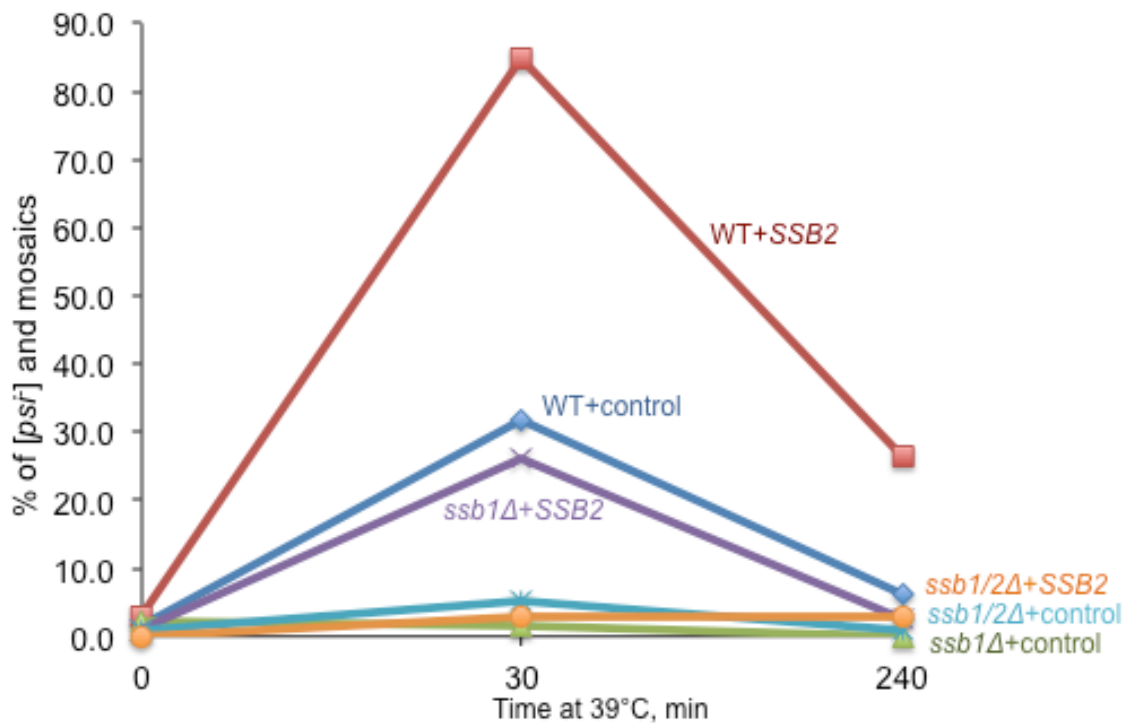


Figure 5-2. Effect of addition of *SSB2* plasmid on $[PSI^+]$ destabilization during mild heat shock. Quantitative mild heat shock assay showing that addition of *SSB2* returns the wild-type result in *ssb1Δ* and increases $[PSI^+]$ destabilization by mild heat shock in the wild-type (WT) strain. Addition of *SSB2* did not affect $[PSI^+]$ destabilization in *ssb1/2Δ*. Preliminary result for only one sample.

Since Ssb has been shown to promote $[PSI^+]$ curing by artificially overproduced Hsp104 (Chernoff *et al.* 1999), and release of Ssb from the ribosome to the cytosol in strains lacking one or both components of the ribosome-associated chaperone complex (RAC),

Zuo1 and/or Ssz1, also leads to increased $[PSI^+]$ curing by excess Hsp104 and destabilization of some weak variants of $[PSI^+]$ (Kiktev *et al.* 2015), we checked the effect of *zuo1Δ* and *ssz1Δ* on $[PSI^+]$ curing by mild heat shock. In contrast to deletion of Ssb, *zuo1Δ* and *ssz1Δ* both dramatically increased heat shock mediated $[PSI^+]$ destabilization (Figure 5-3).

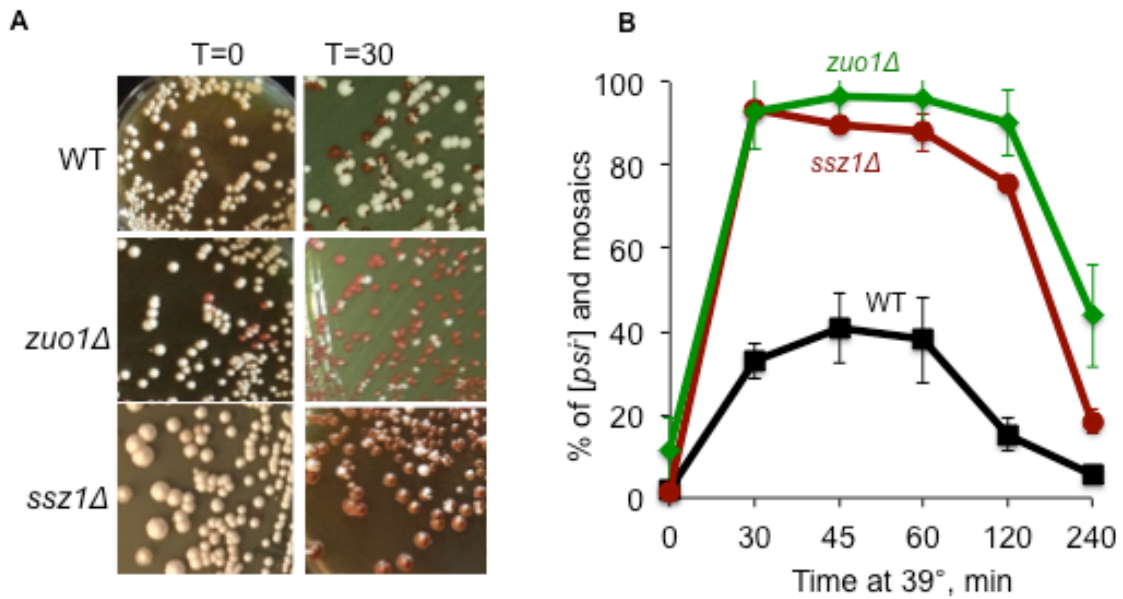


Figure 5-3. Effect of *zuo1Δ* or *ssz1Δ* on $[PSI^+]$ destabilization during mild heat shock. (A) Deletion of *ZUO1* or *SSZ1* increases curing from mild heat shock. (B) Quantitative mild heat shock assay showing that deletion of *ZUO1* or *SSZ1* increases $[PSI^+]$ destabilization by heat shock. WT (wild-type) is a compilation of all runs. Error bars indicate standard deviation. See Table A4 for percent curing and SD.

5.3 Heat shock protein levels in strains deleted in *ZUO1* or *SSB*

As the balance of Hsp104 and Ssa are shown to play the major role in destabilization of $[PSI^+]$ destabilization by mild heat shock, and one explanation for the effect of RAC component deletion or Ssb deletion on $[PSI^+]$ destabilization by mild heat shock could be that Hsp104 or Ssa levels are altered in the deletion strains, we checked

levels of Hsp104 for *ssb1/2Δ* and *zuo1Δ* at mild heat shock. Neither *ssb1/2Δ* nor *zuo1Δ* influenced Hsp104 levels compared to the wild-type strain before or during heat shock as determined by Western blot (Figure 5-4). Ssa levels were also checked for the *zuo1Δ* strain, with no change detected compared to wild-type (Figure 5-4B).

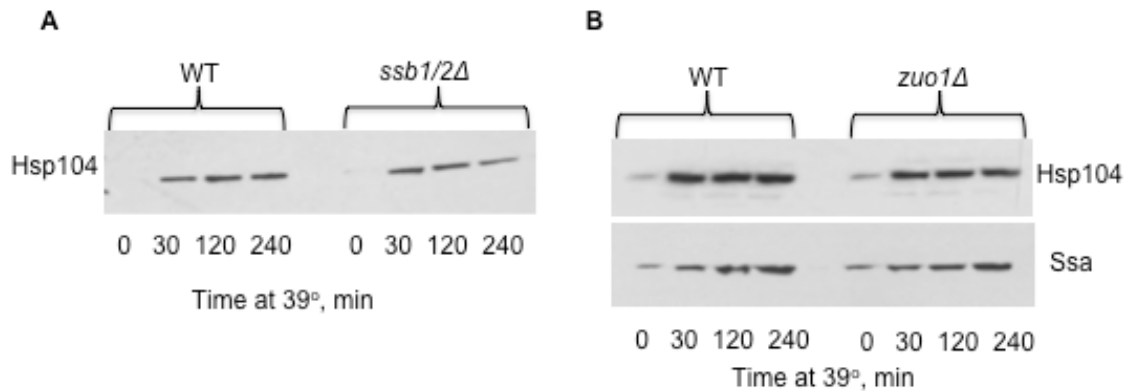


Figure 5-4. Hsp levels in *ssb1/2Δ* or *zuo1Δ* strains during mild heat shock. Hsp104 and Ssa levels in *ssb1/2Δ* or *zuo1Δ* strains. (A) Hsp104 levels are not altered by *ssb1/2Δ*. (B) Hsp104 and Ssa levels are not altered by *zuo1Δ*. Proteins purified after 0 or 30 minutes at 39°C were subjected to Western blotting.

5.4 The intracellular distribution of Ssb during mild heat shock

Release of Ssb from the ribosome to the cytosol in strains lacking one or both components of the RAC, Zuo1 and/or Ssz1, was previously shown to lead to increased $[PSI^+]$ curing by excess Hsp104 and destabilization of some weak variants of $[PSI^+]$ (Kiktev *et al.* 2015). It was demonstrated that this Ssb release is accompanied by a decrease in the proportion of Ssa bound to the Sup35 aggregates, suggesting that cytosolic Ssb impairs the function of the Hsp104/Hsp70-Ssa/Hsp40 chaperone complex in prion propagation by antagonizing Ssa (Kiktev *et al.* 2015, Chernoff and Kiktev 2016). To see if Ssb is released from the ribosome to the cytosol during mild heat shock, we performed sucrose gradient fractionation and subsequent Western blotting for Ssb.

While Ssb is not induced by heat shock (Iwahashi *et al.* 1995, Lopez *et al.* 1999), centrifugation of cell extracts in sucrose gradients demonstrated that a significant fraction of Ssb protein moves from the pellet fraction (corresponding to the ribosomal marker Rpl3) to the top (cytosolic) fractions in the extracts of heat shocked cells, compared to the non-shocked culture (Figure 5-5).

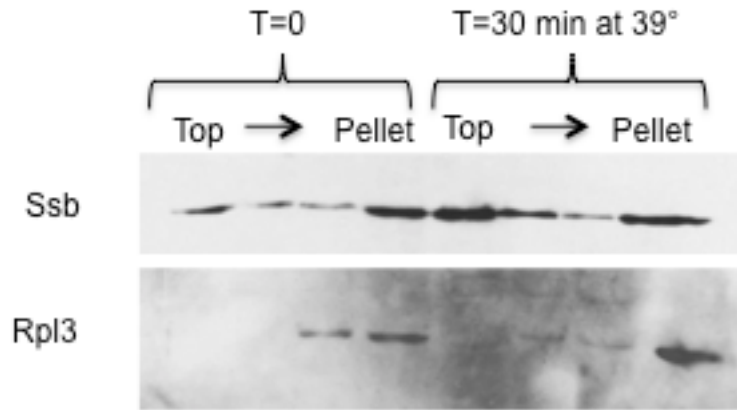


Figure 5-5. Effect of mild heat shock on Ssb localization. Ssb moves to the cytosol during heat shock in wild-type cells. Proteins purified after 0 or 30 minutes at 39°C were subjected to sucrose gradient centrifugation. Fractions from the sucrose gradient are (left to right): top, middle, bottom, pellet. Fractions were run on SDD-AGE tagged with Ssb or Rpl3 (ribosomal protein) antibody. Rpl3 is mostly in the pelleted fraction (some in bottom) but not in top or middle. Ssb is mostly in the pelleted fraction with ribosomes pre-heat shock but moves to the top fraction (cytosol) post-heat shock.

5.5 Discussion of Chapter 5 data

Our work has also uncovered a new role for the Hsp70 chaperone Ssb during heat shock. Ssb is normally found along with the proteins Zuo1 and Ssz as part of the ribosome associated complex (RAC), preventing misfolding of nascent polypeptides exiting the ribosome (Bukau *et al.* 2000; Koplín *et al.* 2010; Willmund *et al.* 2013), and disruption of the ribosome-associated complex of Zuo1 and/or Ssz1 (RAC) releases Ssb from the ribosome into the cytosol. Previous data show that cytosolic Ssb antagonizes

the binding of Ssa to Sup35 prion polymer, resulting in an effective shift of the balance between Hsp104 and prion-bound Ssa, and therefore in a defect in prion fragmentation and propagation (Kiktev *et al.*, 2015). Moreover, release of Ssb from the ribosome to cytosol is also observed in certain unfavorable growth conditions where translational rates go down and the number of the active polysomes is decreased, for example during growth in poor synthetic medium. Here we show that the release of Ssb from the ribosome to the cytosol is also induced by heat shock (Figure 5-5). Apparently, this release has functional consequences, as $[PSI^+]$ destabilization by mild heat shock is decreased in the cells lacking one or both SSB genes (Figure 5-1) therefore releasing less or no Ssb, but increased in *zuo1Δ* cells (Figure 5-3), where release of Ssb is known to be facilitated. Furthermore, addition of Ssb2 into the *ssb1Δ* strain tentatively returns the wild-type level of $[PSI^+]$ destabilization and addition of Ssb2 into the wild-type strain increases curing (Figure 5-2) indicating that $[PSI^+]$ destabilization by heat shock is dependent on total levels of Ssb in the cell. Taken together, our findings support the model of re-localization of Ssb into cytosol serving as a bridge between heat shock and aggregated proteins. Probably acting by further altering the balance between the polymer-associated Ssa and Hsp104 in favor of Hsp104, Ssb acts as an anti-prion agent during stress, impairing proliferation of prion aggregates in post-stress divisions. Heat shock induces massive protein aggregation (Wallace *et al.* 2015) and is shown to promote formation of at least some prions (Tyedmers *et al.* 2008; Chernova *et al.* 2017).

As at least some yeast prions are toxic to cells (Wickner *et al.* 2011), the anti-prion effect of Ssb during stress may have an adaptive role. Notably, transcription of SSB genes is not induced by heat shock (Lopez *et al.* 1999) therefore our data show that in addition to changes in expression, stress-induced alterations in intracellular localization of some chaperone proteins may also play a functional, possibly adaptive, role. This

parallels previous observations showing that re-localization of the Hsp40 protein Sis1 (a co-chaperone of Ssa) between the cytosol and nucleus, mediated by the stress-inducible sorting factor Cur1, also has functional consequences, including the effect on heat shock dependent $[PSI^+]$ destabilization (Barbitoff *et al.* 2017; Matveenko *et al.* 2018).

The model for heat shock mediated destabilization of $[PSI^+]$ that emerges from our data explains this process via the shift in the Hsp104/Ssa balance towards Ssa, which is facilitated by the Ssa-antagonistic effect of Ssb (relocated to the cytosol in stress conditions) and results in Sir2-dependent asymmetric distribution of prion aggregates between the mother and daughter cells in post-stress divisions, leading to malpartition and segregational loss of a prion, as shown in Figure 5-6. This links heritable protein aggregation to the general cellular response to accumulation of aggregated proteins in the stressed cells. Aggregates are prevented from being shorn into seed aggregates as Ssb moves to the cytosol and inhibits Ssa/Hsp104 fractionation of these aggregates, the large aggregates are segregated into the mother cell along with other aggregated proteins in an Hsp104-dependent manner, while smaller aggregates of $[PSI^+]$ remaining in the daughter may be sheared and refolded into monomers or degraded, leading to curing of $[PSI^+]$ in the daughter cells.

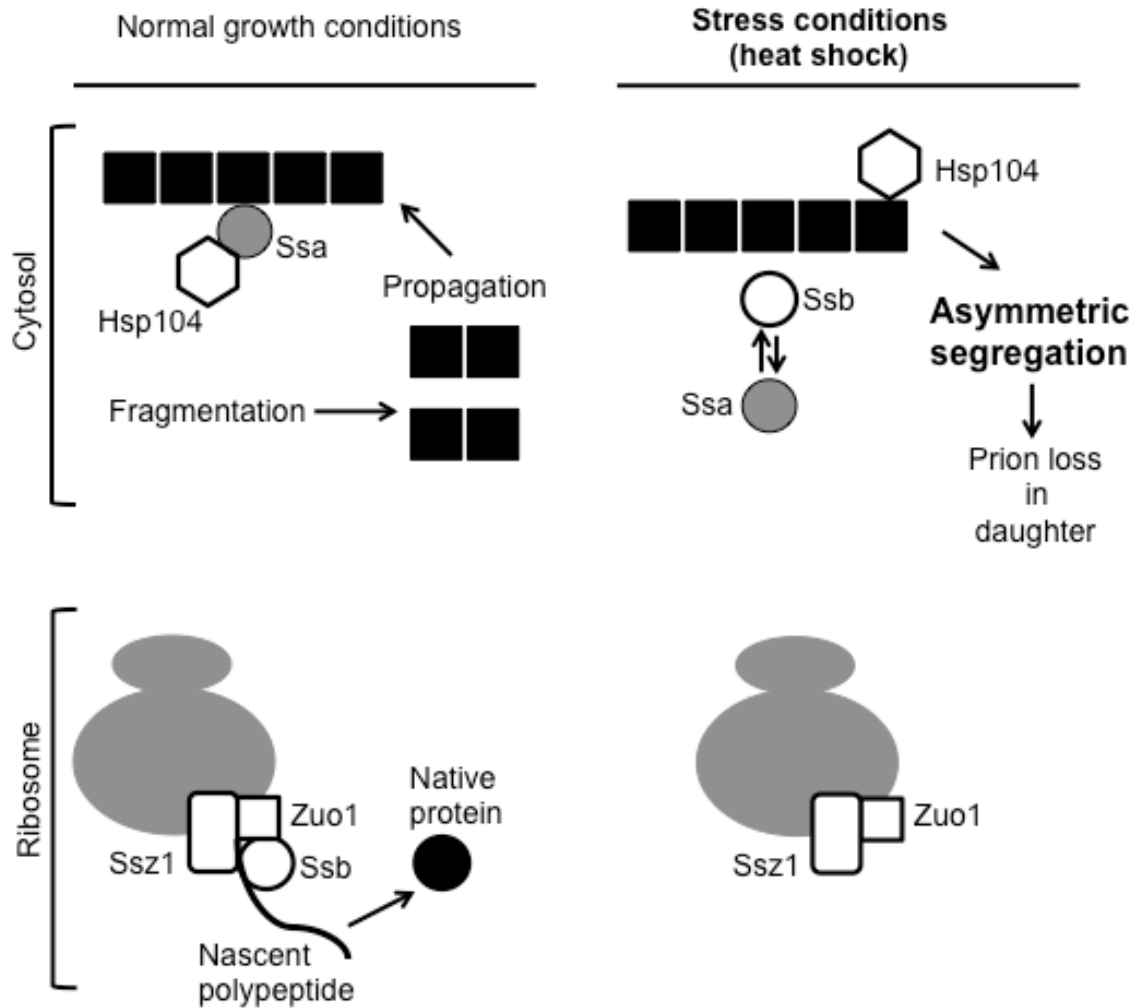


Figure 5-6. The role of Ssb in heat-shock mediated destabilization of $[PSI^+]$. During normal growth, Hsp104 and Ssa fragment $[PSI^+]$, while Ssb and the RAC (along with others) cause nascent polypeptides to fold correctly into their native structure. During heat shock, Ssb is released from the RAC to the cytosol, where it antagonizes Ssa. This prevents fragmentation of the prion and causes subsequent loss in the daughter due to asymmetric segregation during cell division.

5.6 Conclusions of Chapter 5

- Deletion of the RAC components Zuo1 or Ssz increases destabilization of [*PSI*⁺] during mild heat shock.
- [*PSI*⁺] destabilization by mild heat shock is inhibited by loss of the ribosome-associated chaperone Ssb, with deletion of either of the genes encoding Ssb preventing [*PSI*⁺] destabilization.
- Changes to [*PSI*⁺] destabilization by mild heat shock in *zuo1Δ* or *ssb1/2Δ* strains are not associated with detectable changes in the levels of Hsp104 or Ssa induction during heat shock.
- A significant fraction of the Ssb protein is relocated from the ribosome to the cytosol during heat shock.

CHAPTER 6. THE EFFECT OF THE RIBOSOME-ASSOCIATED COMPLEX ON FORMATION OF PRIONS BEYOND $[PSI^+]$

Yeast ribosome associated complex (RAC) and the associated Hsp70 protein Ssb are known to be involved in folding of nascent polypeptides. Defects in this system have previously been found to increase protein misfolding in general and the formation of the $[PSI^+]$ prion in particular. Heat shock is also known to cause massive protein misfolding and is known to induce some prions, in particular the metastable prion form of the cytoskeleton associated protein Lsb2, $[LSB^+]$. This prion can be detected by its ability to promote formation of another prion, $[PSI^+]$. We hypothesized that defects in the RAC or associated Ssb would increase formation of prions other than $[PSI^+]$, as increased protein aggregation should also increase the general likelihood of prion formation. Here we show that deletion of the gene for the RAC component *ZUO1* causes increased spontaneous formation of the prion $[URE3]$, and that the simultaneous deletion of both Ssb-encoding genes greatly increases heat-shock induced formation of prion(s) possessing the $[PSI^+]$ inducing effect (similar to $[LSB^+]$). These results indicate that the RAC and Ssb act as an anti-prion system whose effect is not restricted only to $[PSI^+]$, and that Ssb specifically plays an anti-prion role during stress.

6.1 Introduction to Chapter 6

The build-up of misfolded proteins is the basis of an ever-growing list of diseases (Gregersen *et al.* 2006), thus correct protein folding is of the utmost importance to cells. To ensure correct protein folding, eukaryotic cells possess chaperones linked to protein synthesis that are associated with the nascent polypeptide (Albanèse *et al.* 2006). In *S. cerevisiae*, the ribosome associated complex (RAC), consisting of the Hsp70 Ssz1 and the Hsp40 Zuo1, along with an associated Hsp70 chaperone Ssb (encoded by *SSB1*

and *SSB2*), is associated with the ribosome near the exit tunnel and works to prevent misfolding of nascent polypeptides (Willmund *et al.* 2013; Döring *et al.* 2017). Deletion of *SSB1/2* causes increased [*PSI*⁺] formation (Chernoff *et al.* 1999) and widespread protein aggregation (Willmund *et al.* 2013), and deletion of RAC components leads to increased spontaneous and induced formation of [*PSI*⁺] (Amor *et al.* 2015). While intact Ssb and the RAC are thus demonstrated to work against *de novo* formation of [*PSI*⁺], it is currently unknown whether this effect is generalizable to all prions or if Sup35 is specifically prone to aggregation and prion formation in Ssb/RAC-deficiency. In order to determine whether RAC or Ssb deficiency leads to general prion formation, we tested the effect of *zuo1Δ* and *ssb1/2Δ* on other prions.

6.2 Materials and methods for Chapter 6

6.2.1 Fluctuation test for formation of prion

In order to determine spontaneous induction of [*URE3*], a modified Luria-Delbruck fluctuation assay was used (Lancaster *et al.* 2010, Amor *et al.* 2015), as shown in Figure 6-1. Colonies that were [*ure0*] were streaked to YPD for single colonies. Twelve colonies each from wild-type and *zuo1Δ* platings were selected and suspended in 110 μL of sterile water. Ten microliters of this suspension was diluted and plated to YPD to determine total viable cell counts. The remaining suspension was plated onto synthetic media lacking adenine (-ADE media) in two aliquots of 10 and 90μL, then incubated at 30°C for 21 days to select for [*URE3*] cells. Frequencies and calculated rates include [*URE3*] colonies and cell numbers for both platings combined. In order to determine that colonies were spontaneously formed prion and not mutations, a subset of colonies was checked for curing by guanidine hydrochloride (GuHCl) at a concentration

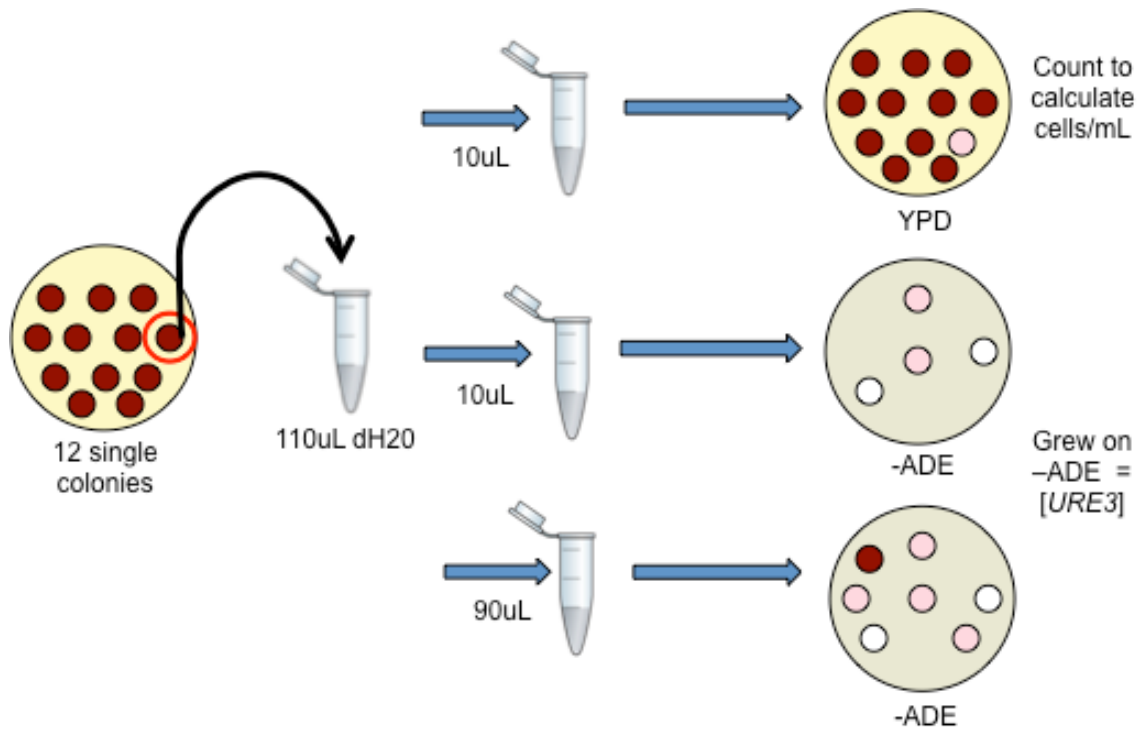


Figure 6-1. Fluctuation test for spontaneous [URE3] formation. Cultures are streaked to YPD and 12 single [*ure0*] colonies are selected. Each colony is suspended in 110µL of sterile water. Ten microliters of suspension is used to quantify cell numbers by dilution plating to YPD. The remaining suspension is plated in two aliquots of 10µL and 90µL to -ADE plates. YPD plates are grown 3-7 days and colonies enumerated to determine cell counts, -ADE plates are grown at 30°C for at least 14 days after which colonies are counted to determine frequency of [URE3]. Frequency and cell counts are then used to calculate rate.

of 2mM, as *zuo1Δ* is known to cause sensitivity to GuHCl. The rate of [URE3] as indicated by ADE⁺ and the 95% Confidence Intervals were estimated as previously described (Amor *et al.* 2015).

6.2.2 Heat shock induction of [PRN⁺] assay

Induction of the prion [PSI⁺] was used to check for a secondary prion, [PRN⁺], presumably [LSB2⁺], as described previously (Chernova *et al.* 2017) and in Figure 6-2. Wild-type and *ssb1/2Δ* cultures that were [*psi*⁻] [*pin*⁻] and possessed the *ade1-14*

background and reporter system for $[PSI^+]$ were first transformed with a Gal-Sup35N plasmid, then grown in YPD liquid overnight at 25°C. Cultures were diluted into YPD to $OD_{600}=0.1$, grown for two hours, then sampled at T=0. Samples were diluted and counted with a hemocytometer, and approximately 500 cells were plated to media selective for plasmid. The remaining culture was shifted to 39°C for 120 minutes, sampled, and plated to selective media. Plates were grown at 30°C for 3 days, velveteened to Gal selective for plasmid, grown 3 days, then velveteened to –ADE. Colonies that grew on –ADE were considered induced, as $[PSI^+]$ does not form appreciably without the existence of a secondary prion (Liebman and Chernoff 2012; Chernova *et al.* 2017), which may be $[PIN^+]$, but in the $[pin]$ background for this assay has been reported to be $[LSB^+]$ (Chernova *et al.* 2017). A subset of ADE+ colonies were passaged on GuHCl to check curability and ensure that growth on –ADE was due to formation of $[PSI^+]$. Colonies that had induced were also checked for stability of $[PRN^+]$ by checking sustained ability to induce. For stability assessment, colonies that had induced were taken from the original selective media plate (prior to Gal induction), streaked onto media selective for the Gal-Sup35N plasmid, and single colonies were patched to selective media. Plates were then velveteened to Gal selective for plasmid, grown 3 days, then velveteened to –ADE. Inducing original colonies that produced at least 2 out of 12 (Chernova *et al.* 2017) inducing subcolonies (grew on –ADE) were considered stable.

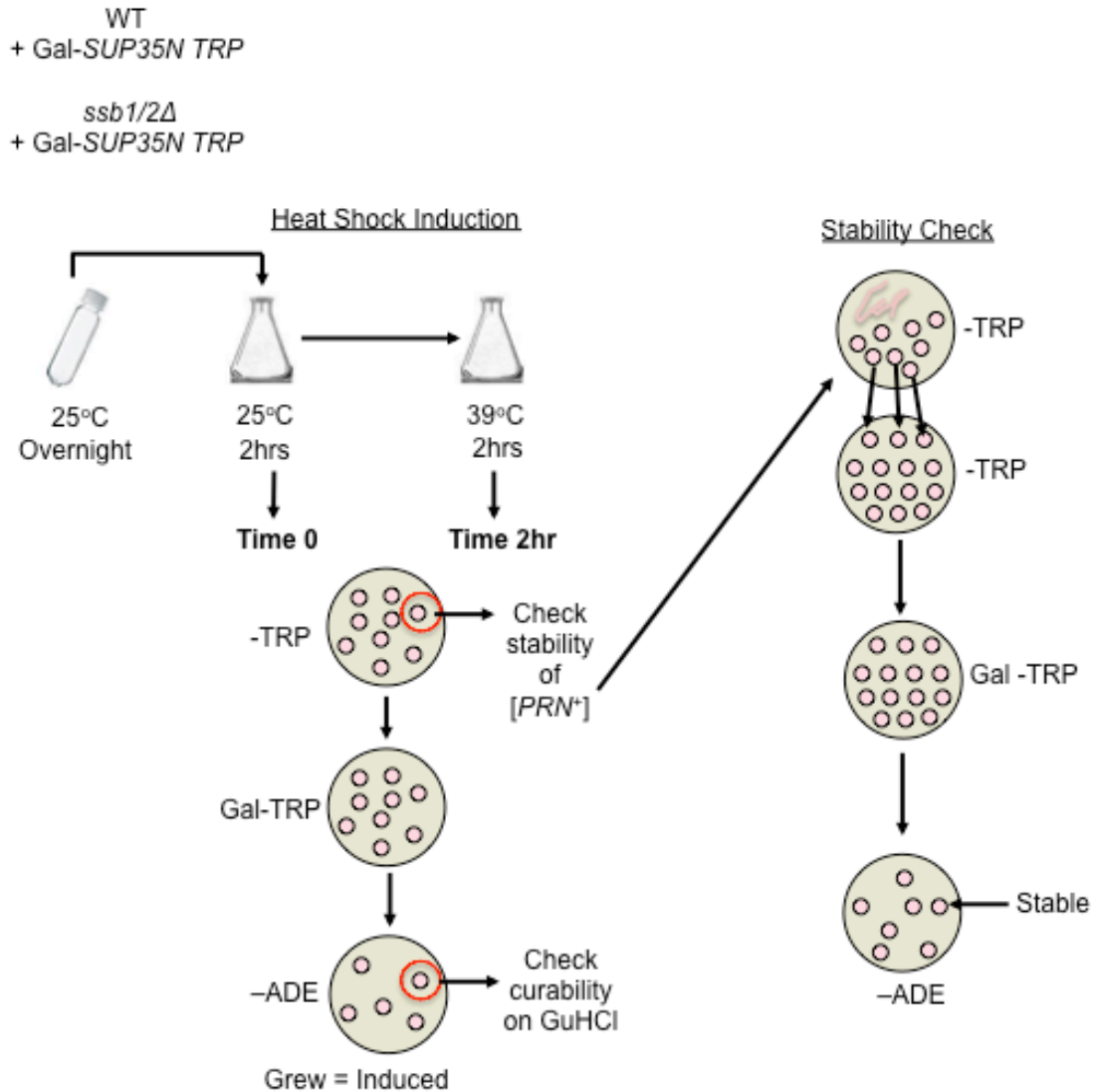


Figure 6-2. Procedure for heat shock induction of a prion $[PRN^+]$. Induction of the prion $[PSI^+]$ is used to check for a secondary prion, presumably $[LSB2^+]$, but designated $[PRN^+]$. Cultures that are $[psi^-]$ $[pin^-]$ are transformed with Gal-Sup35N plasmid, grown in YPD overnight at 25°C, then diluted into YPD to $OD_{600}=0.1$. Cultures are grown two hours, then samples for T=0 were taken and ~500 cells plated to media selective for plasmid (-TRP). Remaining culture was shifted to 39°C for 120 minutes, then sampled and plated. Plates were grown at 30°C for 3 days, velveted to Gal selective for plasmid, grown 3 days, then velveted to -ADE. Colonies that grew on -ADE were considered induced. Several ADE+ colonies were passaged on GuHCl to check curability. Colonies that induced were checked for stability of the $[PRN^+]$ by checking sustained ability to induce.

6.3 The impact of *zuo1Δ* on formation of [URE3⁺]

Deletion of the gene encoding RAC component Zuo1 has previously been shown to increase formation of the prion [PSI⁺] (Amor *et al.* 2015), an aggregated form of the yeast translation termination factor Sup35 that is curable by Hsp104 overexpression. The yeast prion [URE3] is the prion form of a transcription factor, Ure2, which is normally involved in nitrogen metabolism (Wickner 1994; Hong *et al.* 2011; Liebman and Chernoff 2012). To determine whether *zuo1Δ* impacts formation of [URE3], we deleted *ZUO1* in a [*ure0*] strain that had been modified to use the *ade1-14* background and reporter system for [URE3] (Hong *et al.* 2011). In this strain, growth on –ADE media indicates the conversion from [*ure0*] to [URE3]. We first checked to see if *zuo1Δ* affects formation of [URE3] by overexpression of Ure2 (Wickner 1994). For this assay, wild-type and *zuo1Δ* strains were transformed with *URE2* under the *GAL* promoter and passaged on galactose media selective for plasmid before velveteneing to –ADE. Induction of [URE3] was assessed after growth at 30°C for 7 days. To our surprise, we found that induced formation of [URE3] was not detected in the *zuo1Δ* strain (Figure 6-3). In the wild-type strain, 30 out of 30 colonies were induced to [URE3] with overexpression of Ure2, however none (0 of 30) of the *zuo1Δ* colonies became [URE3]. Given that the *zuo1Δ* strains were previously observed to grow slower than wild-type, the plates were allowed to incubate for an additional 9 days (16 days total), but this had no effect on induction of [URE3] in the *zuo1Δ* strain.

As induction of [URE3] by overexpression of Ure2 was not detected in the *zuo1Δ* strain, a fluctuation assay (Figure 6-1) was performed to determine whether *zuo1Δ* has any effect on spontaneous formation of [URE3]. Contrary to the induction assay, the fluctuation test resulted in dramatically increased frequency of formation of [URE3] as

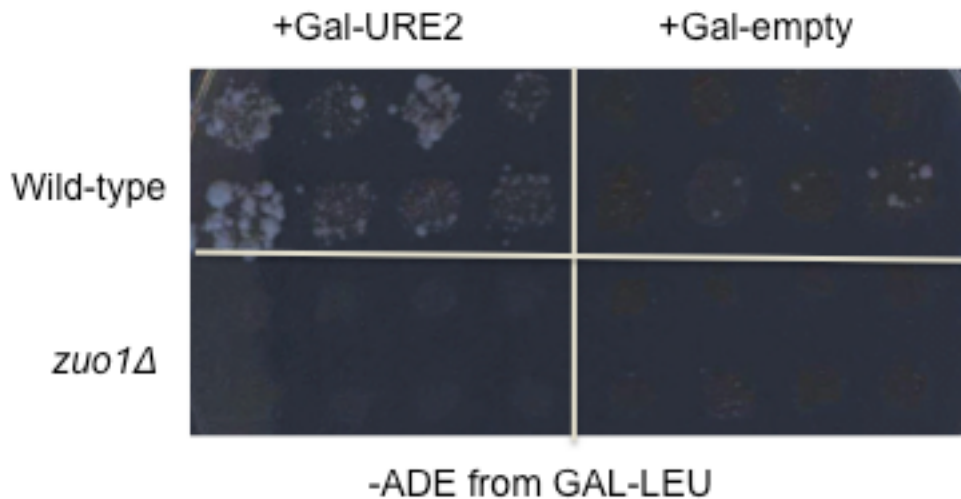


Figure 6-3. Induction of the prion [URE3] in wild-type and *zuo1Δ* strains. Deletion of *ZUO1* decreases detectable induction of [URE3] by overexpression of *URE2*. Strains were transformed with *URE2* under the Gal promoter and passaged on Gal selective for plasmid before velveteneering to –ADE.

well as generational rate of formation in the *zuo1Δ* strain as compared to wild-type (Figure 6-4). Colonies formed by the *zuo1Δ* strain were noticeably smaller than the wild-type (Figure 6-4B), and had a higher proportion of incurable colonies (Table 6-1), however a majority of colonies from both strains were curable by GuHCl (2mM) and stable (Table 6-1), indicating that these colonies were in fact [URE3].

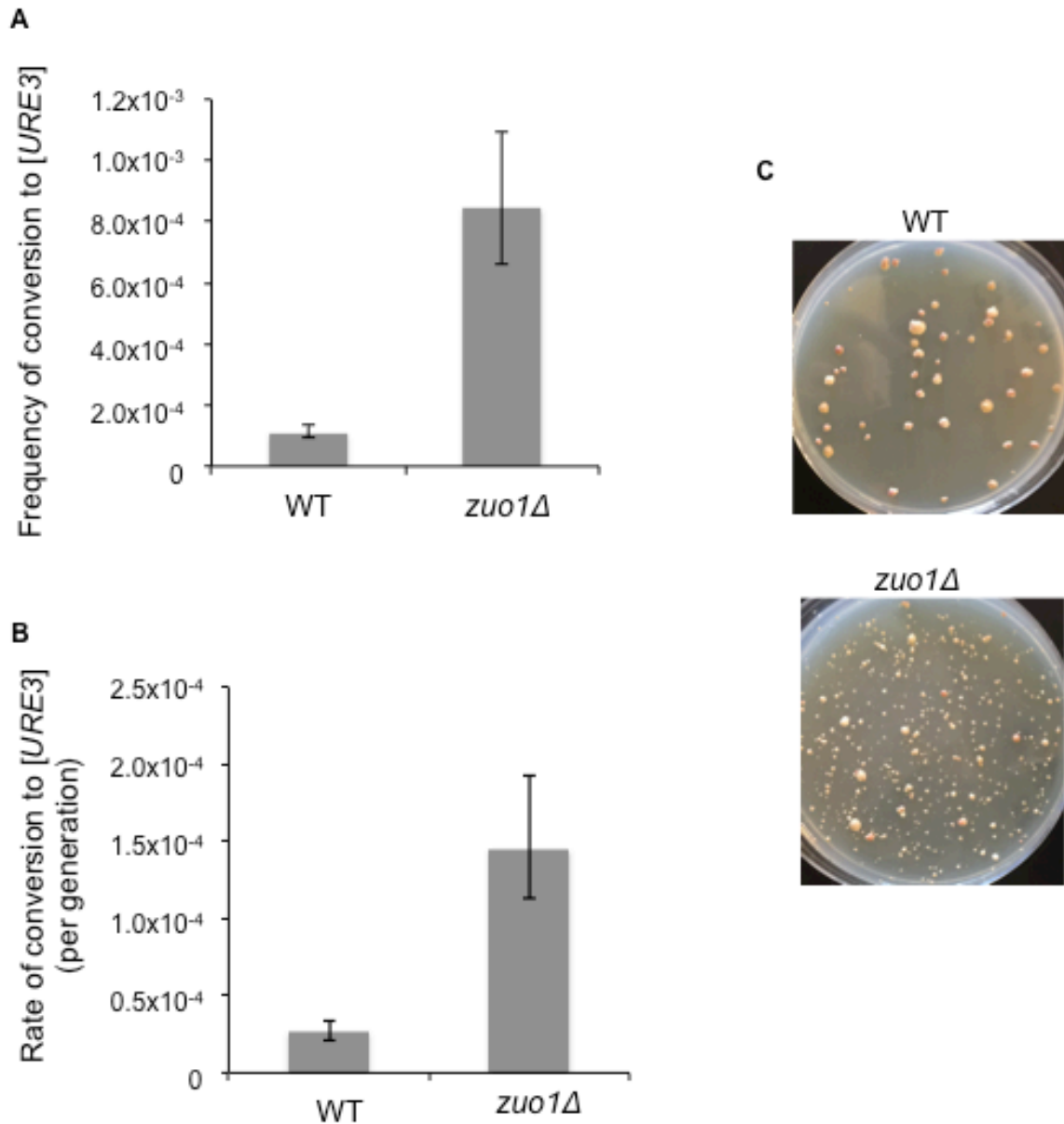


Figure 6-4. Effect of *zuo1Δ* on spontaneous formation of the prion [URE3]. (A) Deletion of *ZUO1* increases frequency of formation of [URE3] as assessed by fluctuation assay. Error bars represent 95% confidence interval. Fluctuation assay performed as described, experiment performed twice with similar results each time, results for one experiment shown. (B) Calculated rate of formation of [URE3]. Error bars represent 95% confidence interval. (C) –ADE plates from *zuo1Δ* had dramatically increased formation frequency of [URE3]. See Tables A8 and A9 for all frequencies and rates.

Table 6-1. Curability and stability rates of spontaneously formed [URE3].

		WT	<i>zuo1Δ</i>
Cured	Stable	9	6
	Unstable	2	2
	Total	11 (100%)	8 (67%)
Not cured	Stable	0	4
	Unstable	0	0
	Total	0 (0%)	4 (33%)
Total tested		11	12

6.4 The effect of *ssb1/2Δ* on induction of prions by heat shock

Formation of [PSI⁺] has previously been demonstrated to increase in *ssb1/2Δ* strains (Chernoff *et al.* 1999) and, although widespread protein aggregation has also been reported (Willmund *et al.* 2013), it is unknown whether *ssb1/2Δ* alters formation of prions beyond [PSI⁺]. In order to address this question, we compared wild-type and *ssb1/2Δ* strains in a heat shock induction of [PRN⁺] assay, which uses induction of the prion [PSI⁺] to check for a secondary prion, presumably [LSB2⁺], as described previously (Chernova *et al.* 2017) and in Figure 6-2. While *de novo* formation of [PSI⁺] is very rare, even with overexpression of Sup35, presence of another prion, such as [LSB⁺] or [PIN⁺],

in the cell causes conversion of monomeric Sup35 to the prion form $[PSI^+]$ (Figure 6-5).

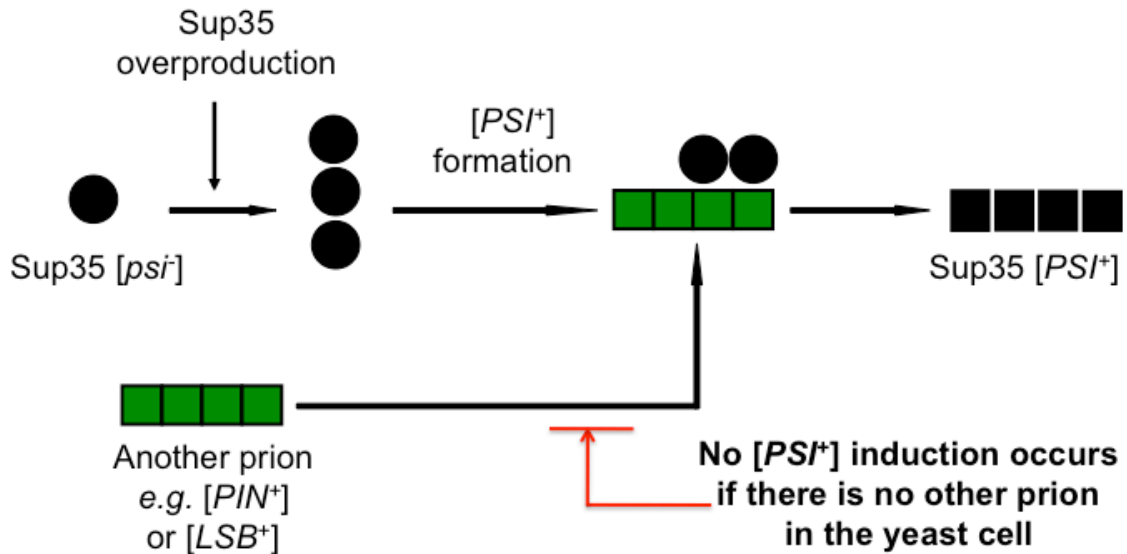


Figure 6-5. Presence of another prion induces $[PSI^+]$ formation. Presence of another prion, e.g. $[PIN^+]$ or $[LSB^+]$, is required to induce formation of $[PSI^+]$ from Sup35 overproduction.

As shown previously in Figure 6-2, the assay used here induces presence of a prion, designated $[PRN^+]$ and possibly $[LSB^+]$ but as yet undetermined, by heat shock. Presence of this prion is then able to promote conversion of Sup35 into $[PSI^+]$ when Sup35 is overproduced as described in Figure 6-2. When this assay was performed, deletion of the genes coding for Ssb, $SSB1$ and $SSB2$, caused dramatically increased induction of prion from heat shock, as shown in Figure 6-6. While inducible colonies were less than 1% of total colonies in wild-type strains or in $ssb1/2\Delta$ prior to heat shock, induction after heat shock in the $ssb1/2\Delta$ strain was over 17% of colonies checked (Table 6-2). The two colonies counted as inducing for the wild-type strain (one at $T=0$, one at $T=120$ min) were both unstable (0% stability), however, 100% and 91% of

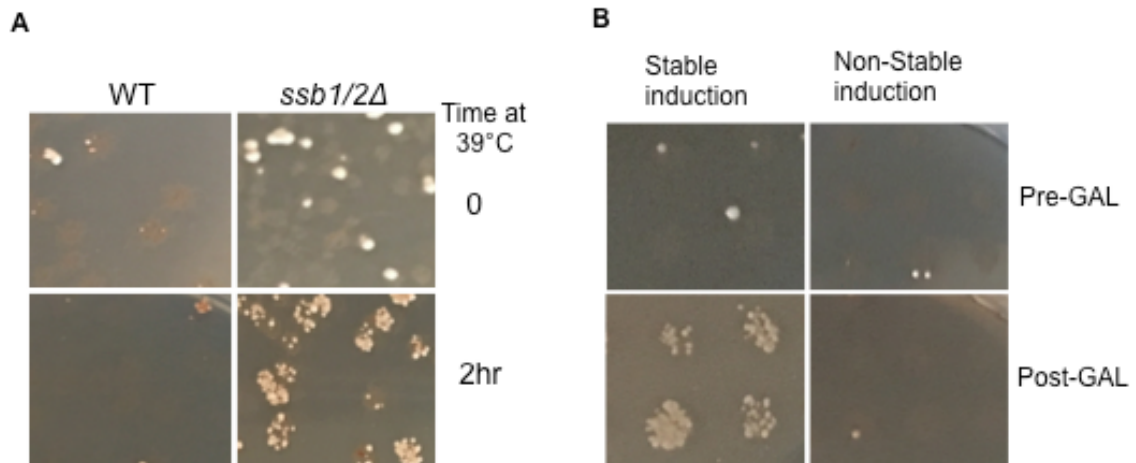


Figure 6-6. Effect of *ssb1/2Δ* on induction of a prion $[PRN^+]$ with $[PSI^+]$ inducing effect by mild heat shock. (A) Deletion of *SSB1/2* promotes induction of a $[PRN^+]$ by mild heat shock as reported by formation of $[PSI^+]$. Plates showing colony induction, with dramatic increase of induction at 2hr for *ssb1/2Δ*. $[psi^-]$ $[pin^-]$ strains transformed with $P_{GAL}SUP35$ were subjected to 39°C; pre- and post- shocked cells were plated and passaged on Gal selective for plasmid then velveted to $-ADE$ to check inducibility of $[PSI^+]$. Inducible colonies are considered to have a prion ($[PRN^+]$), likely $[LSB2^+]$, as $[PSI^+]$ does not induce alone. (B) Stability of inducing colonies. Inducing colonies were streaked on selective media and 14-15 sub-colonies were checked for stability of induction. Stable colony sub-colonies on left, non-stable colony sub-colonies on right.

ssb1/2Δ colonies checked from the same respective time points were stable, (Figure 6-5 and Table 6-3). Curability of a subset of the induced colonies taken from $-ADE$ and passaged on 2mM GuHCl revealed that 100% of colonies were curable (Figure 6-7), confirming that growth on $-ADE$ indicates presence of prion.

Table 6-2. Induction of $[PSI^+]$ by a prion $[PRN^+]$ by mild heat shock in wild-type vs. $ssb1/2\Delta$ strains.

39°C min	WT			<i>ssb1/2Δ</i>		
	Colonies inducible	Total tested	Percent inducible	Colonies inducible	Total tested	Percent inducible
0	1	1882	0.05%	36	10223	0.4%
120	1	2097	0.05%	442	2499	17.7%

Table 6-3. Stability of a prion $[PRN^+]$ with $[PSI^+]$ -inducing effect by mild heat shock in wild-type vs. $ssb1/2\Delta$ strains.

39°C min	WT			<i>ssb1/2Δ</i>		
	Stable colonies	Colonies tested	Percent stable	Stable colonies	Colonies tested	Percent stable
0	0	1	0%	7	7	100%
120	0	1	0%	10	11	91%

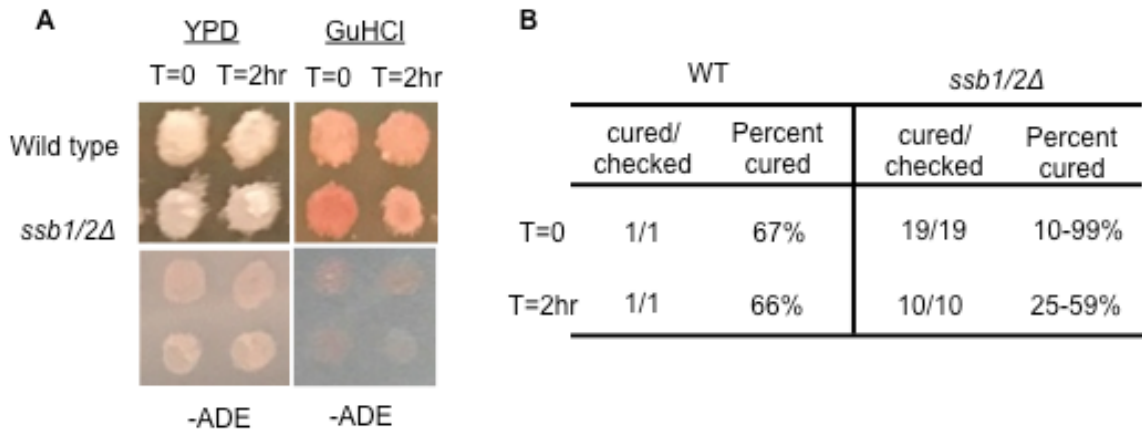


Figure 6-7. Curability of $[PSI^+]$ colonies induced by a prion $[PRN^+]$. (A) Induced colonies are curable by GuHCl (2mM) for both wild type and *ssb1/2Δ* cultures. Passage on YPD or GuHCl and subsequent velveteneing to -ADE. (B) Rates of curing for induced colonies. Number of colonies that cured out of those checked. Colonies were streaked out on YPD after passage on either YPD or GuHCl and reds, mosaics, and pinks counted to determine percent curing. Colonies with higher rates of reds + mosaics after passage on GuHCl compared to YPD passage were considered cured.

6.5 Discussion of Chapter 6 data

The RAC and the associated chaperone Ssb have previously been demonstrated to play a role in preventing protein misfolding (Willmund *et al.* 2013) and to antagonize formation of the prion $[PSI^+]$ (Chernoff *et al.* 1999; Amor *et al.* 2015; Chernoff and Kiktev 2016). The increases in formation of $[URE3]$ (Figures 6-4) and $[PRN^+]$ (Figure 6-6) in RAC or Ssb-deficient strains in this work demonstrate that the role of the RAC and Ssb in prevention of prion formation is not limited to $[PSI^+]$, but includes other prions as well. The most likely explanation for the increase in prion formation seen in this work and others is that increases in protein misfolding overall cause an increased misfolding of prion proteins as well, perhaps even more than normal proteins, as most prion proteins are overly prone to misfolding and aggregation even in the best circumstances. Initial

misfolding of prion proteins off of the ribosome increases prion formation generally, as modeled by Kiktev *et al.* (2015). In this light, the lack of [URE3] induction (Figure 6-3) when Ure2 is overproduced in the *zuo1Δ* strain is unexpected. There are several possibilities for this difference in results. One possibility is toxicity/incompatibility or a defect of viability, as [URE3] formation with no induction is already very high in the *zuo1Δ* strain. Pushing [URE3] formation even higher via Ure2 overexpression may cause toxicity, as previously reported for Sup35^{NM} in a *zuo1Δ* strain (Amor *et al.* 2015). It is also possible that there is a defect in [URE3] stability when Ure2 is overproduced. The relatively small colonies for the *zuo1Δ* strain (Figure 6-4B) compared to wild-type seen in the spontaneous formation assay support the hypothesis that [URE3] is incompatible with the *zuo1Δ* strain, as [URE3] may be gained but quickly lost, limiting colony growth. The relatively high proportion of the seemingly incurable [URE3] in the *zuo1Δ* strain compared to wild-type may be due to problems with curability of *zuo1Δ* in general due to sensitivity of *zuo1Δ* to GuHCl, or it may be due to secondary formation of ADE⁺ mutants on the basis of poorly growing [URE3] derivatives in the *zuo1Δ* background. The latter explanation is consistent with the smaller colony size and supports the concept of incompatibility of the [URE3] prion with the *zuo1Δ* background. It is also possible that transformation and maintenance in the *zuo1Δ* background causes rearrangement, which could be checked by plasmid digestion or sequencing from the *zuo1Δ* transformants, however this is unlikely as overexpression by the same plasmid induced [URE3] in the wild-type strain.

The increase in spontaneous formation of [URE3] prion in the *zuo1Δ* strain (Figure 6-4) supports previous work showing increased formation of [PSI⁺] in RAC-deficient strains (Amor *et al.* 2015; Kiktev *et al.* 2015), and points to a model where the RAC-Ssb system works to prevent prion formation by preventing initial protein misfolding. The

dramatic increase in heat shock-mediated formation of prions with $[PSI^+]$ -inducing effect seen when both *SSB* genes are deleted (Figure 6-6 and Table 6-2) also points to the anti-prion function of Ssb. This result may be due to the role that Ssb plays in initial protein misfolding on the ribosome, as increased protein misfolding causes increased prion protein aggregate load in the cell and this increased aggregate load may then form prion more frequently during heat shock. However, it may also be due to the now demonstrated anti-prion role of Ssb in the cytosol during heat shock. As the Hsp104/Ssa chaperone system is necessary for propagation of $[PSI^+]$ as well as other prions, and is now shown to be antagonized by Ssb during heat shock, prion that is formed during heat shock and then normally lost due to the antagonizing effect of Ssb on Hsp104/Ssa may not be lost in the *ssb1/2Δ* strain. This would help to explain why most isolates with the $[PSI^+]$ -inducing effect generated in the *ssb1/2Δ* strain are mitotically stable, in contrast to the known prion $[LSB^+]$ induced by heat shock in the wild type strain (Table 6-3). It may also be that other more stable prions, such as $[PIN^+]$ are also induced in the *ssb1/2Δ* strain, increasing the stability of $[PSI^+]$ induction.

6.6 Conclusions of Chapter 6

- Deletion of the gene coding for the ribosome-associated chaperone Zuo1 increases spontaneous formation of the $[URE3]$ prion.
- Deletion of any or both *SSB* genes greatly increases heat shock mediated formation of prions with the $[PSI^+]$ -inducing effect.
- Most isolates with the $[PSI^+]$ -inducing effect generated in the *ssb1/2Δ* strain show higher stability than the known prion $[LSB^+]$ induced by heat shock in the wild type strain.

GENERAL CONCLUSIONS

- Sir2, a protein necessary to the cellular asymmetry apparatus, plays a role in the asymmetric segregation of $[PSI^+]$ aggregates after heat stress, leading to destabilization and loss of the prion in daughter cells.
- Replicative aging in yeast is associated with increases in both protein aggregation and formation of the prion $[PSI^+]$.
- $[PSI^+]$ destabilization by mild heat shock is dependent on the ribosome associated Hsp70 chaperone Ssb, which relocates from the ribosome to the cytosol during heat shock and plays an anti-prion role during stress.
- The ribosome associated complex and the associated chaperone Ssb act as an anti-prion system, preventing formation of prions other than $[PSI^+]$.

FUTURE DIRECTIONS

We show in this work that curing of $[PSI^+]$ by mild heat shock relies on asymmetric segregation, however curing by mild heat shock for other prions has not yet been reported. It is possible that other prions are not segregated with aggregated proteins, or it may be that the effect is not adequate to cause curing, but these questions should be addressed in future work. As all known prions rely on Hsp104 and Ssa for propagation by shearing, Ssb movement to the cytosol and subsequent antagonization of Ssa during heat shock should have an effect on prions besides $[PSI^+]$. It is possible that the discrepancy in levels between Hsp104 and Ssa does not last long enough to affect other prions such that they are cured by mild heat stress, or there may be other dynamics at play for other prions, but curing by overexpression of Ssb in concert with Hsp104 overexpression should be tested for prions besides $[PSI^+]$, perhaps $[URE3]$ or $[MOT^+]$ as these have phenotypes that allow relatively easy determination of presence or absence of the prion.

The mammalian ribosome associated complex and chaperone system is highly homologous to the yeast system, but knowledge about the mammalian system in response to stress is lacking. It may be interesting to check whether the mammalian Hsp70 (Ssb homolog) is able to function in a similar manner as Ssb in preventing shearing of prion proteins or assisting in clearance of protein aggregates. The role of asymmetric segregation in prion propagation or curing in mammalian cells is another area of potential future research. Indeed, the mammalian protein Tau, which is implicated in Alzheimer's Disease and the Tauopathies, is also implicated in regulation of the actin cytoskeleton thus further knowledge regarding this apparatus may provide insight into these disorders.

APPENDIX A. TABLES OF STRAINS, PLASMIDS, PRIMERS, AND DATA

Table A1. Strains used in this work

NAME	SOURCE	GENOTYPE
1-1-74-D694 (OT55)	Wegrzyn <i>et al.</i> 2001	<i>MATa ade1-14 his3-Δ200 leu2-3,112 trp1-289 ura3-52 [PSI⁺]</i>
GT1680	This work	<i>MATa ade1-14 his3-Δ200 leu2-3,112 trp1-289 ura3-52 [PSI⁺] sir2Δ::HIS5</i>
GT1792	This work	<i>MATa ade1-14 his3-Δ200 leu2-3,112 trp1-289 ura3-52 [PSI⁺] hst2Δ::HIS5</i>
WTY682 (OT483)	Chernova <i>et al.</i> 2011	<i>MATa ade1-14 his3-Δ200 leu2-3,112 trp1-289 ura3-52 [PSI⁺] lsb2Δ::kanMX4</i>
GT1838	This work	<i>MATa ade1-14 his3-Δ200 leu2-3,112 trp1-289 ura3-52 [PSI⁺], sir2Δ::HIS5, lsb2Δ::kanMX4</i>
GT2059	This work	<i>MATa ade1-14 his3-Δ200 leu2-3,112 trp1-289 ura3-52 [PSI⁺] Hsp104::GFP-HIS5</i>
GT2066	This work	<i>MATa ade1-14 his3-Δ200 leu2-3,112 trp1-289 ura3-52, Hsp104::GFP-HIS5, sir2Δ::kanMX4, [PSI⁺]</i>
GT2197	This work	<i>MATa ade1-14 his3-Δ200 leu2-3,112 trp1-289 ura3-52 [psi⁻]</i>
GT2198	This work	<i>MATa ade1-14 his3-Δ200 leu2-3,112 trp1-289 ura3-52 sir2Δ::HIS5 [psi⁻]</i>
GT2156	This work	<i>MATa ade1-14 his3-Δ200 leu2-3,112 trp1-289 ura3-52 ssb2Δ::URA3, [PSI⁺]</i>
GT2177	This work	<i>MATa ade1-14 his3-Δ200 leu2-3,112 trp1-289 ura3-52 ssb1Δ::HIS3 [PSI⁺]</i>
GT2161	This work	<i>MATa ade1-14 his3-Δ200 leu2-3,112 trp1-289 ura3-52 ssb1Δ::HIS3 ssb2Δ::URA3 [PSI⁺]</i>
GT2188	This work	<i>MATa ade1-14 his3-Δ200 leu2-3,112 trp1-289 ura3-52 zuo1Δ::kanMX4 [PSI⁺]</i>

GT2185	This work	<i>MATa ade1-14 his3-Δ200 leu2-3,112 trp1-289 ura3-52 ssz1Δ::HIS5 [PSI⁺]</i>
3383 (OT537)	Wickner <i>et al.</i> 1994	<i>MATa karl ura2 leu2 his- [ure0]</i>
BY241 (OT539)	Brachmann <i>et al.</i> 2005	<i>MATa leu2 trp1ura3 PDAL5:ADE2 PDAL5:CAN1 kar1 [ure0]</i>
GT2175	This work	<i>MATa leu2 trp1ura3 PDAL5:ADE2 PDAL5:CAN1 kar1 zuo1Δ::kanMX4 [ure0]</i>
GT409	Chernova <i>et al.</i> 2017	<i>MATa ade1-14 his3-Δ200 or 11,15 leu2-3,112 lys2 trp1-Δ ura3-52 [psi⁻] [pin⁻]</i>
GT1786	D. Kiktev	<i>MATa ade1-14 his3-Δ200 or 11,15 leu2-3,112 lys2 trp1-Δ ura3-52 ssb1Δ::HIS3 ssb2Δ::URA3 [psi⁻] [pin⁻]</i>
GT127	P. Bailleul	<i>MATa ade1-14 his3-Δ200 or 11,15 leu2-3,112 lys2 trp1-Δ ura3-52 ssb1Δ::HIS3 ssb2Δ::URA3, [PSI⁺]</i> used for strain construction
YBD401 (OT492)	Liu <i>et al.</i> 2010	<i>MATa, his3Δ1, leu2Δ, met15Δ, ura3Δ, HSP104::GFP-HIS6</i> used for strain construction
YGR285c (OT536)	K. Lobachev	<i>MATa; his3Δ1, leu2Δ0, met15Δ0, ura3Δ0, Δzuo1:kanMX4</i> used for strain construction

Table A2. Plasmids used in this work

Plasmid name	Plasmid type	Yeast marker	Collection number	Use	Source
pGAL104-URA3	<i>CEN</i>	<i>URA3</i>	46	Induction of <i>HSP104</i> under GAL promoter	S. Lindquist
pRS316-GAL	<i>CEN</i>	<i>URA3</i>	3	Control plasmid for pGAL104- <i>URA3</i>	Liu
pYCL-Sp-SUP35NMSc-DsRed	<i>CEN</i>	<i>LEU2</i>	582	Fluorescence tracking of Sup35NM	R. Wegrzyn
pFA6a-KanMX6	bacterial	none (<i>E. coli</i> AMP)	658	Pringle constructs for deletions with <i>KanMX</i>	J. Pringle
pFA6a-His3MX6	bacterial	none (<i>E. coli</i> AMP)	247	Pringle constructs for deletions with <i>HIS5</i>	J. Pringle
YEp351G-URE2	2 micron	<i>LEU2</i>	1514	Induction of [<i>URE3</i>] by <i>URE2</i> under GAL promoter	R. Wickner
p366-6	<i>CEN</i>	<i>LEU2</i>	904	Addition of Ssb2 during heat shock	Chernoff Lab
p366	<i>CEN</i>	<i>LEU2</i>	175	Control plasmid for p366-6	Chernoff Lab
YEp351G	2 micron	<i>LEU2</i>	1513	Control plasmid for Yep351G- <i>URE2</i>	R. Wickner
pFL39GAL-SUP35N	<i>CEN</i>	<i>TRP1</i>	465	Induction of <i>SUP35</i> under GAL promoter	A. Borchsenius

Table A3. Primers used in this work

NAME	SEQUENCE
Sir2DeleteFwd	CATTCAAACCATTTTTCCCTCATCGGGCACATTAAGCT GGCG GATCCCCGGGTTAATTAA
Sir2DeleteRvs	ATTGTTTGCCATACTATGTAAATTGATATTAATTTGGCA CGAATTCGAGCTCGTTTAAAC
Sir2CheckFwd	GCCCATTCTCACGTATTTCAA
Sir2CheckRvs	ACCCGGTACAATGAAAATAGC
Hst2delFwd	GCCCGTCACTGAGCTACCAACCAGACGTACCGCGATC TCTC GGATCCCCGGGTTAATTAA
Hst2delRvs	CGCGCATGCTAGATGAATAAGGAAAAAAAAAAGGGGGA CGGG AATTCGAGCTCGTTTAAAC
Hst2checkFwd	AGCTTCGCCGATCTTAAGAA
Hst2checkRvs	ATGCAATGTCAAACGCGTAG
Hsp104-GFP-For	ATTCCGATGATATGGGTGCA
Hsp104-GFP-Rev	TGAGAAGCTGTCATCGAGGTT
Hsp104-GFP-ckh-fw	TCGTGGATATTCGTTTGAAGG
Hsp104-GFP-ckh-rv	GGGGTTCGTGGGAATTTTAA
SSB2-replacement-F	TTGCACTTGTTACCCATCGTT
SSB2-replacement-R	GTGTATAACCTTAACCAGAATG
SSB2che-F	CGGAAATGGTGTGGAAGAT
SSB2che-R	CAGCCGAAAAGCAGTTTCAT
SSB1replacePRINGFwd	CTTGCTTTTGGATTTTCAGATGTCCCAAGATCATTAC AGTCGGATCCCCGGGTTAATTAA
SSB1replacePRINGRvs	GACATATCAGTAACAGTTATCAAGCTAAATATT TACGCGAGAATTCGAGCTCGTTTAAAC
SSB1-replacement-F	TGTCGCTTTGCTTTTCCTTCT
SSB1-replacement-R	TGGGTCTTGATCAACTTTCCTC
ZUO1_new_FWD	CATCGTTAGCTGGCGTTTTA

ZUO1_new_RVS	ACAACGACAAAGAAGTATGGG
ZUO1 chF	CATAAGGTTTTCTACCGATGC
ZUO1 chR	CGCCTTTCTCATTATCCCTC
SSZ1 delF	GGTGAAATTTTTTCCAAGAGATGATGAGGTCGGATAAT ATCGGATCCCCGGGTTAATTAA
SSZ1 delR	TTTTCTATATACGTATACATACCGTTTTTCTTAGAGCGC TGAATTCGAGCTCGTTTAAAC
SSZ1 checkF	TGGGAGCGGTAAAAGATGTGC
SSZ1 checkR	ATGGCACGATAAGCCTTTCTC

Table A4. Percent of [*psi*] (reds and mosaics) for mild heat shock experiments.

Strain	Averages and SD for each time point (%)						(n) tested
	0	30	45	60	120	240	
wild-type (WT)	1.6 \pm 1.0	32.8 \pm 4.1	41.3 \pm 8.2	38.8 \pm 10.5	15.4 \pm 3.8	5.5 \pm 2.1	14
<i>ssb1/2</i> Δ	3.4 \pm 2.1	5.2 \pm 2.9	10.7 \pm 5.4	9.7 \pm 4.5	4.2 \pm 2.1	3.6 \pm 2.2	7
<i>ssb1</i> Δ	1.2 \pm 1.2	2.2 \pm 1.6	2.2 \pm 1.0	3.1 \pm 1.2	3.0 \pm 2.5	2.0 \pm 0.8	4
<i>ssb2</i> Δ	1.1 \pm 2.2	5.3 \pm 2.7	10.0 \pm 6.6	7.9 \pm 5.8	2.3 \pm 1.0	2.1 \pm 1.0	4
<i>zuo1</i> Δ	11.5 \pm 7.6	92.8 \pm 9.1	96.7 \pm 6.1	96.0 \pm 6.5	90.1 \pm 7.8	43.8 \pm 12.3	7
<i>sir2</i> Δ	1.2 \pm 1.2	3.2 \pm 3.6	4.8 \pm 5.6	4.2 \pm 3.7	2.7 \pm 3.7	1.9 \pm 1.8	9
<i>lsb2</i> Δ	1.1 \pm 1.6	42.4 \pm 1.9	56.3 \pm 1.4	64.1 \pm 3.0	36.9 \pm 2.6	11.8 \pm 5.6	2
<i>lsb2</i> Δ <i>sir2</i> Δ	0.0 \pm 0.0	2.3 \pm 1.1	5.0 \pm 2.8	5.9 \pm 7.0	6.5 \pm 8.2	3.1 \pm 2.4	4
<i>hst2</i> Δ	1.5 \pm 1.3	17.6 \pm 3.0	19.4 \pm 3.1	16.0 \pm 3.0	7.0 \pm 3.3	3.8 \pm 0.7	6
<i>ssz1</i> Δ	1.4 \pm 0.6	93.3 \pm 0.1	89.9 \pm 0.3	87.9 \pm 4.6	75.3 \pm 0.2	18.5 \pm 3.1	2
WT+NAM (10mM)	2.6 \pm 1.9	28.1 \pm 9.7	50.5 \pm 15.3	53.6 \pm 16.3	40.0 \pm 16.5	8.9 \pm 2.6	6
<i>sir2</i> Δ +NAM (10mM)	0.0 \pm 0.0	4.8 \pm 4.2	10.9 \pm 7.9	14.8 \pm 11.7	8.7 \pm 6.9	1.7 \pm 1.4	4

Table A5. Hsp104-GFP tagged aggregate location data.

Time point	Total pairs with aggregates in location, Numbers and (%) Mother, Daughter, Both percents are out of pairs with aggregates only, General Fluorescence is out of total pairs of cells. +/- Standard Error				
		Mother only	Daughter only	Both	General Fluorescence
Pre-heat shock	WT	8 (73 \pm 13%)	0 (0 \pm 9%)	3 (27 \pm 13%)	71 (87%)
	<i>sir2</i> Δ	12 (41 \pm 9%)	9 (31 \pm 9%)	8 (28 \pm 8%)	56 (66%)
T=0 (heat shock)	WT	0 (0 \pm 1%)	0 (0 \pm 1%)	68 (100 \pm 1%)	0 (0%)
	<i>sir2</i> Δ	0 (0 \pm 1%)	0 (0 \pm 1%)	217 (100 \pm 1%)	0 (0%)
120 min recovery	WT	21 (15 \pm 3%)	0 (0 \pm 1%)	118 (85 \pm 3%)	2 (1%)
	<i>sir2</i> Δ	4 (3 \pm 2%)	4 (3 \pm 2%)	116 (94 \pm 2%)	0 (0%)
240 min recovery	WT	18 (67 \pm 1%)	0 (0 \pm 4%)	9 (33 \pm 9%)	2 (7%)
	<i>sir2</i> Δ	26 (55 \pm 7%)	2 (4 \pm 3%)	19 (40 \pm 7%)	4 (8%)

Table A6. Sup35NM-RFP aggregate location data.

Time point	Total pairs with aggregates in location, Numbers and (%) Mother, Daughter, Both percents are out of pairs with aggregates only, General Fluorescence is out of total pairs of cells. +/- Standard Error				
		Mother only	Daughter only	Both	General Fluorescence
Pre-heat shock	WT	4 (40 ± 15%)	0 (0 ± 9%)	6 (60 ± 15%)	57 (85%)
	<i>sir2Δ</i>	7 (58 ± 14%)	0 (0 ± 8%)	5 (42 ± 14%)	43 (78%)
T=0 (heat shock)	WT	16 (55 ± 9%)	2 (7 ± 5%)	11 (38 ± 9%)	17 (37%)
	<i>sir2Δ</i>	5 (9 ± 4%)	4 (7 ± 3%)	47 (84 ± 5%)	10 (15%)
120 min recovery	WT	18 (27 ± 5%)	2 (3 ± 2%)	46 (70 ± 6%)	25 (27%)
	<i>sir2Δ</i>	26 (32 ± 5%)	3 (4 ± 2%)	52 (64 ± 5%)	8 (9%)
240 min recovery	WT	17 (94 ± 6%)	0 (0 ± 5%)	1 (6 ± 6%)	5 (22%)
	<i>sir2Δ</i>	26 (63 ± 8%)	3 (7 ± 4%)	12 (29 ± 7%)	13 (24%)

Table A7. Frequencies of [PSI⁺] in aged, unaged, or average age cells.

Experiment 3 shown	Frequency of [PSI ⁺]					
	WT			<i>sir2Δ</i>		
Experiment #	1	2	3	1	2	3
T=0	1.33x10 ⁻³ +/-5x10 ⁻⁵	3.21x10 ⁻⁴ +/-3x10 ⁻⁵	1.44x10⁻³ +/-2x10 ⁻⁴	1.16x10 ⁻⁵ +/-4x10 ⁻⁶	3.86x10 ⁻⁵ +/-1x10 ⁻⁵	2.06x10⁻⁴ +/-2x10 ⁻⁵
Aged 14 gen	7.19x10 ⁻⁴ +/-8x10 ⁻⁵	4.33x10 ⁻⁴ +/-4x10 ⁻⁵	1.72x10⁻³ +/-1x10 ⁻⁴	5.38x10 ⁻⁴ +/-3x10 ⁻⁴	4.57x10 ⁻⁴ +/-7x10 ⁻⁵	2.26x10⁻³ +/-6x10 ⁻⁴
Average 14 gen	2.82x10 ⁻³ +/-2x10 ⁻⁴	6.69x10 ⁻⁴ +/-5x10 ⁻⁵	2.78x10⁻³ +/-3x10 ⁻⁴	1.78x10 ⁻⁵ +/-1x10 ⁻⁵	3.65x10 ⁻⁴ +/-7x10 ⁻⁵	2.02x10⁻³ +/-6x10 ⁻⁴
Aged 18 gen	3.21x10 ⁻³ +/-2x10 ⁻⁴	3.35x10 ⁻³ +/-4x10 ⁻⁴	1.47x10⁻² +/-1x10 ⁻³	N/T	N/T	N/T
Average 18 gen	5.45x10 ⁻³ +/-6x10 ⁻⁴	5.96x10 ⁻³ +/-7x10 ⁻⁴	2.02x10⁻² +/-7x10 ⁻⁴	N/T	N/T	N/T

Table A8. Frequency of [URE3] spontaneous formation for wild-type vs. *zuo1Δ*.

	WT		<i>zuo1Δ</i>	
	Experiment 1	Experiment 2	Experiment 1	Experiment 2
Median Frequency	3.2x10 ⁻⁵	1.1x10⁻⁴	8.7x10 ⁻⁵	8.5x10⁻⁴
95% CI Frequency	1.9-3.7x10 ⁻⁵	9.4x10⁻⁵-1.3x10⁻⁴	6.8x10 ⁻⁵ -1.1x10 ⁻⁴	6.6x10⁻⁴-1.1x10⁻³
All frequencies Experiment 2 shown	1.7x10 ⁻⁵ 1.7x10 ⁻⁵ 1.9x10 ⁻⁵ 2.1x10 ⁻⁵ 2.3x10 ⁻⁵ 3.2x10 ⁻⁵ 3.2x10 ⁻⁵ 3.2x10 ⁻⁵ 3.3x10 ⁻⁵ 3.7x10 ⁻⁵ 4.0x10 ⁻⁵ 5.4x10 ⁻⁵	7.2x10 ⁻⁵ 8.6x10 ⁻⁵ 9.4x10 ⁻⁵ 9.6x10 ⁻⁵ 1.0x10 ⁻⁴ 1.1x10 ⁻⁴ 1.1x10 ⁻⁴ 1.2x10 ⁻⁴ 1.3x10 ⁻⁴ 1.3x10 ⁻⁴ 1.4x10 ⁻⁴ 1.6x10 ⁻⁴	5.3x10 ⁻⁵ 6.3x10 ⁻⁵ 6.8x10 ⁻⁵ 7.5x10 ⁻⁵ 8.0x10 ⁻⁵ 8.3x10 ⁻⁵ 9.2x10 ⁻⁵ 9.8x10 ⁻⁵ 1.1x10 ⁻⁴ 1.1x10 ⁻⁴ 1.2x10 ⁻⁴ 1.6x10 ⁻⁴	5.0x10 ⁻⁴ 6.3x10 ⁻⁴ 6.6x10 ⁻⁴ 6.7x10 ⁻⁴ 7.3x10 ⁻⁴ 8.0x10 ⁻⁴ 8.9x10 ⁻⁴ 1.0x10 ⁻³ 1.1x10 ⁻³ 1.1x10 ⁻³ 1.2x10 ⁻³ 3.0x10 ⁻³

Table A9. Rates of [URE3] spontaneous formation for wild-type vs. *zuo1Δ*.

	WT		<i>zuo1Δ</i>	
	Experiment 1	Experiment 2	Experiment 1	Experiment 2
Median Rate	7.5x10 ⁻⁶	2.7x10⁻⁵	1.7x10 ⁻⁵	1.5x10⁻⁴
95% CI Rate	4.5x10 ⁻⁶ -1.0x10 ⁻⁵	2.1-3.3x10⁻⁵	1.4-2.2x10 ⁻⁵	1.1-1.9x10⁻⁴
All rates Experiment 2 shown	5.6x10 ⁻⁶ 4.4x10 ⁻⁶ 4.5x10 ⁻⁶ 5.3x10 ⁻⁶ 6.8x10 ⁻⁶ 7.4x10 ⁻⁶ 7.5x10 ⁻⁶ 8.1x10 ⁻⁶ 8.1x10 ⁻⁶ 1.0x10 ⁻⁵ 1.1x10 ⁻⁵ 1.6x10 ⁻⁵	1.8x10 ⁻⁵ 1.8x10 ⁻⁵ 2.1x10 ⁻⁵ 2.3x10 ⁻⁵ 2.3x10 ⁻⁵ 2.7x10 ⁻⁵ 2.8x10 ⁻⁵ 3.0x10 ⁻⁵ 3.1x10 ⁻⁵ 3.3x10 ⁻⁵ 3.3x10 ⁻⁵ 3.9x10 ⁻⁵	1.1x10 ⁻⁵ 1.3x10 ⁻⁵ 1.4x10 ⁻⁵ 1.4x10 ⁻⁵ 1.5x10 ⁻⁵ 1.7x10 ⁻⁵ 1.8x10 ⁻⁵ 1.8x10 ⁻⁵ 2.1x10 ⁻⁵ 2.2x10 ⁻⁵ 2.3x10 ⁻⁵ 3.2x10 ⁻⁵	8.3x10 ⁻⁵ 1.1x10 ⁻⁴ 1.1x10 ⁻⁴ 1.2x10 ⁻⁴ 1.2x10 ⁻⁴ 1.4x10 ⁻⁴ 1.5x10 ⁻⁴ 1.8x10 ⁻⁴ 1.8x10 ⁻⁴ 1.9x10 ⁻⁴ 2.1x10 ⁻⁴ 5.2x10 ⁻⁴

REFERENCES

1. **Aguilaniu H, Gustafsson L, Rigoulet M, and Nystrom T.** 2003. Asymmetric inheritance of oxidatively damaged proteins during cytokinesis. *Science*. 299(5613):1751-1753.
2. **Albanèse V, Yam AY, Baugman J, Parnot C, and Frydman J.** 2006. Systems analyses reveal two chaperone networks with distinct functions in eukaryotic cells. *Cell*. 124:75-88.
3. **Amor AJ, Castanzo DT, Delany SP, Selechnik DM, van Ooy A, and Cameron DM.** 2015. The ribosome-associated complex antagonizes prion formation in yeast. *Prion*. 9(2):144–164.
4. **Audet A, Côté N, Couture C, Bossé Y, Després JP, Pibarot P, and Mathieu P.** 2012. Amyloid substance within stenotic aortic valves promotes mineralization. *Histopathology*. 61:610–619.
5. **Bagriantsev SN, Kushnirov VV, Liebman SW.** 2006. Analysis of amyloid aggregates using agarose gel electrophoresis. *Methods in Enzymology*. 412:33-48.
6. **Baldi S, Bolognesi A, Meinema AC, and Barral Y.** 2017. Heat stress promotes longevity in budding yeast by relaxing the confinement of age-promoting factors in the mother cell. *eLife*. 6:e28329.
7. **Barbitoff YA, Matveenko AG, Moskalenko SE, Zemlyanko OM, Newnam GP, Patel A, Chernova TA, Chernoff YO, and Zhouravleva GA.** 2017. To CURE or not to CURE? Differential effects of the chaperone sorting factor Cur1 on yeast prions are mediated by the chaperone Sis1. *Molecular Microbiology*. 105:242–257.
8. **Baudin-Baillieu A, Fabret C, and Namy O.** 2011. Are prions part of the dark matter of the cell? *Prion*. 5(4):299-303.
9. **Bitterman KJ, Anderson RM, Cohen HY, Latorre-Esteves M, and Sinclair DA.** 2002. Inhibition of silencing and accelerated aging by nicotinamide, a putative negative regulator of yeast Sir2 and human SIRT1. *Journal of Biological Chemistry*. 277(47):45099-45107.
10. **Blanco LP, Evans ML, Smith DR, Badtke MP, and Chapman MR.** 2012. Diversity, biogenesis and function of microbial amyloids. *Trends in Microbiology*. 20(2):66-73.

11. **Boyle JP, Thompson TJ, Gregg EW, Barker LE, and Williamson DF.** 2010. Projection of the year 2050 burden of diabetes in the US adult population: dynamic modeling of incidence, mortality, and prediabetes prevalence. *Population Health Metrics*. 8(29):doi: 10.1186/1478-7954-8-29
12. **Bukau B, Deuerling E, Pfund C, Craig EA.** 2000. Getting newly synthesized proteins into shape. *Cell*. 101:119–122.
13. **Calderwood SK, Murshid A, and Prince T.** 2009. The shock of aging: molecular chaperones and the heat shock response in longevity and aging – A Mini-Review. *Gerontology*. 55:550–558.
14. **Chernoff YO and Kiktev DA.** 2016. Dual role of ribosome-associated chaperones in prion formation and propagation. *Current Genetics*. 62(4):677-685.
15. **Chernoff YO, Lindquist SL, Ono B, Inge-Vechtsov SG, and Liebman SW.** 1995. Role of the chaperone protein Hsp104 in propagation of the yeast prion-like factor [*PSI⁺*]. *Science*. 268:880-884.
16. **Chernoff YO, Newnam GP, Kumar J, Allen K, and Zink AD.** 1999. Evidence for a protein mutator in yeast: role of the Hsp70-related chaperone Ssb in formation, stability, and toxicity of the [*PSI⁺*] prion. *Molecular Cell Biology*. 19(12):8103-12.
17. **Chernova TA, Kiktev DA, Romanyuk AV, Shanks JR, Laur O, Ali M, Ghosh A, Kim D, Yang Z, Mang M, Chernoff YO, and Wilkinson KD.** 2017. Yeast short-lived actin-associated protein forms a metastable prion in response to thermal stress. *Cell Reports*. 18(3):751-761.
18. **Chernova TA, Romanyuk AV, Karpova TS, Shanks JR, Ali M, Moffatt N, Howie RL, O'Dell A, McNally JG, Liebman SW, Chernoff YO, and Wilkinson KD.** 2011. Prion induction by the short-lived, stress-induced protein Lsb2 is regulated by ubiquitination and associated with the actin cytoskeleton. *Molecular Cell*. 43:242-252.
19. **Chernova TA, Wilkinson KD, and Chernoff YO.** 2014. Physiological and environmental control of yeast prions. *Federation of European Microbiological Societies Microbiology Reviews*. 38(2):326–344.
20. **Chiti F and Dobson CM.** 2006. Protein misfolding, functional amyloid, and human disease. *Annual Review of Biochemistry*. 75:333-66.

21. **Cohen A, Ross L, Nachman I, and Bar-Nun S.** 2012. Aggregation of PolyQ proteins is increased upon yeast aging and affected by Sir2 and Hsf1: novel quantitative biochemical and microscopic assays. *Public Library of Science One.* 7(9):e44785.
22. **Dang W, Steffen KK, Perry R, Dorsey JA, Johnson FB, Shilatifard A, Kaeberlein M, Kennedy BK, and Berger SL.** 2009. Histone H4 lysine-16 acetylation regulates cellular lifespan. *Nature.* 459(7248):802-807.
23. **Derdowski A, Sindi SS, Klaips CL, DiSalvo S, Serio TR.** 2010. A size threshold limits prion transmission and establishes phenotypic diversity. *Science.* 330:680–683.
24. **Derkatch IL, Bradley ME, Masse SV, Zadorsky SP, Polozkov GV, Inge-Vechtomov SG, and Liebman SW.** 2000. Dependence and independence of $[PSI^+]$ and $[PIN^+]$: a two-prion system in yeast? *European Molecular Biology Organization Journal.* 19:1942–1952.
25. **Döring K, Ahmed N, Riemer T, Suresh HG, Vainshtein Y, Habich M, Riemer J, Mayer MP, O'Brien EP, Kramer G, Bukau B.** 2017. Profiling Ssb-nascent chain interactions reveals principles of Hsp70-assisted folding. *Cell.* 170(2):298-311.
26. **Dubrey, SW and Comenzo, RL.** 2012. Amyloid diseases of the heart: current and future therapies. *Quarterly Journal of Medicine.* 105(7):617–631.
27. **Dulle JE, Stein KC, and True HL.** 2014. Regulation of the Hsp104 middle domain activity is critical for yeast prion propagation. *Public Library of Science One.* 9(1):e87521.
28. **Erjavec N, Larsson L, Grantham J, and Nystrom T.** 2007. Accelerated aging and failure to segregate damaged proteins in Sir2 mutants can be suppressed by overproducing the protein aggregation-remodeling factor Hsp104p. *Genes and Development.* 21:2410-2421.
29. **Espargaro A, Villar-Pique A, Sabate R, and Ventura S.** 2012. Yeast prions form infectious amyloid inclusion bodies in bacteria. *Microbial Cell Factories.* 11(1):89.
30. **Ferreira PC, Ness F, Edwards SR, Cox BS, and Tuite MF.** 2001. The elimination of the yeast $[PSI^+]$ prion by guanidine hydrochloride is the result of Hsp104 inactivation. *Molecular Microbiology.* 40(6):1357-69.

31. **Gietz D, St Jean A, Woods RA, and Schiestl RH.** 1992. Improved method for high efficiency transformation of intact yeast cells. *Nucleic Acids Research.* 20(6):1425.
32. **Glover JR and Lum R.** 2009. Remodeling of protein aggregates by Hsp104. *Protein Peptide Letters.* 16:587-97.
33. **Gregersen N, Bross P, Vang S, Christensen JH.** 2006. Protein misfolding and human disease. *Annual Review of Genomics and Human Genetics.* 7:103-24.
34. **Hebert, LE, Scherr, PA, Bienias, JL, Bennett, DA, and Evans, DA.** 2003. Alzheimer's disease in the U.S. population: Prevalence estimates using the 2000 Census. *Archives of Neurology.* 60(8):1119–1122.
35. **Helsen CW and Glover JR.** 2012. A new perspective on Hsp104-mediated propagation and curing of the yeast prion [*PSI*⁺]. *Prion.* 6(3): 234-239.
36. **Heron M.** 2012. Deaths: leading causes for 2008. *National Vital Statistics Reports.* 60(6):1-95.
37. **Hill SM, Hanzén S, Nyström T.** 2017. Restricted access: spatial sequestration of damaged proteins during stress and aging. *European Molecular Biology Organization Reports.* 19(3): 377-391.
38. **Holmes DL, Lancaster AK, Lindquist S, and Halfmann R.** 2013. Heritable remodeling of yeast multicellularity by an environmentally responsive prion. *Cell.* 153:153–165.
39. **Hong JY, Mathur V, and Liebman SW.** 2011. A new color assay for [*URE3*] prion in a genetic background used to score for the [*PSI*⁺] prion. *Yeast.* 28(7): 555–560.
40. **Huh W, Falvo JV, Gerke LC, Carroll AS, Howson RW, Weissman JS, and O'Shea EK.** 2003. Global analysis of protein localization in budding yeast. *Nature.* 425:686-691.
41. **Hung GC and Masison DC.** 2006. N-terminal domain of yeast Hsp104 chaperone is dispensable for thermotolerance and prion propagation but necessary for curing prions by Hsp104 overexpression. *Genetics.* 173:611-620.
42. **Inge-Vechtomov SG, Zhouravleva GA, and Chernoff YO.** 2007. Biological roles of prion domains. *Prion.* 1(4):228-235.

43. **Iwahashi H, Wu Y, and Tanguay RM.** 1995. Detection and expression of the 70 kDa heat shock protein Ssb1p at different temperatures in *Saccharomyces cerevisiae*. *Biochemical and Biophysical Research Communications*. 213:484–489.
44. **Kiktev DA, Melomed MM, Lu CD, Newnam GP, and Chernoff YO.** 2015. Feedback control of prion formation and propagation by the ribosome-associated chaperone complex. *Molecular Microbiology*. 96(3):621-32.
45. **Kiktev DA, Patterson JC, Muller S, Bariar B, Pan T, and Chernoff YO.** 2012. Regulation of chaperone effects on a yeast prion by cochaperone Sgt2. *Molecular Cell Biology*. 32:4960–4970.
46. **Klaips CL, Hochstrasser ML, Langlois CR, and Serio TR.** 2014. Spatial quality control bypasses cell-based limitations on proteostasis to promote prion curing. *eLife*. 3:e04288.
47. **Koplin A, Preissler S, Ilina Y, Koch M, Scior A, Erhardt M, and Deuerling E.** 2010. A dual function for chaperones Ssb–RAC and the NAC nascent polypeptide–associated complex on ribosomes. *Journal of Cell Biology*. 189(1):57-68.
48. **Kourtis N and Tavernarakis N.** 2011. Cellular stress response pathways and aging: intricate molecular relationships. *European Molecular Biology Organization Journal*. 30(13):2520-2531.
49. **Kushnirov VV, Vishnevskaya AB, Alexandrov IM, Ter-Avanesyan MD.** 2007. Prion and nonprion amyloids: a comparison inspired by the yeast Sup35 protein. *Prion*. 1:179–84.
50. **Lancaster AK, Bardill JP, True HL, Masel J.** 2010. The spontaneous appearance rate of the yeast prion [*PSI⁺*] and its implications for the evolution of the evolvability properties of the [*PSI⁺*] system. *Genetics*. 184:393–400.
51. **Liebman SW and Derkatch IL.** 1999. The yeast [*PSI⁺*] prion: making sense of nonsense. *Journal of Biological Chemistry*. 274:1181-1184.
52. **Li C, Qin R, Liu R, Miao S, Yang P.** 2018. Functional amyloid materials at surfaces/interfaces. *Biomaterials Science*. 6(3):462-472.
53. **Liu B, Larsson L, Caballero A, Hao X, Oling D, Grantham J, and Nyström T.** 2010. The polarisome is required for segregation and retrograde transport of protein aggregates. *Cell*. 140(2):25-267.

54. **Liu B, Larsson L, Franssens V, Hao X, Hill SM, Andersson V, Höglund D, Song J, Yang X, Öling D, Grantham J, Winderickx J, and Nyström T.** 2011. Segregation of protein aggregates involves actin and the polarity machinery. *Cell*. 147(5):959-61.
55. **Longtine MS, McKenzie A, Demarini DJ, Shah NG, Wach A, Brachat A, Philippsen P, and Pringle JR.** 1998. Additional modules for versatile and economical PCR-based gene deletion and modification in *Saccharomyces cerevisiae*. *Yeast*. 14:953-961.
56. **Lopez N, Halladay J, Walter W, Craig EA.** 1999. SSB, encoding a ribosome-associated chaperone, is coordinately regulated with ribosomal protein genes. *Journal of Bacteriology*. 181:3136–3143.
57. **Lum R, Niggemann M, and Glover JR.** 2008. Peptide and protein binding in the axial channel of Hsp104. *Journal of Biological Chemistry*. 283(44):30139-30150.
58. **Ma J, Ward EM, Siegel RL, and Jemal A.** 2015. Temporal trends in mortality in the United States, 1969-2013. *Journal of the American Medical Association*. 314(16):1731-1739.
59. **Madania A, Dumoulin P, Grava S, Kitamoto H, Schärer-Brodbeck C, Soulard A, Moreau V, and Winsor B.** 1999. The *Saccharomyces cerevisiae* homologue of human Wiskott-Aldrich syndrome protein Las17p interacts with the Arp2/3 complex. *Molecular Biology of the Cell*. 10:3521–3538.
60. **Maji SK, Perrin MH, Sawaya MR, Jessberger S, Vadodaria K, Rissman RA, Singru PS, Nilsson KP, Simon R, Schubert D, Eisenberg D, Rivier J, Sawchenko P, Vale W, Riek R.** 2009. Functional amyloids as natural storage of peptide hormones in pituitary secretory granules. *Science*. 325(5938):328-32.
61. **Majumdar A, Cesario WC, White-Grindley E, Jiang H, Ren F, Khan MR, Li L, Choi EM, Kannan K, Guo F, Unruh J, Slaughter B, Si K.** 2012. Critical role of amyloid-like oligomers of *Drosophila* Orb2 in the persistence of memory. *Cell*. 148(3):515-29.
62. **Matveenko AG, Barbitoff YA, Jay-Garcia LM, Chernoff YO, and Zhouravleva GA.** 2018. Differential effects of chaperones on yeast prions: CURrent view. *Current Genetics*. 64(2):317-325.

63. **Michishita E, Park JY, Burneskis JM, Barrett JC, and Horikawa I.** 2005. Evolutionarily conserved and nonconserved cellular localizations and functions of human SIRT proteins. *Molecular Biology of the Cell*. 16:4623-4635.
64. **Moriyama H, Edskes HK, and Wickner RB.** 2000. [URE3] prion propagation in *Saccharomyces cerevisiae*: requirement for chaperone Hsp104 and curing by overexpressed chaperone Ydj1p. *Molecular Cell Biology*. 20:8916-22.
65. **Nakayashiki T, Kurtzman CP, Edskes HK, Wickner RB.** 2005. Yeast prions [URE3] and [PSI⁺] are diseases. *Proceedings of the National Academy of Sciences*. 102(30):10575-80.
66. **Ness F, Cox BS, Wongwigkarn J, Naeimi WR, Tuite MF.** 2017. Over-expression of the molecular chaperone Hsp104 in *Saccharomyces cerevisiae* results in the malpartition of [PSI⁺] propagons. *Molecular Microbiology*. 104(1):125-143.
67. **Newman GP, Birchmore JL, and Chernoff YO.** 2011. Destabilization and recovery of a yeast prion after mild heat shock. 2011. *Journal of Molecular Biology*. 408:432-448.
68. **Park KW, Hahn JS, Fan Q, Thiele DJ, and Li L.** 2006. *De novo* appearance and “strain” formation of yeast prion [PSI⁺] are regulated by the heat-shock transcription factor. *Genetics*. 173: 35–47.
69. **Park Y, Morales D, Rubinson EH, Masison D, Eisenberg E, and Greene LE.** 2012. Differences in the curing of [PSI⁺] prion by various methods of Hsp104 inactivation. *Public Library of Science One*. 7(6): e37692.
70. **Park YN, Zhao X, Yim YI, Todor H, Ellerbrock R, Reidy M, Eisenberg E, Masison D C, and Greene LE.** 2014. Hsp104 overexpression cures *Saccharomyces cerevisiae* [PSI⁺] by causing dissolution of the prion seeds. *Eukaryotic Cell*. 13:635–647.
71. **Prusiner SB.** 1998. Prions. *Proceedings of the National Academy of Sciences*. 95(23):13363-13383.
72. **Prusiner SB.** 2012. A unifying role for prions in neurodegenerative diseases. *Science*. 336:1511-1513.
73. **Reidy M and Masison DC.** 2011. Modulation and elimination of yeast prions by protein chaperones and co-chaperones. *Prion*. 5(4):245-249.

74. **Ridley RM, Baker HF, Windle CP, Cummings RM.** 2006. Very long term studies of the seeding of beta-amyloidosis in primates. *Journal of Neural Transmission.* 113(9):1243-51.
75. **Saarikangas J and Barral Y.** 2015. Protein aggregates are associated with replicative aging without compromising protein quality control. *eLife.* 4:e06197.
76. **Schwimmer C, Masison DC.** 2002. Antagonistic interactions between yeast [*PSI⁺*] and [*URE3*] prions and curing of [*URE3*] by Hsp70 protein chaperone Ssa1p but not by Ssa2p. *Molecular Cell Biology.* 22:3590-8.
77. **Sharma D, Masison DC.** 2008. Functionally redundant isoforms of a yeast Hsp70 chaperone subfamily have different anti-prion effects. *Genetics.* 179:1301-11.
78. **Sherman F.** 2002. Getting started with yeast. *Methods in Enzymology.* 350:3-41.
79. **Shewmaker F and Wickner RB.** 2006. Ageing in yeast does not enhance prion generation. *Yeast.* 23:1123–1128.
80. **Shorter J and Lindquist S.** 2005. Prions as adaptive conduits of memory and inheritance. *Nature Reviews Genetics.* 6(6):435-50.
81. **Si K, Lindquist S, Kandel ER.** 2003. A neuronal isoform of the aplysia CPEB has prion-like properties. *Cell.* 115(7):879-91.
82. **Speldewinde SH, Doronina VA, Tuite MF, and Grant CM.** 2017. Disrupting the cortical actin cytoskeleton points to two distinct mechanisms of yeast [*PSI⁺*] prion formation. *Public Library of Science Genetics.* 13(4): e1006708.
83. **Spokoini R, Moldavski O, Nahmias Y, England JL, Schuldiner M, and Kaganovich D.** 2012. Confinement to organelle-associated inclusion structures mediates asymmetric inheritance of aggregated protein in budding yeast. *Cell Reports.* 2(4):738-747.
84. **Steffen KK, Kennedy BK, Kaeberlein M.** 2009. Measuring replicative life span in the budding yeast. *Journal of Visualized Experiments.* 25(28):e1209.
85. **Stöhr J, Watts JC, Mensinger ZL, Oehler A, Grillo SK, DeArmond SJ, Prusiner SB, and Giles K.** 2012. Purified and synthetic Alzheimer's amyloid beta (A β) prions. *Proceedings of the National Academies of Sciences.* 109(27):11025-11030.

86. **Suzuki G, Shimazu N, and Tanaka M.** 2012. A yeast prion, Mod5, promotes acquired drug resistance and cell survival under environmental stress. *Science*. 336:355-359.
87. **Taneja V, Maddelein ML, Talarek N, Saupe SJ, Liebman SW.** 2007. A non-Q/N-rich prion domain of a foreign prion, [*Het-s*], can propagate as a prion in yeast. *Molecular Cell*. 27:67–77.
88. **Tessarz P, Schwarz M, Mogk A, and Bukau B.** 2009. The yeast AAA+ chaperone Hsp104 is part of a network that links the actin cytoskeleton with the inheritance of damaged proteins. *Molecular Cell Biology*. 29(13):3738-45.
89. **Trevitt CR and Singh PN.** 2003. Variant Creutzfeldt-Jakob disease: pathology, epidemiology, and public health implications. *The American Journal of Clinical Nutrition*. 78(3): 651S–656S.
90. **Tsuchiya M, Dang N, Kerr EO, Hu D, Steffen KK, Oakes JA, Kennedy BK, and Kaeberlein M.** 2006. Sirtuin-independent effect of nicotinamide on lifespan extension from calorie restriction in yeast. *Aging Cell*. 5:505-514.
91. **Tuite MF and Cox BS.** 2007. The genetic control of the formation and propagation of the [*PSI⁺*] prion of yeast. *Prion*. 1(2):101-109.
92. **Tyedmers J, Madariaga ML, and Lindquist S.** 2008. Prion switching in response to environmental stress. *Public Library of Science Biology*. 6(11):e294.
93. **Uptain SM and Lindquist S.** 2002. Prions as protein-based genetic elements. *Annual Reviews of Microbiology*. 56:703-41.
94. **Vergheze J, Abrams J, Wang Y, and Morano KA.** 2012. Biology of the heat shock response and protein chaperones: budding yeast (*Saccharomyces cerevisiae*) as a model system. *Microbiology and Molecular Biology Reviews*. 76(2):115-158.
95. **Wach A, Brachat A, Alberti-Segui C, Rebischung C, and Philippsen P.** 1997. Heterologous *HIS3* marker and GFP reporter modules for PCR-targeting in *Saccharomyces cerevisiae*. *Yeast*. 13:1065-1075.
96. **Wallace EW, Kear-Scott JL, Pilipenko EV, Schwartz MH, Laskowski PR, Rojek AE, Katanski CD, Riback JA, Dion MF, Franks AM, Airoidi EM, Pan T, Budnik BA, and Drummond DA.** 2015. Reversible, specific, active

aggregates of endogenous proteins assemble upon heat stress. *Cell*. 162(6):1286-98.

97. **Wickner RB.** 1994. [*URE3*] as an altered *URE2* protein: evidence for a prion analog in *Saccharomyces cerevisiae*. *Science*. 264(5158):566-569.
98. **Wickner RB, Edskes HK, Bateman D, Kelly AC, and Gorkovskiy A.** 2011. The yeast prions [*PSI⁺*] and [*URE3*] are molecular degenerative diseases. *Prion*. 5(4):258-262.
99. **Willmund F, del Alamo M, Pechmann S, Chen T, Albanèse V, Dammer EB, Peng J, Frydman J.** 2013. The cotranslational function of ribosome-associated Hsp70 in eukaryotic protein homeostasis. *Cell*. 152(1-2):196–209.
100. **Wu Y, Greene LE, Masison DC, and Eisenberg E.** 2005. Curing of yeast [*PSI⁺*] prion by guanidine inactivation of Hsp104 does not require cell division. *Proceedings of the National Academy of Sciences of the United States of America*. 102(36):12789–12794.
101. **Zhou C, Slaughter BD, Unruh JR, Eldakak A, Rubinstein B, and Li R.** 2011. Motility and segregation of Hsp104-associated protein aggregates in budding yeast. *Cell*. 147(5):1186–1196.
102. **Zhou C, Slaughter BD, Unruh JR, Guo F, Yu Z, Mickey K, Narkar A, Ross RT, McClain M, Li R.** 2014. Organelle-based aggregation and retention of damaged proteins in asymmetrically dividing cells. *Cell*. 159(3):530-42.